Effective Safety Message Dissemination in V2X Communications

Minglong Zhang

A thesis submitted to

Auckland University of Technology

in fulfilment of the requirements for the degree of

Doctor of Philosophy (PhD)

2020

School of Engineering

Abstract

Over the last decade, the advent of vehicular ad-hoc networks (VANETs) fulfilled various functionalities in intelligent transportation systems (ITS). Typical safety applications in ITS include exchange of mutual awareness messages among vehicles, broadcast of warning messages, cooperative driving and so on. The main purposes of these applications are to mitigate the risk of road accidents and improve the traffic efficiency. All of them rely on the technologies of vehicle-to-everything (V2X) communications, in which vehicles can communicate with vehicles, portable devices, as well as infrastructures. However, due to the highly dynamic topology of VANETs, lossy channels and limited bandwidth, the reliability and effectiveness of V2X communications is of great concern in both academic research and commercial applications. In this thesis, we aim to address the existing issues of unreliability and inefficiency in safety message dissemination. We propose a novel medium access control (MAC) protocol, enhancing the performance of the network through optimizing the MAC, and bettering resource allocation in (fifth generation) 5G cellular-V2X.

A hybrid MAC protocol, namely NC-PNC MAC, for basic safety message (BSM) dissemination is proposed, based on the framework of Dedicated Short-Range Communications (DSRC). In the protocol, BSMs are chiefly broadcast during a centralized session, while a distributed session is reserved for unqualified vehicles that may only apply legacy DSRC MAC. Such characteristic not only can effectively suppress the transmission collisions but possess the compatibility with IEEE 802.11p. In addition, the integration of Physical-Layer Network Coding (PNC) and Random Linear Network Coding (RLNC) further strengthens the reliability and efficiency for BSM dissemination. Comprehensive simulations indicate that, compared with existing schemes, the proposed protocol can significantly improve the packet delivery ratio (PDR) by a range of 20% to 300%. Meanwhile, the normalized throughput of the whole network is substantially boosted by a varying percent between 20% and 160%.

Extended studies involved in the hybrid NC-PNC MAC are conducted with the purpose of shedding light on the protocol and enhancing its performance further. The relevant studies include: 1) developing a mathematical model to analyse the subcarrier collision probability in an OFDMA scheme, the communication complexity of the MAC as well as the average PDR performance of the network; 2) identifying the key factors and investigating how they affect the PDR performance and delivery latency; 3) proposing two distinct strategies of performance enhancement based on the prior analysis and investigation. One is to adjust the parameters of the protocol, while the other is to add extra relay nodes. Under the consideration of the requirement on delivery latency, the PDR can be boosted by 10% to 40% higher at an insignificant cost.

Except for V2X in DSRC, V2X communications in 5G cellular networks are becoming a spotlight, and more advanced services are enabled in the 5G networks. To support those services, cutting-edge techniques are employed in both physical layer and MAC layer of the 5G cellular V2X. Among those techniques, resource allocation is an essential part as it determines how effectively the limited resources are utilized.

In addition to studies carried in DSRC-based V2X networks, in the thesis, we also conduct research on 5G-V2X networks, focusing on dynamic resource allocation in mode 3 and developing three algorithms. The first one is based on random allocation as a benchmark method, in which resources are randomly and exclusively allocated to different users. The second one is based on location-aware resource allocation (LARA) strategy tries to reuse the spectrum according to vehicle's instant locations. To investigate their performances, we develop a network model for 5G V2X communications in urban areas, and then employ typical V2X services in the analysis. Simulation results reveal that the two algorithms for resource allocation, while able to eliminate or reduce interference at reception, cannot provide guaranteed services, especially for the enhanced V2X services. The third proposed algorithm is a self-adaptive fuzzy logic-based resource allocation strategy (named FUZZRA). In FUZZRA, multiple factors are considered, such as data rate, interference level and message priority. By comprehensively processing the factors, the FUZZRA can intelligently dedicate resources to vehicles and other devices. Compared with the two prior proposed schemes, the fuzzy approach can effectively improve the resource utilization and boost the network performance; thereby satisfying the stringent requirements of the services.

Attestation of Authorship

I hereby declare that this submission is my own work and that, to the best of my knowledge and belief, it contains no material previously published or written by another person (except where explicitly defined in the acknowledgements), nor material which to a substantial extent has been submitted for the award of any other degree or diploma of a university or other institution of higher learning.

Minglong Zhang

Signature

Date: 25-08-2020

Acknowledgement

I would like to express my most genuine gratitude to my primary supervisor Professor Peter Chong. He provided me with guidance, inspiration, and encouragement in my academic research in past years. His patience and perseverance in research, generous sharing with his experience and knowledge, as well as constructive suggestions impressed me so much in past years. Without his colossal help, I cannot complete my studies. I would also like to acknowledge very important assistance from my secondary supervisor Professor Boon-Chong Seet. He offered me a lot of helpful suggestions and discussions in my research, especially in revising papers, selecting research topics and so on.

Apart from the above, I would deeply appreciate indispensable work from my wife, who spent her most time on looking after our child and the whole family. I also would like to thank my four-year-old Christina, who accompanied me in Auckland over the past years. Finally, I give my sincere thanks to all staff of School of Engineering in AUT and other people who supported me in my study and life.

Table of Contents

List of Figures

List of Tables

List of Abbreviations

3GPP   Third Generation Partnership Project

5G   Fifth Generation

AIFS   Arbitrary Interframe Space

BPSK   Binary Phase Shift Keying

BS   Base Station

BSM   Basic Safety Message

CAM   Cooperative Awareness Message

CCH   Control Channel

COG   Centre of Gravity

CSMA/CA   Carrier-Sense Multiple Access with Collision Avoidance

C-V2X   Cellular Vehicle-to-Everything

CW   Contention Window

D2D   Device-to-Device

DCF   Distributed Coordination Function

DIFS   DCF Interframe Space

DSRC   Dedicated Short-Range Communication

EDCA   Enhanced Distributed Channel Access

eNB or eNodeB   evolved Node B

ETSI   European Telecommunications Standards Institution

eV2X   enhanced V2X

FCC   Federal Communication Commission

FL   Fuzzy Logic

GNSS   Global Navigation Satellite System

GPS   Global Positioning System

GSM   Global System for Mobile Communications

IPv6   Internet Protocol version 6

ITS   Intelligent Transportation System

LTE   Long-Term Evolution

MAC   Medium Access Control

MCS   Modulation and Coding Scheme

MUD   Multi-user Detection

NC   Network Coding

NLOS   Non-Line-Of-Sight

OBU   On-Board Unit

OFDM   Orthogonal Frequency-Division Multiplexing

OFDMA   Orthogonal Frequency Division Multiple Access

PDR   Packet Delivery Ratio

PHY   Physical Layer

PLNC   Packet-Level Network Coding

PNC   Physical layer Network Coding

PSCCH   Physical Sidelink Control Channel

PSSCH   Physical Sidelink Shared Channel

QPSK   Quadrature Phase Shift Keying

16-QAM   16 Quadrature Amplitude Modulation

64-QAM   64 Quadrature Amplitude Modulation

RB   Resource Block

RLNC   Random Linear Network Coding

RoI   Region of Interest

RSU   Roadside Unit

SC-FDMA   Single Carrier Frequency Division Multiple Access

SCI   Sidelink Control Information

SIFS   Short Interframe Space

SINR   Signal Interference Noise Ratio

SLNC   Symbol-Level Network Coding

SNR Signal Noise Ratio

SPS Semi-persistent Scheduling

STR Successful Transmission Ratio

SU-SIC Single User Successive Interference Cancellation

TCP Transmission Control Protocol

TDMA Time-Division Multiple Access

UDP User Datagram Protocol

UE User Equipment

UTMS Universal Mobile Telecommunications Systems

V2I Vehicle-to-Infrastructure

V2N Vehicle-to-Network

V2P Vehicle-to-Pedestrian

V2V Vehicle-to-Vehicle

V2X Vehicle-to-Everything

VANETs Vehicular Ad-hoc Networks

VUE Vehicular User Equipment

WAVE Wireless Access in Vehicular Environments

Chapter 1 Introduction

In this Chapter, we present the background information about services provided in the intelligent transportation system (ITS) and how vehicle-to-everything (V2X) communications supporting those services. Following the background, important technological advances in V2X communications are stated, and then research motivations, objectives and main contributions are described.

1.1 Background

1.1.1 Basics about V2X Communications

Over the past decades, propelled by the economic development and explosion of global population, demands of motor vehicles soared significantly. Vehicles have dominated land transportation and de facto became a necessity in most of daily circumstances. With the increasing concerns of environmental issues, the beginning of 21st century witnessed the revival of kinds of electrified vehicles and emergence of other vehicles driven by new energy sources, further enriching the automobile market. Especially in recent years, along with the progress in computation capability, wireless communication technologies and other related technologies, people's attention has been transferred from basic demands like speed and convenience to safety, comfort, autonomy and intelligence, while considering modern vehicles and transportation system. Among those objectives, road safety is highly prioritised. However, according to the World Health Organization (WHO) Report on road safety [1], road accidents result in deaths of approximately 1.3 million people over the world each year and leave more than 20 million people with non-fatal injuries. To reduce the risk of road crashes, an intelligent transportation system (ITS) that incorporates advanced technologies and management solutions was devised [2]. The ITS targets on creating an accident-free vehicular environment, enhancing the transportation efficiency, and providing on-board infotainment services at the same time. To achieve these goals, a series of services need to be supported. They include basic safety services [3] (e.g., collision prevention and hazard warning), enhanced safety services [4-5] (e.g., cooperative sensing, advanced driving and traffic efficiency) as well as infotainment [6-7] (e.g., multi-media streaming, advertisement and Internet surfing).

V2X communication is a key determinant in the framework of ITS [8]. The concept of V2X communications contains vehicle-to-vehicle (V2V), vehicle-to-infrastructure (V2I), vehicle-to-pedestrian (V2P), and vehicle-to-network (V2N) communications [9]. V2V communications expect vehicles that are in proximity of each other to directly exchange information, such as basic safety message (BSM) that include dynamics and status of vehicles, including current location, instantaneous speed, acceleration, direction and so on. V2I communications involve in vehicles transmitting data to a roadside unit (RSU), which is typically installed in fixed infrastructure such

as lamp posts or traffic lights, or obtain information (e.g., traffic information, warning messages, etc) from an RSU[1]. Vehicles supporting V2N communications are communicating with a server also supporting the V2N applications via the Evolved Packet System (EPS) [25]. Regarding V2P communications, it is to protect the vulnerable road users carrying portable devices like smart phones in some dangerous traffic situations. Nevertheless, both V2N and V2P communications are distinct from the other two cases due to the properties of devices. For instance, V2P has limited communication range and radio sensitivity because of lower battery capacity and antenna design.

Most of the services supported by V2X communications described above in ITS fall into two categories: safety-related services and non-safety-related ones. The purpose of the former is to assist drivers in improving consciousness of surrounding vehicles and potential dangers, thereby avoiding accidents in dangerous situations. In fact, most of the accidents are due to distracted driving or improper behaviours of the drivers, who also face to unknown hazards, such as the presence of vehicles in their blind zones, abrupt braking by the vehicles in front and so on. Without adequate knowledge of locations and status of vehicles in the vicinity, a driver cannot completely avoid accidents even if he or she drives a car in a precautionary way. To solve the problem, safety messages are broadcast in vehicular networks including vehicles, pedestrians and infrastructure. According to their distinctive functionalities, typical safety services include intersection collision avoidance, emergency call services (police, fire, ambulance), lane-change warning, and blind-zone assistance [11-12]. They can be further divided into two types: services with periodic transmissions and event-trigger applications. The first type is used to prevent accidents by periodically exchanging BSMs[2] (also known as safety beacons) or other safety information among neighbouring vehicles, whereas the second is for conveying emergency messages (e.g., traffic accidents and hazardous weather conditions) to vehicles in a specific geographical area. A BSM generated by each vehicle usually contains a vehicle's instantaneous status information, such as velocity, direction, acceleration, and position. These data are yielded by various sensors and Global Positioning System (GPS) rigged on each vehicle. A periodic exchange of BSM packets can create mutual awareness and alert drivers in time, thus avoiding road accidents. It is remarkable that safety beacons are massively generated at all times, but event-trigger information only originates from a few sources when urgent situations or events take place.

On the other hand, the non-safety services have drawn a great deal of attention as well by affording on-board infotainment and other personal or commercial services. Typically, these services may include audio-visual contents, Internet surfing, road navigation, on-board virtual conference

---

[1] Data sent from RSU to vehicle is also referred to I2V communications, which can be regarded as a special type of V2I communications.

[2] BSM is a term in the US standard [13], and it is also referred to as Cooperative Awareness Message (CAM) in the European standard [14].
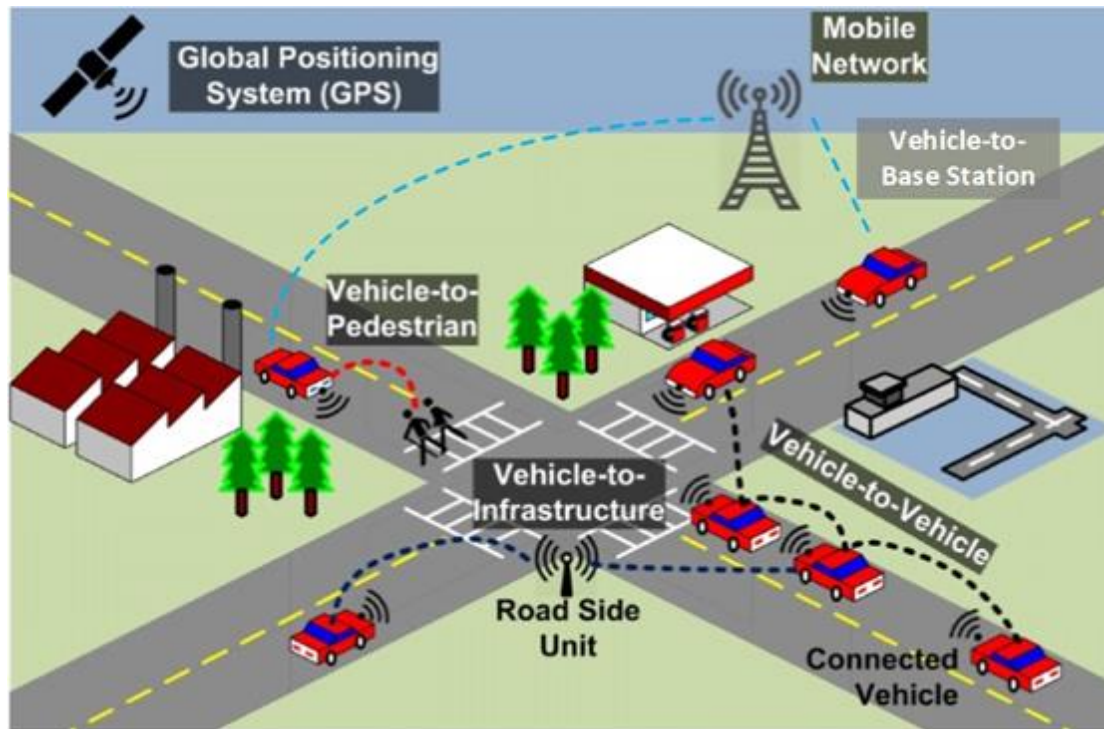
Fig. 1.1: Typical V2X communications in ITS [10].

and so on [3-8] [82-84]. The non-safety services can offer commercial information, entertain people who are travelling or commuting by vehicles like bus, and convey different types of useful information and social interactions via social medias, emails, and other on-line applications. These functions make them become a necessary part in ITS. In short, they can greatly enrich people's lives and provide convenience. However, the non-safety services generally have lower priority than the safety-related counterparts in many vehicular networks, according to the Third Generation Partnership Project (3GPP) standard [9].

Fig. 1.1 shows some typical V2X communications at an intersection in ITS. It includes V2V, V2P and V2I communications. Those different types of V2X communications can support various services. For instance, V2V communication can enable vehicles in proximity to be aware of each other, while V2I communications may enlarge the range of communications among vehicles by forwarding messages further. V2P communications can alert the drivers that pedestrians are approaching or crossing road, which can prevent accidents due to unawareness or aggressive driving.

Experts from both academia and industry have endeavoured to fulfil various functionalities envisioned in ITS by creating technologies for V2X communications, and two widely recognised technologies have been proposed. One specific technology is Dedicated Short Range Communication (DSRC) [15]. Technically, DSRC consists of a stack of protocols [13] [16]. The IEEE Standard 802.11p [17] is the basis to provide specifications for physical (PHY) layer and medium

access control (MAC) layer. Middle and high layers of DSRC are structured by the IEEE 1609 working group [18-21]. More details of these protocols will be elaborated in Chapter 2.

Since the debut of DSRC in the first decade of the 21st century, concerted efforts have been made by experts from both industry and academia. In 2002 the U.S. Department of Transportation (DOT) and a consortium of automakers started a collaboration in the study of DSRC-based collision prevention. The project VSC and CAMP [128], which were both supported by DOT, have demonstrated the feasibility of a few of V2V safety applications including forward collision warning, blind spot warning, control loss warning, hard-brake warning, intersection movement assist and so on. Meanwhile, numerous similar projects involved in DSRC have also been conducted all over the world. The CVIS [129] platform initiated by European Union can support multichannel terminals that enabled continuous Internet access, open communication architecture, enhanced positioning and commercial applications by adopting different radio interfaces including Global System for Mobile Communications (GSM), Universal Mobile Telecommunications Systems (UTMS) and DSRC. Similarly, the SAFESPOT [130] realised applications like accurate localization, dynamic local traffic maps and scenario-based evaluation of safety applications. Based on experimental data, the authors in [35] showed the characteristics of DSRC networks and analysed how typical factors affected the network performance. Researchers attempted to address discovered issues and improve the reliability and scalability for inter-vehicle communications by introducing new techniques, such adding congestion control [34] [40] [44], adopting repetitive transmissions [36], exploiting network coding [45-47] and so on.

Apart from DSRC, another technology is cellular V2X or C-V2X, which is based on long-term evolution (LTE) networks and fifth generation (5G) networks. The concept of C-V2X was firstly proposed as a part of cellular networks by 3GPP in 2016 in Release 14 [24-27], which established the foundation for communications to support 27 basic use cases [9]. Those basic use cases comprise basic safety and non-safety applications, such as collision warning, dynamic traffic control, which can warn drivers early in case of potential collisions or improve traffic efficiency. C-V2X has been evolving since the advent of 5G networks. In order to satisfy the requirements of advanced application from automotive industry, the latest Release 15 in 2019 has additionally defined four types of enhanced V2X (eV2X) services [28], including extended sensing, vehicle platooning, advanced driving and remote driving. Different from IEEE 802.11p, which only has one radio interface and applies carrier-sense multiple access with collision avoidance (CSMA/CA) at MAC layer and orthogonal frequency-division multiplexing (OFDM) at PHY layer, the 5G C-V2X contains two radio interfaces. One is cellular interface (called *uU*) that supports vehicle-to-infrastructure communications, while the other, known as PC5 interface, supports direct V2X (i.e.,

vehicle-to-vehicle and vehicle-to-RSU) communications (also known as sidelink communications) between vehicles and vehicles; and vehicles and other user equipment[3] (UEs).

In recent years, numerous projects and studies have been carried out in various respects of C-V2X. To show the performance of 5G C-V2X, the 5G Automotive Association (5GAA)[4] firstly launched a series of benchmark tests on BSM delivery [131]. The tests include congestion control, V2V message exchange in both line of sight (LOS) and non-line of sight (NLOS), as well as interference tests. The report confirms better performance of C-V2X than DSRC in key performance indices. In Europe, the 5GCAR project [133], supported by EU Commission, developed an overall 5G system architecture to provide optimized end-to-end V2X connectivity. It demonstrated a lane-merge coordination use case in France in 2019. A central planning system in the demonstration can recommend individual actions, including acceleration, deacceleration and lane changes, by collecting status information of connected vehicles. Meanwhile, researchers from institutes also performed important investigations to either promote the feasibility or provide more insights in C-V2X communications. Some studies were conducted for dedicated services in C-V2X. For instance, researchers have developed different strategies to match the latency and reliability demands of platooning applications in cooperative driving [115] [132]. There are also a number of works that contributed to the content dissemination. A case in point is a regional-centralized heterogeneous content dissemination scheme for 5G C-V2X using millimetre-wave communications [6]. The scheme can ensure a low-delay service in multimedia content dissemination. Advanced resource allocation and scheduling approaches were proposed to enhance the packet reception [50-51]. The work in [52] theoretically modelled the average PDR as a function of the distance between transmitter and receiver.

Vehicular networks running DSRC protocols are distributed networks, where mobile nodes contend for accessing channels. Such distributed networks are flexible and have lower management overhead. However, the ability of DSRC supporting reliable communications has been questioned by research that revealed its poor performance in scalability. In addition, due to its limited bandwidth, it is hard to meet the demands of high-speed communication for advanced safety applications and in-vehicle Internet access. Compared to DSRC, 5G C-V2X is promising to overcome those shortcomings and provide high data rate as well as large coverage V2X communications [31]. Although C-V2X seems to have more advantages than DSRC, it is not clear whether the cellular network can additionally accommodate V2X data traffic, especially in the background of

---

[3] To be more accurate, in 5G era, the concept of UE contains cellular user equipment, vehicular user equipment and other equipment involved in V2X communications, such as RSU.

[4] The 5GAA is a global, cross-industry organisation was founded by companies including AUDI AG, BMW Group, Daimler AG, Ericsson, Huawei, Intel, Nokia, and Qualcomm Incorporated in 2016. Its main role is to help develop, test, and promote 5G standards.

explosive increase of data traffic from its existing cellular users. Therefore, a potential hybrid architecture where DSRC and cellular are interworking has also been considered [32-33].

In the coming era of ITS, traditionally mechanical vehicles will be transformed to moving smart nodes that are equipped with diverse sensors and transceivers, by which colossal amount of data are generated, transmitted and received. The various functionalities envisioned in ITS can satisfy people's increasing needs on safe, comfortable and convenient travelling. Nevertheless, it is still full of technological challenges. On the one hand, constantly changing wireless channels, highly dynamic network topology and widely ranging traffic density are critical tests of network's performance, scalability, and robustness. On the other hand, many safety applications like BSM have stringent requirements on reliability and latency. The challenges impose considerable difficulty on system design, especially on protocols and schemes in PHY layer and MAC layer. To fight against the adversities and meet the requirements, this study strives for betterment of the MAC protocol in the framework of DSRC, optimization of parameters of the MAC protocol to boost the network performance and effective resource allocation for 5G cellular V2X communications.

1.1.2 Seminal V2X Cases in Industries

Due to the fast development of V2X technologies in past decade and imperative of improving road safety, some organizations have pioneered to deploy V2X in ITS. As a global leader with V2X solutions, Cohda Wireless provides various V2X products including both OBU and RSU, which has the potential to eliminate or mitigate up to 80% of non-impaired-driving collisions [137]. Cohda's products are widely being deployed or being tested in different scenarios. For example, in a trail of autonomous platooning in Australia's newest motor-racing circuit, tests confirmed Cohda's platooning solution can deliver impressive gap management of 5 metre + 0.4 seconds at 95 KM/h by utilizing inter-vehicle communications [138]. In Germany, DIGINET-PS that is funded by the German Federal Ministry of Transport and Digital Infrastructure has been developed to test automated and connected driving under real-life conditions in the centre of Berlin. In the test field, V2X-locate technology, as an important application in V2X services, enables accurate positioning of vehicles in environments where Global Navigation Satellite System (GNSS) performs poorly such as urban tunnels and underground car-parks [139]. Another remarkable large-scale deployment of V2X is the New York city connected vehicle pilot, which is a milestone development in the adoption of connected vehicle technology around the world [140]. The New York pilot encompasses three distinct areas and comprises of over 3000 vehicles consisting of cars, buses, and fleet vehicles. Its goal is to reduce the number of fatalities and injuries resulting from traffic accidents through the deployment of connected vehicle technologies that allow vehicles to 'speak to each other,' extending their perception horizon far beyond that of human capability. The NYC deployment is primarily focused on safety applications – which rely on vehicle-to-vehicle (V2V), vehicle-to-infrastructure (V2I) and infrastructure-to-pedestrian

(IVP) communications. About 14 applications have been developed and these applications provide drivers with alerts so that the driver can take action to avoid a crash or reduce the severity of injuries or damage to vehicles and infrastructure.

1.2 Research Motivations

This section presents our motivations of the conducted studies pertaining to effective safety message dissemination in V2X communications. Three projects constitute the entire study. The motivation of each project is described below.

1.2.1 Unreliability of BSM Dissemination in DSRC-Based V2X

With the dramatic growth of global traffic accidents in past decades, road safety issue has become a cause of great concern in daily life. According to the Global Status Report on Road Safety [1] from WHO, road traffic crashes have led to approximate 1.35 million deaths, numerous injuries, and huge number of property loss. Many factors contribute to vehicle accidents, most of which are due to distracted or improperly behaved drivers, who also have to face potential hazards at the same time, such as the presence of vehicles in their blind zones, abrupt braking by the vehicles in front, and so on.

The proposal of ITS was expected to create an accident-free transportation. In recent years, the advent of vehicular ad-hoc networks (VANETs) fulfilled various functionalities in ITS. One typical and foremost application in ITS is to reduce the risk of road accidents by providing a series of safety-related services, such as collision prevention and hazard warning, etc. The DSRC aimed to realize such safety applications, which can be divided into two categories: periodic and event-trigger application. The former is used to prevent accident by periodically broadcasting basic safety message (BSM, also known as safety beacon) to neighbouring vehicles, while the latter is for disseminating event-trigger messages (e.g., traffic accidents and hazardous weather condition) to vehicles in a specific geographical area. A BSM generated by each vehicle usually contains a vehicle's current status information, such as velocity, direction, acceleration, and position. A periodic exchange of BSM packets can create mutual awareness in surrounding environment, thus avoiding potential accidents.

In DSRC, vehicles access channels and broadcast BSMs via a mechanism called carrier-sense multiple access with collision avoidance (CSMA/CA). However, this mechanism only works effectively in very sparse networks (e.g., less than 10 vehicles in a vehicular network) [34]. With the increase of traffic density, transmission collisions abound and result in a poor service for safety message delivery. Unlike other unicast communications, there is no retransmission on the occasion of loss of BSMs. Thus, such unreliability is unacceptable for many periodic applications. Meanwhile, BSM packets delivery ratio (PDR) is worsened by 1) highly dynamic topology; and 2) fading channels caused by buildings, bridges and other large objects on road [35]. Moreover,

another challenge comes from the stringent requirement on rather low delivery latency. Being distinct from the event-trigger messages, BSMs need to be rapidly disseminated to all vehicles in the proximity within the lifetime, i.e., 100 milliseconds in DSRC.

Towards tackling the issues of BSM broadcasting in vehicular networks based on DSRC, relevant studies have been carried out, and most of them either attempted to design completely new MAC protocols or enhance the originally CSMA/CA-based MAC protocol. Among all those studies, there are mainly three sorts of strategies proposed by researchers so far, with respects to their attributes. The first type is to replace the original MAC (i.e., IEEE 802.11p) and adopt a new distributed MAC protocol, in which each safety message is broadcast repeatedly in several times [36-37]. Although such approaches can undoubtedly improve the PDR to some extent, they still do not perform well in moderate and dense networks as the collisions caused by repetitive transmissions rise exponentially. To alleviate the adverse effect of lossy channels, network coding (NC) [38] or random linear network coding (RLNC) [39] are employed. However, packet loss rate is still too high to be accepted in dense networks due to the essence of its distributed manner that vehicles still face contentions for medium access and transmission collisions rise. Based on the observation, the second type is centralized MAC protocols that employ time-division multiple access (TDMA) have been proposed to eliminate transmission collisions [40-42]. The flaw of such centralized schemes is that some nodes need to work on coordination for transmissions, which inevitably incur large delay or occupy extra spectrum resources. The third type relates to hybrid MAC. However, they are either more suitable for non-safety message dissemination [47] or far from feasible [93] [104].

Predicated on the above observations, the work in Chapter 3 proposes a hybrid MAC protocol that contains both distributed session and centralized session. It not only effectively suppresses the transmission collisions but possesses compatibility with IEEE 802.11p and good robustness in dense networks.

1.2.2 Performance Analysis and Optimization Problems in the Proposed MAC

Driving safety became a spotlight in recent years, as traffic accidents rose sharply all over the world during past years. Meanwhile, new technologies emerged to prevent road crashes. The advent of vehicular ad hoc networks brought a solution to tackle this issue. As a realization, DSRC was proposed to support a variety of safety applications in VANETs. In DSRC, each vehicle broadcasts its basic safety message periodically to its neighbours. Vehicles that receive those BSM packets can build a neighbourhood map, which could assist drivers in avoiding accidents, since a BSM usually contains a vehicle's instant information, such as velocity, moving direction, and position. However, due to transmission collisions, non-retransmission mechanism and fading

channels, most of vehicular networks suffer a high packet loss rate and a large delivery latency, which are intolerable of many safety applications.

To cope with low reception ratio of BSM in vehicular networks, various methods have been proposed and applied in vehicular networks. To reduce reception failure, vehicles repeatedly broadcast every safety message more than one time during one control channel (CCH) interval in a so-called repetitive transmission scheme [36] in which the repetition times can be adjusted. However, it also increases the probability of simultaneous transmissions. To reduce the transmission collisions, one method is to use a positive orthogonal code [37] or a protocol sequence [43] in transmission scheme, and the other is to lower transmission frequency when the number of detected collisions rises. The authors in [44] attempted to reduce the congestion by dropping certain packets containing redundant or derivable information. Random linear network coding was applied to enlarge the packet reception probability [45-46]. These approaches only perform effectively in sparse networks. The packet delivery rate plummets in dense networks as vehicles still need to contend for accessing channels in those distributed schemes. Furthermore, although centralized MAC protocols seem to be able to eradicate transmission collisions, attempts of applying TDMA-based schemes cannot be deemed as success, because they may lead to a large delay that is unacceptable for BSM delivery.

Recently, researchers developed hybrid MAC protocols that contain both centralized and distributed manners for VAENTs. K. Liu *et. al* [47] presented a network coding assisted scheduling algorithm to disseminate data via V2X communication, but it mainly targets on non-safety applications. The proposed MAC (called NC-PNC MAC) protocol elaborated in Chapter 3 provides a more effective solution, compared with all previous counterparts. It not only exploits joint effect of V2V and V2I communication, but also integrates RLNC and physical-layer network coding (PNC) [62] for safety message dissemination. The protocol outstrips its counterparts in packet delivery ratio (PDR) without causing too much delay for both sparse and dense networks.

However, interesting but challenging questions appears while considering the proposed NC-PNC MAC in depth. At first, it lacks theoretical examination of the MAC. Even though some analytical models, such as Markov chain, have been used to evaluate the network performance in [48] and [49], they are only appropriate for the MAC of DSRC (i.e., IEEE 802.11p). Furthermore, the models opined in the aforementioned works [36-37] [43-46] to analyse the corresponding protocols are evidently apt to either distributed protocols or centralized ones. The analysis in hybrid protocols [47] is not applicable NC-PNC MAC as well, as it does not include PNC in the model. Therefore, to validate the claimed performance and provide more insights on our proposed NC-PNC MAC, it is nontrivial to perform a theoretical analysis on the NC-PNC MAC. Moreover, can the PDR performance of NC-PNC MAC be further improved? Which factor(s) affect(s) its

performance and how to enhance it at the minimum cost? These questions motivate us to carry out a deeper study on the MAC and offer more knowledge for deploying vehicular networks.

1.2.3 Research Gap for Dynamic Resource Allocation for 5G V2X in Mode 3

C-V2X communications in 5G are conducted via the PC5 interface, which is independent on the *uU* interface supporting uplink and downlink communications with base station. As pointed out in the above, only mode 3 or mode 4 is used for the safety-related applications due to their stringent requirements. The difference between mode 3 and mode 4 lies at how the resource allocation and transmission scheduling are managed. Although the mode 3 allows diverse UEs either to select resources by themselves (like the working mechanism in mode 4) or to be assisted by the eNodeB in mode 3, the latter is more preferable in most of the situations because it is promising to provide a more effective resource allocation within the coverage of the eNodeB.

The sidelink communications [5] adopt single-carrier frequency division multiple access (SC-FDMA) with channel of 10 MHz or 20 MHz in bandwidth. At the physical layer, time is segmented into subframes with the length of one millisecond, while the frequency spectrum is divided into subchannels consisting of a number of resource blocks (RBs). An RB is the minimum unit that can be managed and allocated. In addition, data are transmitted over the physical sidelink shared channel (PSSCH), and the sidelink control information (SCI) that indicates modulation and coding scheme (MCS) is transmitted over the physical sidelink control channel (PSCCH).

Much attention has been paid on 5G C-V2X communications in recent years. The authors in [30] compared features among four different work modes and concluded that vehicles working in mode 1 and 2 may incur large latency. Based on mode 4, the project in [50] studied link-level packet reception ratio and the study in [51] designed a novel scheduling mechanism for eV2X services. In addition, with the application of the standardised semi-persistent scheduling (SPS), analytical models were built to analyse the performance in mode 4 [52-53]. Apparently, none of the above analysed the C-V2X performance in mode 3, in which the transmission scheduling and resource allocation of all V2X communications are controlled by an eNodeB.

Resource allocation is an indispensable element in C-V2X networks as it has a tremendous impact on the network performance. Schemes of resource allocation were studied in [54] and [55], but they are either for uplink or downlink communications in the LTE cellular networks. In fact, a few of studies about dedicating spectrum resources have been conducted previously. For example, the authors in [56-58] proposed different resource allocation schemes to minimize co-channel interference between device-to-device (D2D) communications and uplink/downlink communications. Nevertheless, such schemes do not work for 5G V2X communications that use separate

---

[5] Interchangeable term for C-V2X communications in 5G

frequency band with the uplink/downlink links. An autonomous reuse partitioning scheme described in [59] tried to reuse channels among different base stations, but it is far from V2X communications as the base stations have static positions. The subcarriers allocation scheme in work [60], though with lower complexity, does not allow to reuse the subcarriers among different users for the OFDMA system. The objective of resource optimization in paper [61] relies on the connections between Fog Computing-Zone Controllers and Fog Computing BBU Controllers in 5G VANETs rather than resource blocks (RBs) in PHY layer.

From above discussions, on the one hand, all prior studies in 5G C-V2X emphasized on analysing either link-level performance or a partial cellular network in mode 4. On the other hand, regarding how to allocate resources of physical layer, previous algorithms in LTE D2D communications cannot be directly applied in 5G C-V2X. Moreover, unlike mode 4, 3GPP does not specify how to reserve resources for UEs in mode 3. Apparently, there is a research gap in resource allocation in C-V2X communications, especially for mode 3. For instance, can C-V2X communications meet the stringent requirements including latency and reliability specified in the standard, especially in urban areas with dense vehicles? Which algorithm is competent to allocate resources properly in mode 3 and how about the performance of an entire cellular network if the algorithm is adopted? Moreover, it is also worth studying how resource allocation affects network performance. Unfortunately, answers to these questions are still unknown and prior studies cannot respond to them. Motivated by these research incentives, we work on analysing network performance of a 5G network for C-V2X and propose a fuzzy logic-based strategy for resource allocation to boost resource utilization.

1.3 Research Objectives

In this thesis, we chiefly study information dissemination via V2V and V2I communications. Since the safety-related services are the foremost parts in ITS as well as the unsolved issues in V2X communications pointed in the above section, the objectives of this thesis concentrate on how to effectively disseminate safety messages. Three main research objectives of this thesis are described as follows.

- The BSM reception rate needs to be improved, especially in dense networks. To ensure drivers having enough time to take measure in case of danger, the interchange of BSMs among vehicles should be done in a large area and completed within BSM's lifetime (i.e., 100 ms in DSRC). To reach such goals, we first propose a novel MAC protocol based on DSRC. In addition, the compatibility of our proposed MAC with the IEEE 802.11p is also noteworthy as legacy users of DSRC may also exist at the same time.

- Taking into account the deployment of our proposed MAC, mathematically modelling the new MAC can provide more insights while adopting the MAC in the vehicular

networks. Based on the analysis, the thesis will explore how to optimize the protocol in order to enhance the overall performances.

- Regarding the C-V2X communications in 5G networks, we will endeavour to satisfy the stringent requirements on the latency and the reliability. To this aim, various strategies of allocating physical resource blocks and time resources to different vehicles will be studied as resource allocation is the main determinant of the network performance. Moreover, different types of services, including both safety and non-safety services, are considered in the research.

1.4 Main Contributions

As motivated by the discovered problems existing in V2X communications presented in Section 1.2 and the objectives defined in Section 1.3, studies have been conducted to grapple with those problems. The following parts summarise the main contributions made in this thesis.

1. In Chapter 3, in order to improve the reliability and the efficiency for BSM dissemination in V2X networks, we propose a hybrid MAC protocol based on the framework of DSRC. The hybrid MAC is partially centralized and partially distributed. It not only effectively suppresses the transmission collisions, but also shows compatibility with IEEE 802.11p and good robustness of PDR performance in dense networks. The main contributions of this study include:

- A novel MAC protocol is proposed for BSM broadcast. It consists of two centralized sessions and one distributed session. The BSM broadcasting, which is coordinated by an RSU mainly takes place in a centralized contention-free session, while a distributed session is reserved for legacy vehicles only supporting IEEE 802.11p and other ineligible nodes to transmit their BSMs via CSMA/CA.

- It integrates PNC and random linear network coding (RLNC) to exchange BSMs efficiently and reliably. It can be widely adopted because both roadway and intersection scenarios have been considered.

- A system model is built, and comprehensive simulations are conducted to evaluate the performances of the proposed protocol, and its communication complexity is also analysed.

2. Chapter 4 is a continuation of study based on Chapter 3. It firstly mathematically analyses the hybrid MAC protocol, and then enhances the performance based on the analytical results. The main contributions of this study include:

- A mathematical model is developed to analyse the subcarrier collision probability in an OFDMA session, the total number of transmissions of the MAC as well as the PDR performance of the network.

- We identify the factors that influence the PDR performance and investigate how they affect the BSM dissemination in V2X networks.

- With the consideration of time constraints, one strategy to improve PDR is to tune the parameters of the protocol. The PDR performance can be improved by 10% to 30% as compared to the previous one (in Chapter 3) with insignificant costs (i.e., only by selecting proper parameters rather than increasing transmission power, etc).

- Based on the observation from simulations, another strategy for performance enhancement is proposed other than adjusting the parameters. One or two pairs of auxiliary relay nodes are identified and designated by the RSU. The auxiliary relay nodes can significantly boost the PDR by applying RLNC as well as leveraging the idle remaining time which is at the end of each transmission period.

3. In Chapter 5, we evaluate the performance of an entire cellular network in urban areas and attempt to shed light on how resource allocation influences the overall network performance in C-V2X networks. For V2X communications in mode 3, three distinct algorithms of resource allocation (RA), including a random selection one, a location-aware one and a fuzzy-logic based one have been proposed.

- Random Selection RA: A simple resource allocation scheme is derived at first as a benchmark for comparison. The two-dimensional frequency-time resources are randomly assigned for each request from vehicles.

- Location-aware RA: In this algorithm, the base stations utilize the instantaneous location information of vehicles. To boost the resource utilization, the BS may allocate the same resources to different transmitters, according to their locations and service types (unicast or broadcast services).

- Self-adaptive fuzzy-logic based RA: In the algorithm, multiple factors, such as interference level, service priority and half-duplex radio, are input variables to the fuzzy system that tries to allocate the optimal resources for each transmission of vehicles.

- A complete network-level simulation model is built based on the NS-3 [63] based on the traffic and road model from SUMO [64] to simulate various V2X services. The network performance is analysed and compared among the above 3 resource allocation schemes.

1.5 Thesis Organization

The remainder of this thesis is organized as follows. Chapter 2 reviews the basic knowledge and technologies of DSRC V2X as well as 5G cellular V2X, the fundamental concepts of random linear network coding and physical-layer network coding, and other related works of V2X communications for safety-related services. Chapter 3 presents a novel hybrid MAC protocol (named NC-PNC MAC) for basic safety message broadcast based on the framework of DSRC. Chapter 4

Chapter 1: Introduction
Background, Research Motivations, Research Objectives and Contributions

Chapter 2: Fundamental Concepts and Literature Review
DSRC, C-V2X in 5G, Network Coding, Fuzzy Logic Theory and Related Works in V2X for Safety Message Dissemination

Main Contributions

Chapter 3: A Hybrid MAC Protocol for BSM Dissemination
System Model, Protocol Design (NC-PNC MAC), and Simulations

Chapter 4: Performance Analysis and Enhancement for the NC-PNC MAC
Analytical Model, Two Strategies for Performance Boost

Chapter 5: A Fuzzy Logic Based Resource Allocation for 5G V2X
Algorithm Design and Performance Evaluation

Chapter 6: Conclusions and Future Work

Fig. 1.2: Organizations and relationships of chapters in the thesis.

builds a mathematical model to analyse the communication complexity and PDR performance of the NC-PNC MAC. It also figures out how to boost the network performance in two different ways: configuring the MAC mechanism by assigning appropriate parameters or resorting to adding extra relay nodes. Chapter 5 studies various resource allocation algorithms and compares their performance in 5G C-V2X networks. An efficient fuzzy-logic based approach resource allocation algorithm is proposed to allocate PHY resources. The proposed allocation method can maximise the utilization of RBs and make sure the quality of service. Chapter 6 concludes the thesis with some directions for future research.

To be more evident, a flow chart depicting the relationships among those chapters is provided in Fig. 1.2. Chapter 1 introduces background knowledge of V2X communications, research motivations and main contributions, while Chapter 2 reviews related works done previously and discusses fundamental theories. The main technological contents are concentrated in Chapter 3, 4 and 5. The chief contents and features of each chapter are included as well in the figure.

1.6 Summary

In this chapter, we first introduce the background of the emergence of ITS and typical services provided in ITS and their corresponding features. To realise the ITS, the concept of V2X communications was proposed. Key technologies and important research activities for V2X communications are described. Based on the observations and discussions of prior studies, research motivations of the thesis are stated, and the corresponding research objectives and contributions are presented.

Chapter 2 Fundamental Concepts and Literature Review

In this Chapter, fundamental concepts that are intimately bound up with the innovations made in the thesis will be presented. The underlying knowledge includes characteristics of two V2X technologies (DSRC and C-V2X), random linear network coding, physical layer network coding and fuzzy logic theory. Following this, the relevant state-of-the-art studies will then be discussed.

2.1 V2X Network Architecture

More and more vehicles are connected to the Internet or each other through the V2X communication and networks, changing the automotive industry and the transportation system. Being embedded by computing and radio devices into cars, roads, streets, and transit equipment (such as street signs, radars, traffic cameras, and others), vehicles are able to autonomously exchange data with other vehicles (V2V communications), with the network infrastructure (V2I communications), with pedestrians (V2P communications), and so forth. Data is processed and translated into useful information and recommendations to assist users of the transportation system and transit authorities. Such sophisticated communication network is commonly referred to as vehicular network. Vehicular networks connect vehicles to provide a platform for the future deployment of large-scale and highly mobile applications, such as safety applications in ITS described in the first Chapter.

The underlying system architecture of the vehicular network is shown in Fig 2.1. The architecture model mainly comprises four components: In-vehicle domain, ad hoc domain, infrastructure domain, and service domain. The in-vehicle domain contains transceiver modules with radio frequency antenna for each communication interface to enable interactions with different wireless access technologies such as DSRC, Wi-Fi, and 4G/5G. It is also responsible for reliable data transmission, security, IP mobility, and other essential features via OBU. The ad hoc domain is a special class of Mobile Ad-hoc Network (MANET), where the wireless network is created spontaneously for inter-vehicle communications. The two main components are vehicle and RSU. The inter-vehicle communications can be one hop or multi-hop. The presence of RSUs can extend the range of communication by forwarding the messages to other vehicles or serves as a hotspot for Internet access. The infrastructure domain includes the roadside wireless infrastructure and the backbone wired network with middleboxes. The roadside wireless infrastructure can be RSUs (DSRC), Base Stations (eNB) or other smart infrastructure. The wired network infrastructure components can be access switches, routers, open flow switches and controllers (in case of Software Defined Network), edge nodes, fog nodes, and gateways. The service domain is the top layer of the architecture that provides services to the vehicles using the infrastructure domain via V2I/I2V connectivity. They are divided into two main classes: traffic-related services and generic services.
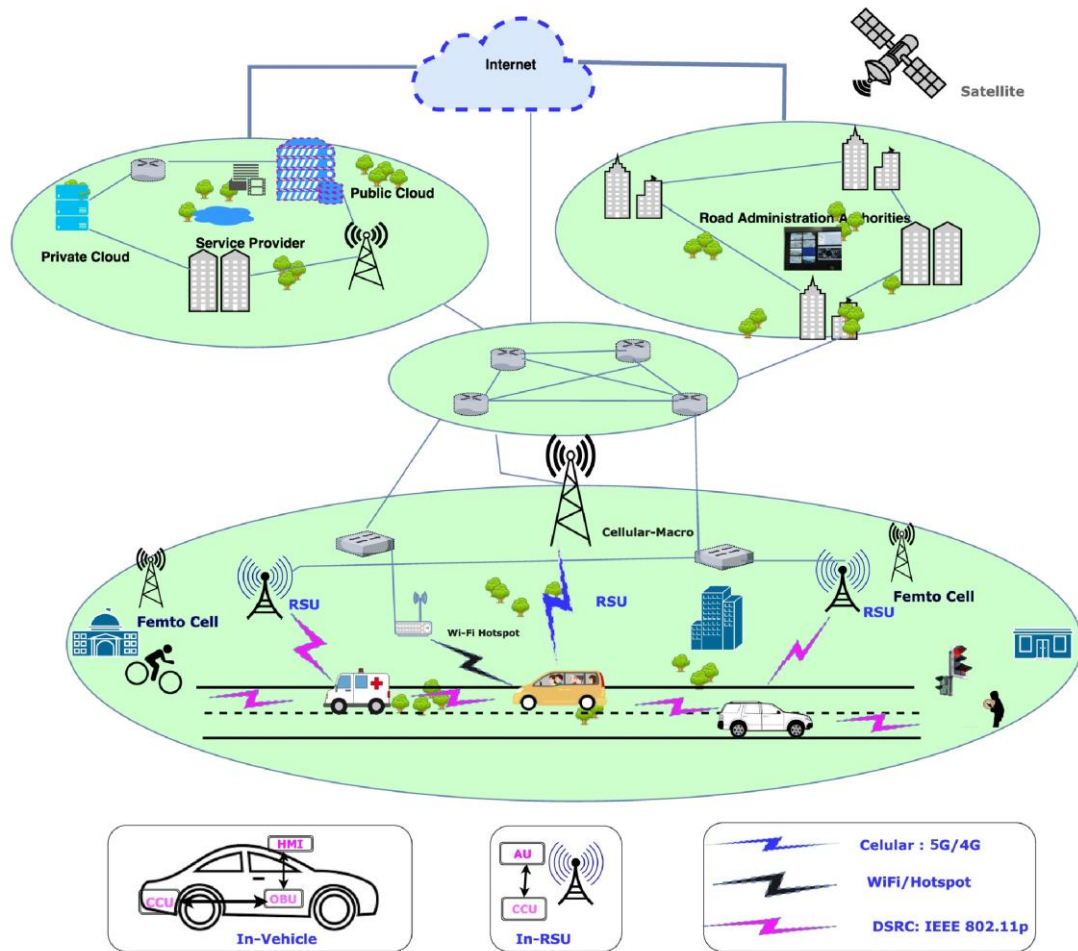
Fig. 2.1: Vehicular network architecture [141].

To support communications in vehicular networks, different standards and protocols are developed by different standardization bodies including the Institute of Electrical and Electronics Engineers (IEEE) in North America, the European Telecommunications Standards Institute (ETSI) in Europe, and the Association of Radio Industries and Businesses (ARIB) in Japan. Those standards are different in operating spectrum band and the supported applications, etc. Fig 2.2 overviews the stacks of protocols by comparing with the famous Open System Interconnection (OSI) reference model.
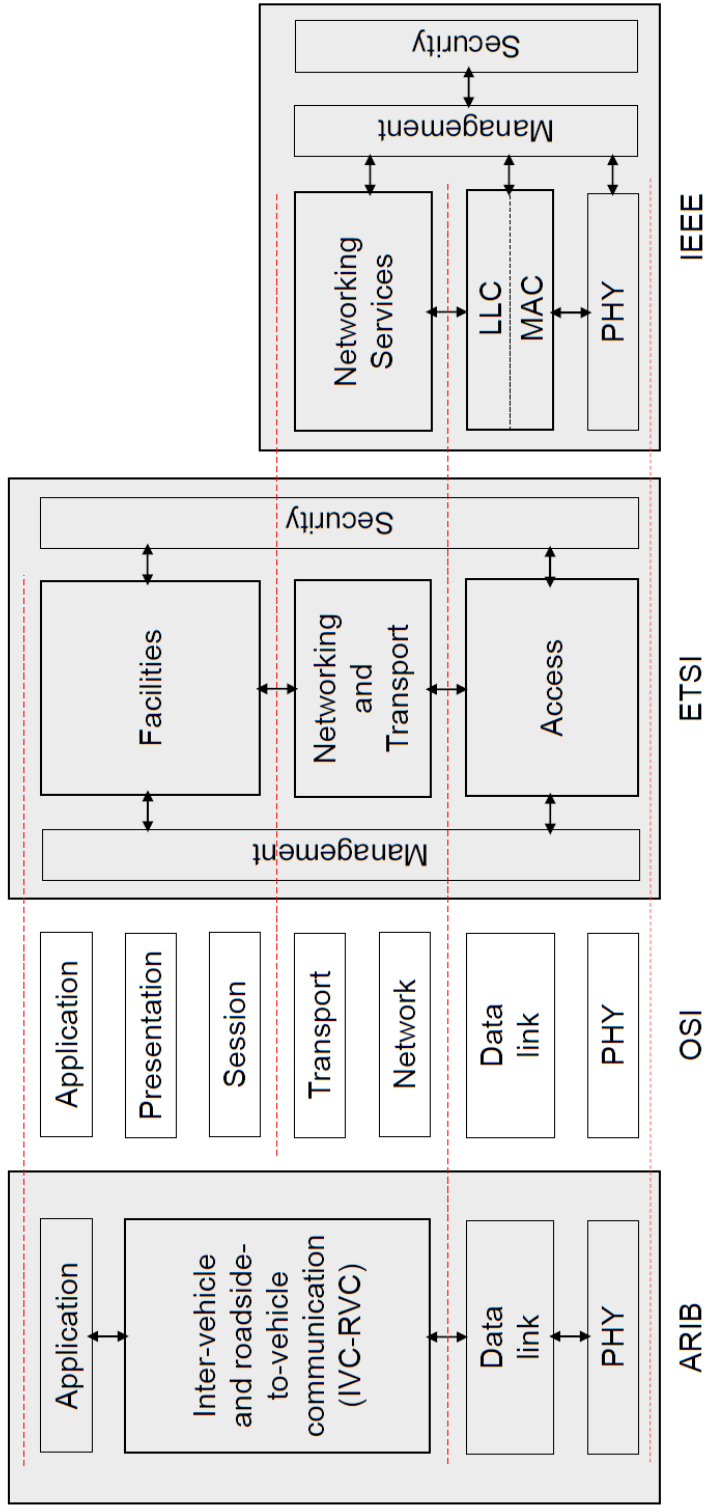
Fig. 2.2: Vehicular network protocols as defined in the standards IEEE 1609.0 (North America), ETSI EN 302 665 (Europe), and ARIB STD-T109 (Japan), in comparison with the Open System Interconnection (OSI) reference model [32].

2.2 Specifications for V2X Technologies

This subsection succinctly describes the key features and specifications of two standardised V2X technologies: DSRC and C-V2X in 5G, which are the basis of the V2X technologies used for our research in this thesis. Table 2.1 lists all notations included in Chapter 2.

Table 2.1: List of Notations in Chapter 2

Notations	Description
P_x	A packet sent by node/vehicle x
$\tilde{A}$ / $\mu_{\tilde{A}}(x)$	A fuzzy set / The membership function of x in fuzzy set $\tilde{A}$
COG(A)	The *centre of gravity* of A
w	The number of time slots
L	The total number of time slots during a period

2.2.1 Dedicated Short-Range Communications

As illustrated in Fig. 2.3 (a), DSRC consists of a stack of protocols [13] and [16]. DSRC adopts IEEE 802.11p [17], a modified version of the well-known IEEE 802.11 (WiFi) standard, as its PHY and MAC layers. Middle layers are structured by IEEE 1609 working group [18-21]. Specifically, IEEE 1609.4 is utilized for MAC sublayer extension with functions including channel switching. IEEE 1609.3 takes care of the network and transport layer, while IEEE 1609.2 is for security services. There are two options at Network and Transport Layers. One is famous Internet protocols for the Network and Transport layers, i.e., Internet Protocol version 6 (IPv6), User Datagram Protocol (UDP) and Transmission Control Protocol (TCP). The other is Wireless Access in Vehicular Environments (WAVE) short message protocol (WSMP). The choice of using whether WSMP or IPv6+/UDP/TCP depends on the requirements of a given application. Single-hop messages, such as BSM, typically use the bandwidth-efficient WSMP, while multi-hop disseminations prefer to use IPv6 due to its routing capability. At the top, SAE J2735 Message Dictionary standard supports a variety of safety applications [65]. The most important of these applications is the BSM, while SAEJ2945.1 specifies performance requirements. In short, the IEEE 1609 family of standards defines the architecture, communications model, management structure, security mechanisms and physical access for WAVE [22-23].

Regarding the spectrum used in DSRC, DSRC operates at 5.9 GHz (from 5.850 GHz to 5.925 GHz) and the spectrum is divided into seven sub channels of 10 MHz bandwidth with a 5 MHz guard band; consisting of six service channels (SCH) and one control channel (CCH), as shown in Fig. 2.3 (b). Channel 172 and Channel 184 are reserved for advanced safety applications and
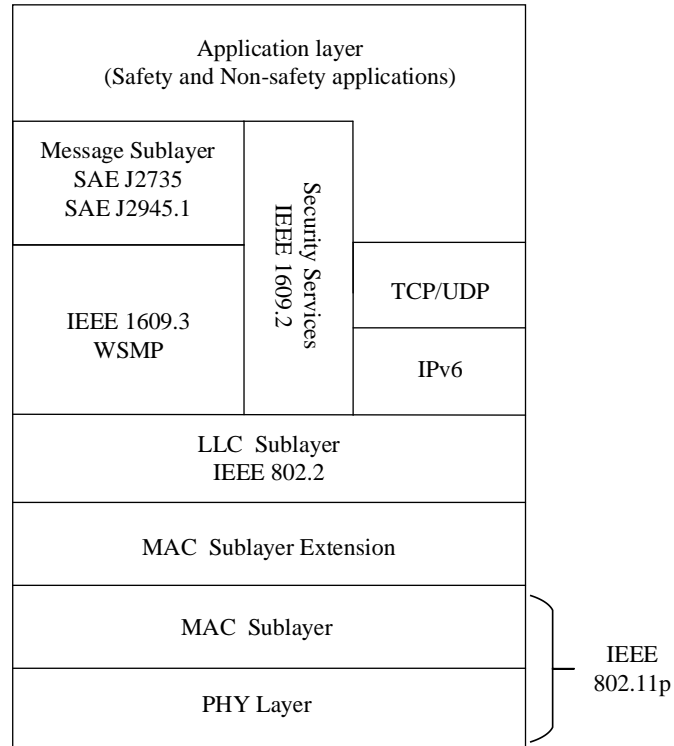
(a)
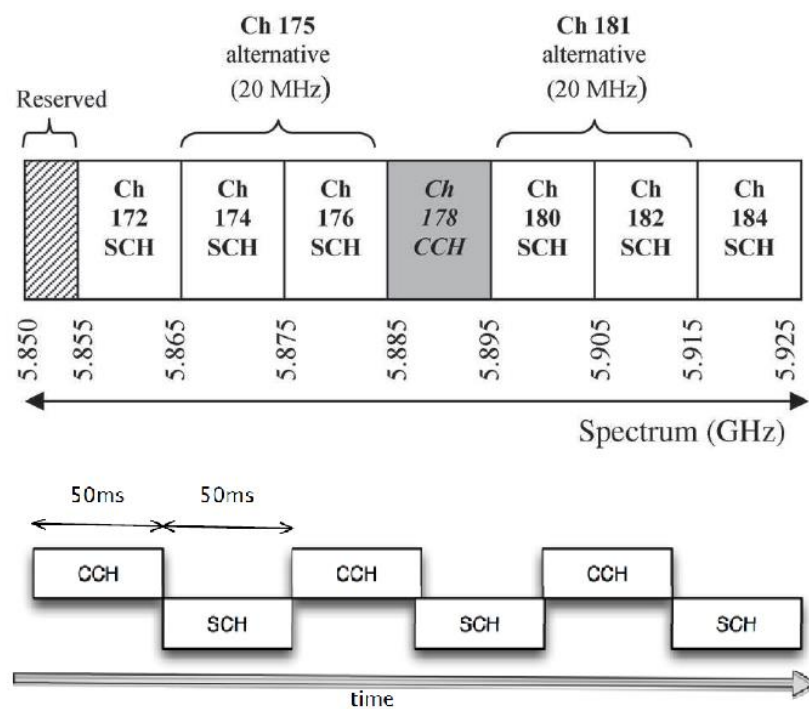
(b)

Fig. 2.3: (a) Stack of protocols in DSRC; (b) Channel division and switching [13].

high-power public safety usages [66]. Some studies shift the safety message communication to Channel 172 for multi-channel uses [13]. For generality, this work only considers vehicles equipped with a single radio. Therefore, BSM packets are usually broadcast during the CCH interval using CCH, Channel 178. The radio devices can work in a switching mode, in which they switch between CCH and SCH every 50 ms. Since the DSRC devices should be in the same channel to communicate, the channel switching for all devices is synchronized. The synchronization mechanism is described in IEEE 1609.4 standard [67]. Besides periodic switching mode, they can also work in a continuous mode, in which the channel is fixed during certain of time until being alternated [68].

Table 2.2: Basic Parameters for DSRC 10 MHz OFDM Channel.

Parameter	Value
Number of data subcarrier	48
Number of Pilot subcarrier	4
Total number of subcarriers	52
Subcarrier band width	156.25 KHz
Guard interval (GI)	1.6 us
Symbol interval (including GI)	8 us

Table 2.3: Supported data rates in DSRC 10MHz OFDM Channel.

Modulation	Coded Bit Rate (Mbps)	Coding Rate	Data Rate (Mbps)
BPSK	6	1/2	3
BPSK	6	3/4	4.5
QPSK	12	1/2	6
QPSK	12	3/4	9
16-QAM	24	1/2	12
16-QAM	24	3/4	18
64-QAM	36	1/2	24
64-QAM	36	3/4	27

At the physical layer, DSRC utilizes the orthogonal frequency division multiplexing (OFDM) to support low-latency delivery of messages to vehicles. The basic parameters of the 10 MHz OFDM

channel are shown in Table 2.2. There are four modulation schemes are available for adoption, including binary phase shift keying (BPSK), quadrature phase shift keying (QPSK), 16 quadrature amplitude modulation (16-QAM), and 64 quadrature amplitude modulation (64-QAM). In addition, channel coding is also employed to correct errors in decoding process. With different combinations of coding rate and modulation, the supported data rate in DSRC is from 3 Mbps to 27 Mbps as listed in Table 2.3.

For the MAC layer, the enhanced distributed channel access (EDCA) is adopted. The EDCA merges the carrier sensing multiple access with collision avoidance (CSMA/CA) and the slotted binary exponential backoff mechanism, which are well-known in IEEE 802.11 [101]. Since this study mainly focuses on the lower 2 layers and the higher layers, like TCP/IP protocol, are well documented in other places [134], the higher layers are not further discussed here.

2.2.2 Cellular V2X in 5G

At the physical layer, C-V2X in 5G adopts single-carrier frequency-division multiple access (SC-FDMA) and supports 20 MHz or 10 MHz channel width at 5.9 GHz band. A channel is divided into subframes in time dimension and subchannels in frequency dimension. A subchannel comprises multiple consecutive resource blocks (RBs) in the same subframe. Each RB has180 KHz wide in frequency that is made of 12 subcarriers of 15 KHz each. One RB is the smallest unit of frequency resources that can be assigned to vehicles. The number of RBs in a subchannel can vary, and it is set up by the size of data to be transmitted. Fig. 2.4 shows the structure of two-dimensional time-frequency pool.

Since each vehicle has two radio interfaces (*uU* and *PC5*, aforementioned in Chapter 1)*,* a vehicle can communicate with eNodeB via conventional uplink/downlink, or it can exchange data with other vehicles, RSUs and devices via sidelink.

Whenever a vehicle transmits a data packet via sidelink, also known as a transport block (TB), the corresponding sidelink control information (SCI) must be transmitted at the same time. The SCI includes information such as MCS used in the associated TB, the RBs being used by the UE and so on. Therefore, SCI is crucial for receivers to decode the data transmitted in the TB. The data are transmitted over physical sidelink shared channels (PSSCH), while the SCI message is transmitted over physical sidelink control channels (PSCCH). According to 3GPP Release 14 or later release, there are two arrangements of PSSCH and PSCCH: 1) Adjacent configuration means that the SCI occupies the first two RBs and the TB occupies the following RBs for each SCI + TB transmission. 2) Nonadjacent configuration is structured by two separate RB pools. One of the pools is dedicated to SCI and the other is reserved for TB only.

Since Release 15, data can be transmitted using QPSK, 16-QAM, 64-QAM, whereas SCIs are always transmitted using QPSK. C-V2X subcarriers have 14 symbols per subframe, and four of

these symbols are dedicated to the transmission of demodulation reference signals (DMRSs) to combat the Doppler effect at high speeds.
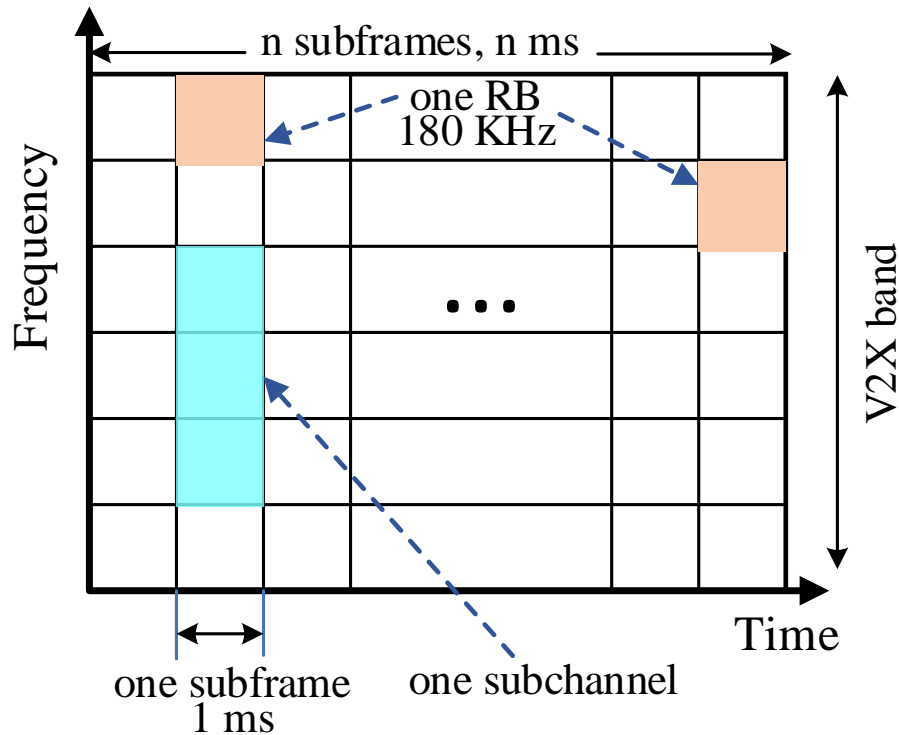
Fig. 2.4: Two-dimensional (time and frequency) resource pool for 5G sidelink.

To manage resources and schedule transmissions, four work modes were introduced for sidelink communications in the 3GPP 5G standard [29]. The first two operation modes, mode 1 and mode 2, are dedicated to device-to-device (D2D) communications. According to the studies [30] and [51], the delivery latency in mode 1 and 2 is too large to satisfy the low latency requirement of eV2X services. In fact, the initial proposal of the two first modes reflected an intentional consideration of the limited battery storage for mobile devices. That is, the prolonged lifetime is at the cost of a large latency. In Release 14 or later, two additional modes, mode 3 and mode 4, are dedicatedly designed for ultra-reliable low latency used in V2X communications. In mode 4, VUEs and other UEs autonomously select their radio resources for transmission whether they are in the coverage of base stations. The selection method called sensing-based semipersistent scheduling (SPS), which has been explained in research papers [50-51] and the 3GPP standards [69-70]. The main idea is that each UE continuously senses all subchannels and reserves resources for a number of consecutive transmissions based on the prior sensing results. A reselection counter is introduced to control when the next reselection occurs. As opposed to mode 4, mode 3 does not specify a resource management algorithm to allow the telecommunication operators to implement their own algorithms. The algorithm in mode 3 should be either a dynamic scheduling and

allocation or a SPS-based one. The former is assisted by the base station that assigns subchannels and transmission time per request from UEs, while the latter is analogous to the standardized SPS scheme in mode 4. Obviously, the dynamic approach is advantageous in resource utilization, but it also may increase overhead or cause bottleneck if not well designed. The main research targets of Chapter 5 in this thesis is to maximise resource utilization, and meanwhile keep a low overhead in resource management at base station.

2.3 Fundamental Knowledge of Network Coding Theory

In this subsection, the network coding theory is introduced. It revolutionizes the traditional method for information dissemination in networks. In the reality, random linear network coding shows superior feasibility in ad hoc networks. Additionally, physical layer network coding, which involves in processing two superposed radio signals at the physical layer, is also introduced.

2.3.1 Random Linear Network Coding

In a traditional network, an intermediate node executes a store-and-forward mode. However, with the network coding (NC), it turns to be a encode-and-forward mode instead. To achieve the maximum flow of a network for multicasting information, the initial idea of NC was proposed by Ahlswede *et al*. in 2000 [38]. Linear network coding was soon constructed in [71] based on the basic idea of NC. Paper in [39] proposed a random linear network coding (RLNC) approach for transmitting and compressing information in the multicast networks, and paper in [72] built a more feasible model for applying RLNC in multicast. Compared with the conventional mode of direct forwarding, the advantages of RLNC are in two folds: 1) the coefficients of network codes are distributed and randomly generated; and 2) the random linear network coding is robust to the dynamic network topology and it obviates the need for centralized knowledge of network topology. Based on the advantage of random linear network coding, numerous schemes apply it in different situations.

To better understand the concept of NC and RLNC, we use a simple example shown in Fig. 2.5 (a) to give a concise explanation. Both packet P_A and packet P_B need to be multicast to receivers D_1 and D_2. The line between two nodes represents a communication link and the number of links between any two nodes indicates the channel capacity. Intermediate node R_3 performs random linear network coding on the two incoming packets and forwards an encoded packet. For instance, node R_3 randomly selects two coefficients α and β from Galois field (GF) [73] and encodes two incoming packets as $\alpha P_A + \beta P_B$. Coefficients are sent along with the payload of the packet. When the receiver D_1 receives P_A and $\alpha P_A + \beta P_B$, it can recover two original packets P_A and P_B by operating a simple algebraic calculation. Similarly, D_2 can also obtain both P_A and P_B after carrying out the similar decoding process. One possible decoding method is Gaussian Elimination [74].
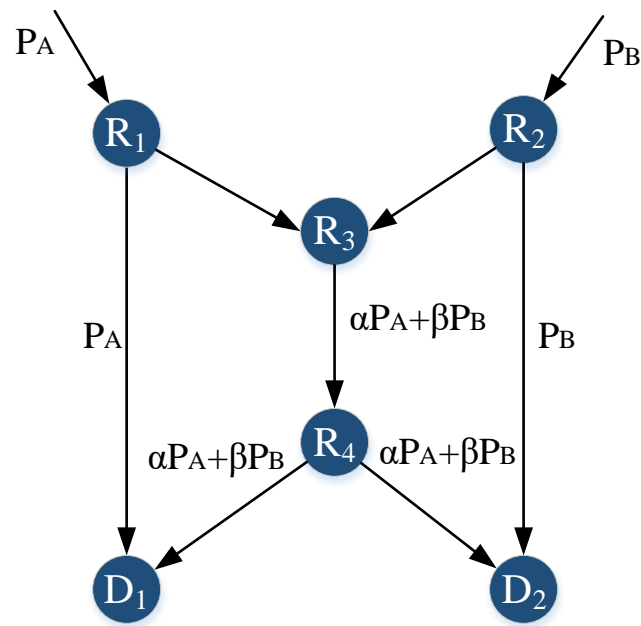
(a)
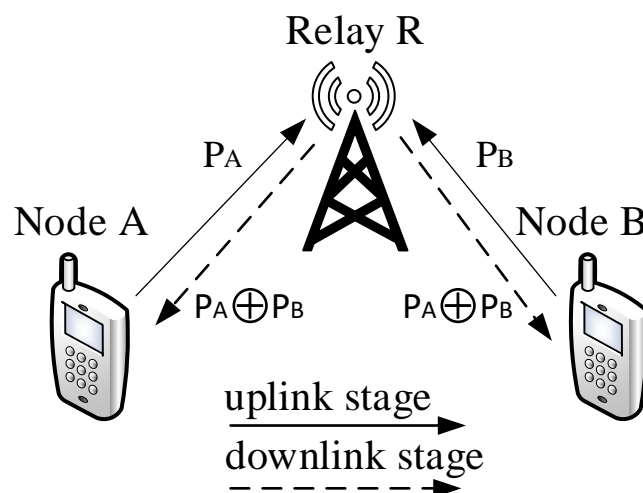
(b)

Fig. 2.5: (a) Basic concept of RLNC; (b) basic concept of PNC.

The application of RLNC in wireless communication shows more superiority in reliability and efficiency than its application in the wired circumstance. Suppose node x and node y need to exchange a packet between them. However, they are not within each other's transmission range. A relay node R that locates in the middle can assist them in completing the exchange. Without network coding, the node R first receives packet P_x from node x and then forwards it to node y.

The same process is repeated for packet P_y from node y. Given the erasure probability of channel between x (or y) and R is P, the successful exchange probability is $(1-P)^4$ and time consumption is 4 timeslots. By contrast, if node R employs network coding, it can broadcast an encoded packet (e.g., P_x+P_y) at the third timeslot. The two nodes can obtain their desired packet after decoding the encoded packet. Apparently, in this situation, the successful probability turns to be $(1-P)^3$ and time consumption is reduced to 3 timeslots.

In fact, network coding can be implemented either in packet level or symbol level. In symbol-level network coding (SLNC), each data packet is divided into symbols and network coding is operated on symbols to achieve high data rate and high protocol efficiency. However, the over-head of SLNC is larger than that of packet-level network coding (PLNC), making it inefficient for the transmission of small-size packets, such as BSM packets, which are typically 200 to 400 bytes in length. Over the years, network coding has been studied and applied in different respects, including network security [75-77], network error correction coding [78-79], peer-to-peer content distribution and downloading [80-81], vehicular networks [82-85] and so on.

2.3.2 Physical-layer Network Coding

Physical-layer network coding (PNC), first appeared in [62], is a subfield of network coding. The simplest system in which PNC can be applied is the two-way relay channel (TWRC), as depicted in Fig. 2.5 (b), where two end nodes A and B exchange information via a relay node R. We assume half-duplex operation and no direct channel between A and B. In traditional mechanism, it needs four timeslots to finish the exchange process. Node A sends a message to relay R at the first timeslot, and then R sends it to B at the second timeslot. Node B takes the third timeslot to transmit its message to R, and R broadcasts it at the last time slot. Compared with the conventional relay system, PNC doubles the throughput of TWRC by reducing the number of time slots for the exchange of one packet from four to two. In PNC, in the first timeslot, the two end nodes send signals simultaneously to the relay; in the second phase, the relay node processes the superimposed signals of the simultaneous packets and maps them to a network-coded packet (e.g., $P_A \oplus P_B$) for broadcast back to the end nodes.

PNC makes full use of the natural property of electromagnetic waves that can overlap each other during propagation if in the same carrier frequency. Therefore, PNC benefits from transmission collisions, which should be obviated in other communication systems. The key point of PNC lies in decoding the overlapped electromagnetic signals. In another word, the relay node needs to map superimposed signals to eXclusive OR (XOR) symbols. A variety of decoding methods have been investigated. Those methods developed diverse algorithms. Typical ones include belief-propagation based solutions in time domain [86-88] and OFDM-based PNC in frequency domain [89-90].

Since PNC can substantially increase the efficiency of information exchange in networks, it has been adopted in vehicular networks. For instance, work in [91] adopted PNC for message unicast in bidirectional shared links in vehicular networks, and paper in [92] used PNC to predict vehicles' positions. The authors in [93] designed a MAC protocol for information broadcasting in VANETs where PNC is employed to restrain transmission collisions.

2.4 Fundamental Knowledge of Fuzzy Logic

Fuzzy logic is a theory that is closely linked with imprecise predicates. The truth values of variables in fuzzy logic can be any real number between two extremes: 0 and 1 both inclusive. It deals with vague and imprecise information, like decision making in human brain. By contrast, on Boolean logic, the truth values of variables may only be 0 or 1.

2.4.1 Basic Definitions

A *classical* (crisp) *set* is usually defined as a collect of elements or objects $x \in X$. Each single element can either belong to or not belong to a subset A, $A \in X$. For a classical set, the member elements can be defined by using the characteristic function, in which **1** means membership and **0** non-membership. By contrast, for a fuzzy set, the characteristic function allows various degrees of membership rather than two values for an element of a given set [94].

Definition 2.1: If X is a set of objects denoted by x, then a fuzzy set $\tilde{A}$ in X is a set of ordered pairs:

$$\tilde{A} = \{(x, \mu_{\tilde{A}}(x)) \mid x \in X\} \tag{2.1}$$

where $\mu_{\tilde{A}}(x)$ is called membership function of x in $\tilde{A}$. The value of the membership function is nonnegative real numbers no larger than 1.

For example, $\tilde{A}$ = "real number close to 10" can be represented by $\tilde{A} = \{(x, \mu_{\tilde{A}}(x)) \mid x \in X\}$, where $\mu_{\tilde{A}}(x) = \left(1 + (x-10)^2\right)^{-1}$. The membership function is plotted in Fig. 2.6.

From Fig. 2.6, we can see that for any real number x, the closer the x to 10, the larger degree it has. Such conclusion is consistent with people's judgement.

A fuzzy set $\tilde{A}$ can be represented in one of the two ways as follows:

- The set X is discrete and finite:

$$\tilde{A} = \left\{ \frac{\mu_{\tilde{A}}(x_1)}{x_1} + \frac{\mu_{\tilde{A}}(x_2)}{x_2} + \frac{\mu_{\tilde{A}}(x_3)}{x_3} + ... \right\} = \left\{ \sum_{i=1}^{n} \frac{\mu_{\tilde{A}}(x_i)}{x_i} \right\} \tag{2.2}$$

- The set X is continuous and infinite:

$$\tilde{A} = \left\{ \int \frac{\mu_{\tilde{A}}(x)}{x} \right\} \tag{2.3}$$
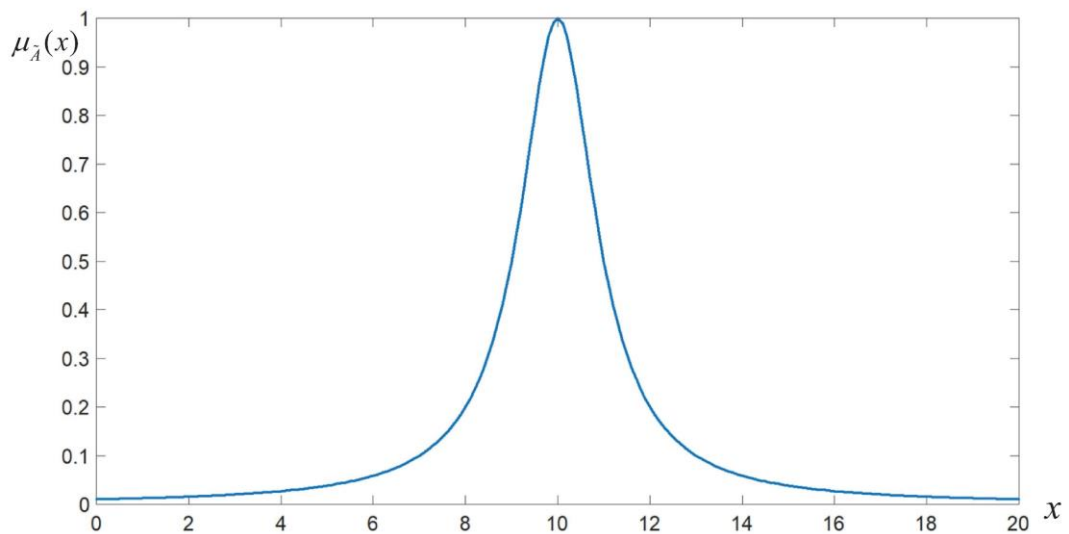
Fig. 2.6: Membership function for $\tilde{A}$ = "real number close to 10".

The basic operations with fuzzy sets are defined via their membership functions. According to the theory proposed by Zadeh [95], there are three basic operations for fuzzy sets: *intersection*, *union* and *complement*, as follows.

Definition 2.2: The membership function $\mu_{\tilde{C}}(x)$ of the *intersection* $\tilde{C} = \tilde{A} \cap \tilde{B}$ is pointwise defined by

$$\mu_{\tilde{C}}(x) = \min\left\{\mu_{\tilde{A}}(x), \mu_{\tilde{B}}(x)\right\}, x \in X \ . \tag{2.4}$$

Definition 2.3: The membership function $\mu_{\tilde{D}}(x)$ of the *union* $\tilde{D} = \tilde{A} \cup \tilde{B}$ is pointwise defined by

$$\mu_{\tilde{D}}(x) = \max\left\{\mu_{\tilde{A}}(x), \mu_{\tilde{B}}(x)\right\}, x \in X \ . \tag{2.5}$$

Definition 2.4: The membership function of the *complement* of a fuzzy set by $\tilde{A}$ is defined by

$$\mu_{\not\subset A}(x) = 1 - \mu_{\tilde{A}}(x), x \in X \ . \tag{2.6}$$

2.4.2 Main Stages of A Fuzzy-logic based Algorithm

Differing with variables in mathematics, fuzzy logic algorithms often take linguistic variables to facilitate the expression of rules and facts. There are three main stages in fuzzy algorithms: fuzzification, inference and defuzzification.

Fuzzification is the process of mapping numerical input of a system into fuzzy sets with degree of membership. Membership functions are used to complete this mapping process. For instance, Fig. 2.6 delineates such a mapping, in which input variables can be any real numbers, membership

function is $\mu_{\hat{A}}(x)=\left(1+(x-10)^2\right)^{-1}$ and output values are between 0 and 1. In fact, for any membership function, the degree of membership should be real numbers within the range [0,1]. If it is **0** then the value does not belong to the given fuzzy set, and **1** means the value completely belongs to the fuzzy set.

As shown in Fig. 2.7, a fuzzification process converts measured temperature into linguistic variables *low*, *moderate*, and *high*. The vertical line in the figure denotes a specific input value (i.e., 22 °C). Three values at three interceptions represent the degree that the temperature belongs to three fuzzy sets. From the bottom to the top along the vertical line, three values are 0, 0.2 and 0.8, which are the degree of the *low*, *moderate,* and *high*, respectively. More specifically, the value 0 pointed by the blue arrow means that the temperature of 22 °C has zero membership in fuzzy set *low*. Similarly, it has 0.8 membership in set *moderate*.
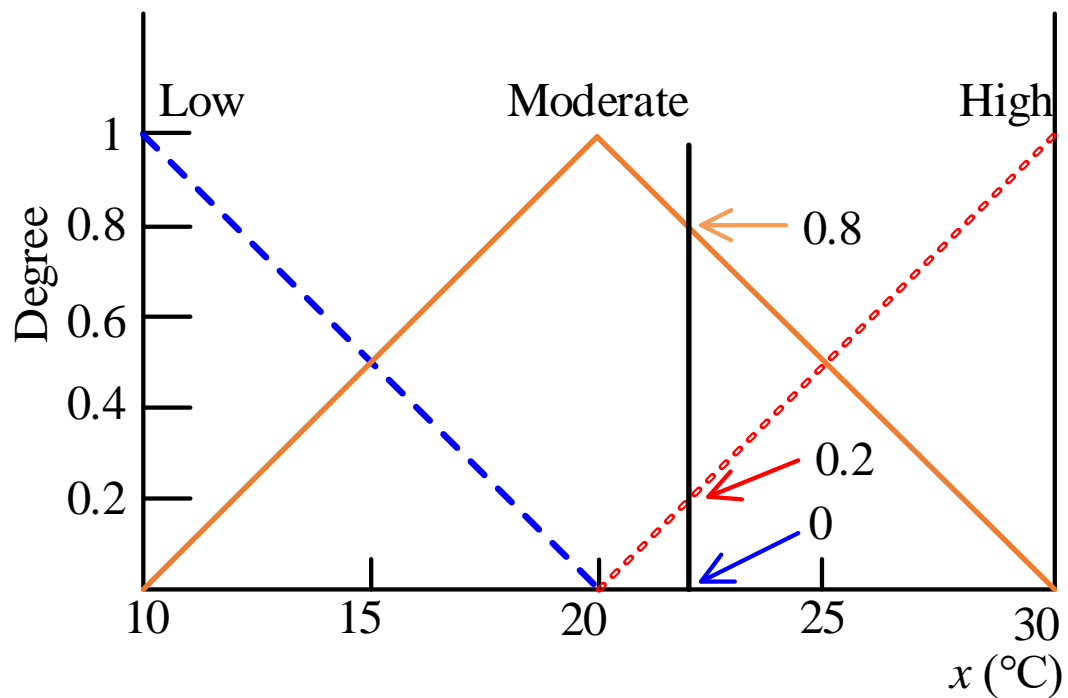
Fig. 2.7: Linguistic variable "temperature".

Inference is a process that pre-defined rules are applied to generate ranks or verdicts according to the results of fuzzification. The rules are usually conditions and inferred results based on IF/THEN process. For example, in a temperature control system like Fig. 2.7, the rules can be:

- Rule 1: If the temperature is low, then start to turn on the heating system;
- Rule 2: If the temperature is high, then start to turn on the cooling system.

Defuzzification is a process computing a crisp output, which is widely used for decision making and control system. There are different types of defuzzification strategies given different criteria.

Those criteria include core selection, scale invariance and so on [96]. Therefore, corresponding typical defuzzification methods can be extreme value strategy and centroid strategy. In extreme value strategy, extremal values of membership function are adopted to define the crisp output. The extremal values can be randomly elected or from a certain position of the core. By contrast, the centroid strategy chooses a value that corresponds to the centre of the area with membership greater than zero. The best known one is the *centre of gravity* (COG) [94] and [96]. From a mathematical point of view, the COG can be calculated by:

$$COG(A) = \frac{\int x\mu_{\tilde{A}}(x)dx}{\int \mu_{\tilde{A}}(x)dx} . \tag{2.7}$$

2.5 Literature Review in V2X Communications for Safety Services

This subsection reviews the relevant research studies for safety message dissemination in V2X communications. In vehicular networks based on DSRC, most of the innovative designs focus on MAC layer. Their goal is to boost the reception probability of safety messages by mitigating the transmission collisions, leveraging network coding or developing other novel approaches. Regarding C-V2X in 5G, pioneers devoted to improving the spectrum utilization as well as constraining the interference to match the requirements of the services.

2.5.1 Basic Safety Message Dissemination in DSRC-Based V2X

Due to transmission collisions, being lack of feedback in case of lost messages for broadcasting and highly dynamic channels, DSRC is incompetent to guarantee the delivery of safety messages, especially for BSMs, in vehicular networks. To tackle the issue, colossal efforts have been made from different respects, and they largely focus on innovation at MAC layer. They can be categorized into distributed, centralized and hybrid schemes.

A repetitive transmission approach was proposed in [36]. In this paper, a control channel (CCH) interval is slotted into L length-fixed time slots. Vehicles repeatedly broadcast each safety beacon several times to enlarge the likelihood of reception. This idea develops into six variations: asynchronous fixed repetition (AFR), synchronized fixed repetition (SFR), asynchronous p-persistent repetition (APR), synchronized persistent repetition (SPR), AFR with Carrier Sensing (AFR-CS), and APR with Carrier Sensing (APR-CS). In SFR or AFR, w ($w<L$) time slots are randomly selected to broadcast a packet repeatedly, while in SPR or APR a packet is sent with a predetermined probability p at each time slot. AFR-CS and APR-CS, both of which listen to the channel status before transmissions, are compatible with the DSRC. The authors in [36] also modelled the upper bound for packet reception failure and acquired the optimal repetition number for different schemes. Although both schemes can diminish the reception failure, they also increase the chance of concurrent transmissions and the interference at the same time, especially in a network with a

high density of vehicles. Therefore, the schemes only work effectively in sparse networks. To limit the number of collisions, a positive orthogonal code is introduced in [37], while protocol sequence is adopted in [43]. A collision-recording based scheme is introduced to control the congestions in [97]. When the number of detected collisions increases, vehicles begin to decrease the frequency of BSM transmission. By contrast, in [44], the authors tried to reduce the number of packets by omitting certain packets containing redundant or derivable information in between consecutive sending packets. Y. Park *et. al* proposed an application-level control scheme [98], in which a CCH interval is divided into a number of asynchronous epochs. To minimize the chance of transmission collisions, the application layer hands over a BSM to the MAC layer in an epoch that is unlikely used by other vehicles.

Additionally, some researchers also explored applying RLNC in distributed schemes to enhance the reliability. Based on DSRC, paper [45] presented an application of RLNC for safety message dissemination among a cluster of nodes. Each node has multiple opportunities to rebroadcast network coded packets that is produced by encoding its own packet with the ones overheard from its counterparts. Paper in [99] built a model to analyse the delivery delay in a highway situation where vehicles broadcast encoded BSM packets. A loss probability upper bound was derived by using discrete phase type model. The dissemination of BSM packets at an intersection of two roads was investigated in [46] and [100]. The former only allows an intersection vehicle to carry out encoding buffered packets before broadcasting, while the latter integrates the repetitive transmissions with RLNC at each vehicle to repetitively transmit encoded packets. In the proposed scheme RT-NC, each vehicle first applies RLNC, in which the vehicle linearly combines packets overheard from others and its own safety packet, and then broadcasts the encoded packets repeatedly. For each repetition, the randomly selected coefficients are applied to do the encoding. The authors adopted Markov chain to mathematically analyse the packet delivery ratio. The analytical results tightly follow the simulation results, which validates the correctness of the analytical model. Compared with DSRC, the RT-NC scheme is able to significantly improve the packet delivery rate to almost 100%, but the packet reception rate plummets when there are more than 50 vehicles in the network. Studies in [91] and [92] try to make use of collisions by means of adopting physical-layer network coding (PNC), but both schemes only work for unicast communications rather than broadcast.

Since the distributed schemes unlikely eliminate transmission collisions for the safety messages in dense vehicular networks, a few centralized protocols based on TDMA have been designed. In [40], a road is divided into numerous segments and each segment has a fixed transmission period. Different vehicles transmit safety beacons in different time slots assigned by a coordinator vehicle. In [41] and [42], an RSU measures the traffic in its coverage and manages the time slots for

different nodes to ensure that every vehicle has its exclusive time slot to broadcast BSMs without contention.

There are also hybrid MAC protocols for VANETs. The authors in [47] developed a NC-assisted scheduling algorithm that fully exploits the joint effect of V2V and V2I communication. Nodes in the network work in both centralized and distributed way. However, the algorithm only suits the non-safety data dissemination due to the large delay. Two papers in [102] and [103] firstly proved the feasibility of implementing PNC at physical layer in vehicular environment. The former examined the impact of motion-induced carrier frequency offset (CFO) and inter-carrier interference (ICI) by applying conventional equalization methods, while the latter delineated an algorithm based on belief propagation to mitigate the CFO/ICI effect on signal decoding. Ndih *et. al* designed a PNC-based MAC protocol named VPNC-MAC [93] and [104], which consists of a centralized period and a distributed period for BSM exchange. In VPNC-MAC, among a cluster of vehicles on road, one vehicle is dynamically designated as a relay vehicle according to vehicles' current positions. The rest of non-relay vehicles apply PNC to exchange their BSM packets with the coordination of the relay vehicle. Each time, a pair of vehicles transmit BSMs at the same time. The relay vehicle plays a similar role of the relay node R in Fig. 2.5 (b). After mapping the overlapped signals from two simultaneous transmissions, the relay vehicle will broadcast a XOR packet. At the end, a contention period is reserved for vehicles that fail to obtain opportunity for transmission in the PNC period. The VPNC protocol can increase the communication efficiency by taking advantage of PNC and reduce the transmission collisions by arranging a centralized session. However, the protocol also has many drawbacks. Firstly, it is based on so many unrealistic assumptions (e.g., one-dimension road in its system model and all vehicles being aware of each other's instant location in advance, etc) that it is far from reality. In addition, the scheme is not robust because the performance is largely affected by the location of the relay. Lastly, the numerical results from theoretical analysis has not been validated by simulations.

More recently, in order to alleviate the broadcast storm and enhance the message delivery rate, some complicated broadcast protocols have been put forward. Protocols in [105] and [106] use fuzzy logic to determine the next hop relay nodes. Comparably, a forwarding node selection scheme that integrates directional broadcast was presented in [107]. The authors in [108] even tried to use a service channel to relay safety messages. Unfortunately, all of them are only suitable for multi-hop dissemination of event-trigger messages rather than BSMs.

2.5.2 Performance Analysis and Enhancement for V2X communications in DSRC

Performance analysis for V2X communications in DSRC have been investigated in previous studies. The mathematical models built in [109-110] are only suitable for unicast scenarios rather than broadcast situations, in which retransmission will not take place if packets are lost. The broadcast

behaviour was modelled by using a Markov chain in [111] for both the saturation and non-saturation states. Gao *et .al* also adopt a similar approach to examine network performance such as packet delivery ratio for BSM broadcast [100-101] where RLNC is applied in the schemes. Although these theoretical models can correctly predict network performance for broadcast, they only work for distributed MAC protocols rather than the hybrid MAC protocol proposed in Chapter 3. Similar conclusions can also be reached while considering the studies in [36-37], [43-45] and [97-99] discussed in the above section.

As mentioned in the previous section, centralized MAC protocols have been developed [40-42]. These protocols are mainly based on TDMA, in which a vehicle [40] or an RSU [41-42] is elected as a coordinator to schedule transmissions. Unfortunately, due to the overhead of coordination, the delivery latency is usually too large to meet the requirement of some safety applications (e.g., BSMs) in vehicular networks. Again, the models included in those works are exclusively apt to centralized protocols.

A few of hybrid MAC protocols were designed for message dissemination in vehicular networks. Partially centralized and partially distributed working manners are the features of those hybrid protocols. K. Liu *et. al* [47] presented a network coding assisted scheduling algorithm to disseminate data via V2X communication, but it mainly targets on non-safety applications. The study in [93] delineated a protocol that applies PNC to enhance the performance. However, it is far from achievable because of its one-dimension network model and other ideal assumptions. Our proposed hybrid MAC protocol in Chapter 3, known as NC-PNC MAC, which not only exploited joint effect of V2V and V2I communications, but also integrated RLNC and PNC for safety message dissemination. The protocol outstrips its counterparts in PDR for both sparse and dense networks. However, more insights need to be provided given the consideration of deployment. On the one hand, despite analytical models have been provided to evaluate the performance of hybrid protocols [48] and [93], they cannot be used to examine NC-PNC MAC. The reason is that the model does not include PNC in the analysis in [48], whereas the model in [93] only considers V2V communications. On the other hand, a mathematical model is helpful to optimize the performance of a vehicular network. Several studies are dedicated to enhancing the DSRC. The optimization of contention window (CW) for MAC based on DSRC standard indicated the CW size should be determined by traffic density on road [112]. Rossi *et al*. [113] theoretically analysed the relationship between the CW and the throughput in order to acquire the optimal CW size. The proposed technique is studied through numerical examples. The DSRC performance was evaluated when the network load was saturated. In [114], the authors proposed a vehicle-density estimation approach that utilizes the PHY attainable information to measure the traffic density. Based on the estimation and Markov chain, an analytical solution to getting the optimal CW size was introduced. Although there are relevant research in performance enhancement for DSCR

networks, there is a research gap in performance optimization for hybrid MAC like NC-PNC MAC as the studies mentioned above only work effectively for the distributed MAC.

Table 2.4: Summary of MAC protocols for safety message dissemination.

Protocol Types	Features	Typical Papers	Contributions	Drawbacks
Distributed MAC Protocols	Repetitive transmission	[36]	Diminish the reception failure by transmitting the same packet multiple times.	Increase the transmission collisions
	Collision reduction and congestion control	[37] [43] [44] [97] [98]	Reduce the concurrent transmissions by leveraging various strategies including: 1) positive orthogonal code [37]; 2) protocol sequence [43]; 3) congestion control [97]; 4) getting rid of redundant packets [44]; 5) asynchronous transmission [98].	Transmission collisions cannot be eliminated, and the network performance degrades sharply in dense networks.
	RLNC based schemes	[45] [46] [99] [100]	The RLNC is applied to improve the reliability and reduce latency for BSM broadcast as vehicles may have higher opportunity to derive the original information by decoding.	Transmission collisions cannot be eliminated, and the network performance degrades sharply in dense networks.
	PNC based schemes	[91] [92]	PNC is used to promote the efficiency of information dissemination.	Only works for unicast scenarios.
Centralized MAC protocols	TDMA based schemes	[40] [41] [42]	A coordinator dedicates different time slots to different vehicles to obviate collisions	Not compatible to DSRC and overhead results from coordination.
Hybrid MAC protocols	Contains both centralized and distributed elements	[47] [93] [104]	1) Partial vehicles broadcast in a centralized way and the left in a distributed way [93] [104]; 2) All vehicles disseminate their information in a centralized way during one period and switch to a distributed mode in another mode [47].	The performance may be negatively affected by a relay node.
Others	Cooperative forwarding [105-107] or occupy extra channels	[105] [106] [107] [108]	1) A relay node is elected by using a particular approach to forward messages [105-107]; 2) SCH channel in DSRC is occupied to relay safety messages [108].	Only work for event-trigger message dissemination in multiple hops. They cannot be used for periodic transmission like BSM.

2.5.3 Resource Allocation in 5G Cellular V2X Communications

V2X communications in 5G networks have four work modes. However, only mode 3 and mode 4 can support Ultra-Reliable Low-Latency Communications (URLLC), according to their different resource reservation approaches. When vehicles are out of the coverage of base stations, they switch to mode 4 and select time and spectrum resources autonomously using a sensing-based SPS scheme. By contrast, in mode 3, when vehicles fall into the communication range of base stations, there are two options for resource allocation. The resources are either managed and allocated dynamically by base stations or reserved via the SPS scheme.

Even though the SPS scheme, which works in a distributed way among vehicles, is flexible for implementation, it manifests a drawback of resource selection collisions that may cause transmission collisions, thereby reception failure. Toward dealing with the issue, papers in [30] and [51] proposed a cooperative scheduling method that decreases the transmission collisions. The authors firstly evaluate the link-level performance of mode 3 and mode 4 with all configurations and scheduling method based on the standard [29]. Based on the simulation using Matlab, they showed how the block error rate (BLER) is affected by factors like Doppler shift, modulation, and retransmission. The simulation results proved that the modulation and the retransmission have enormous impact on BLER. Their simulation further revealed that the probability of transmission collisions, induced by resource selection collisions, is between 1% and 5%, when there are only 10 vehicles in the simulation. To lower the collision probability, the authors proposed a cooperative solution, in which counter values are appended in the transmitted packets. Such method can make surrounding vehicles be aware of the surrounding vehicles' counters, thus obviating two or more vehicles' counters arrive to zero at the same time. Consequently, it leads to a collision-free resource selection. However, there are some drawbacks in the study. The authors only consider the case of rather light traffic in the simulations, and the capacity of the network is unknown if the proposed scheme is applied. In addition, the study omits the other performance indicators such as packet reception ratio and latency. Although the transmission collisions are mitigated, the probability for packet reception was not verified as low transmission collisions do not necessarily result in good reliability.

The study in [50] identified the inefficiency of the SPS scheme in subchannel reselection due to size difference between two packets in two consecutive selections. Based on the findings, a modification to the original SPS was proposed to make full use of subchannels. Nardini *et.al* [115] considered feasibility and evaluated system-level performance of two dynamic scheduling; a sequential mode resembling TDMA and simultaneous transmissions with frequency reuse for a platooning application, which is a typical cooperative driving use case envisioned in C-V2X. However, the authors only considered the platooning application in their simulations and the network-level performance is unknown if more applications are employed in networks. Through extensive

simulations, the study revealed how the resource allocation in mode 4 affects some key performance indicators like latency and packet delivery rate in high-density vehicular networks [53]. Modelling C-V2X mathematically was also provided. As a case in point, the authors of [52] quantified four transmission errors and provided PDR against distance in mode 4. To maximize the number of concurrent V2V links, a belief propagation-based algorithm was developed to allocate RBs for vehicles [116]. Unfortunately, the algorithm only works for a simplified situation of V2V using unicast case. From above discussions, most of these studies in resource allocation for 5G V2X relate to mode 4.

In fact, to improve spatial frequency reuse, comprehensive research has been conducted in LTE cellular networks. Study in [54] presented a heuristic algorithm to assign RBs to CUEs. The algorithm aimed to make the network achieve the largest throughput in uplink. To boost the throughput in downlink of LTE-Advance (LTE-A) networks, Rostami *et. al* [55] addressed the problem of optimization of RB allocation by solving an integer linear programming when carrier aggregation and Multiple-Input Multiple-Output (MIMO) are enabled in downlink. Although such resource allocation algorithms can well deal with the problem in uplink or downlink, they are far from sidelink communications where both unicast and broadcast are included.

Radio resource management was studied thoroughly in D2D communications in LTE, which shares certain features with V2V communications in 5G C-V2X networks. Authors in [56] proposed an interference-aware resource allocation (IARA) scheme, which can dynamically assign channels based on two-way channel gain estimation and interference measurements. The IARA can substantially diminish adverse effect of cochannel interference, thus enlarging the system throughput. The research in [57] focused on alleviating the interference between the eNB relaying and D2D using fractional frequency reuse (FFR), in which D2D and cellular UEs use the different frequency bands chosen according to users' locations. Researchers in [58] firstly discussed resource allocation problems in a multi-cell environment, and then studied intra-inter-cell D2D communications. They have evaluated their proposed novel resource allocation and power optimization scheme by exploiting FFR. A more recent project in [117] studied the joint resource allocation and power control problem for energy efficient V2V communications underlaying cellular networks. The authors transformed the issue as combinatorial and fractional programming and designed a two-layer scheme to solve the problem. The work in [118] introduced a reverse iterative combinatorial auction as a resource allocation mechanism for D2D in LTE-A. In the auction, resources act as bidders competing to obtain D2D links. D2D pairs were auctioned off in each auction round. Toshihito Kanai designed an autonomous reuse partitioning that is an adaptive channel allocation in cellular systems [59]. It coordinates how to allocate radio channels among multiple base stations and minimizes the interference. Though D2D communications are similar to V2V communications in C-V2X network, the above algorithms cannot be adopted

because C-V2X communications consist of unicast and broadcast, and use different spectrum of cellular users rather than as an underlay that sharing with the same channels in the downlink in LTE-A.

Fuzzy logic was also employed for resource allocation in cellular networks. In [61], network resources such as connections between Fog Computing-Zone Controllers and Fog Computing BBU Controllers in 5G VANETs are allocated in a flexible and scalable way. However, the fuzzy-logic-based strategy in this work cannot solve the problems in resource allocation in 5G C-V2X networks because the research objective in [61] focuses link connectivity among vehicles in the networks rather than allocation of RBs and subframes at time dimension. Wu *et. al* [119] proposed a fuzzy logic method to address the issues of the interference coordination among cells as well as the resource allocation among the users served by the same cell. In the proposed fuzzy logic method, four factors are considered and fuzzified as inputs. There are required data rate, signal strength at reception, interference level and fading level. The outcome of the fuzzy system includes a three-state judgement (i.e., positive, neutral, and negative) for allocability and transmission power. Finally, a decision-making algorithm was used to allocate RBs to mobile stations (MSs) in the same cell in accord with the suitability scores obtained from the defuzzification. The proposed algorithm can improve the system throughput and allow the base stations of different small cells work autonomously. However, the authors did not consider the interference between MSs associated with the pico-base station and MSs associated with macro-base station. In addition, the algorithm cannot work on the resource allocation in the circumstance of 5G C-V2X where many services are based on broadcast rather than the unicast communications between BS and mobile stations via downlink and uplink.

2.6 Summary

In Chapter 2, we first introduce specifications of two main technologies in V2X communications: DSRC and 5G C-V2X. Following the specifications, fundamental knowledge of network coding theory and fuzzy logic theory are described. In the literature review of V2X communications, relevant studies of both DSRC-based and cellular-V2X-based protocols or algorithms are discussed. In the discussions, innovations, features, drawbacks, and research gaps in previous studies are included.

Chapter 3 A Novel Hybrid MAC Protocol for BSM Broadcasting in Vehicular Networks

3.1 Introduction

This chapter devotes to investigating how to disseminate BSMs effectively and reliably in vehicular networks. The BSMs periodically broadcast by every vehicle can improve the cooperative awareness on road, thus preventing road accidents. However, due to transmission collisions, fading channels and highly dynamic topology, vehicular networks usually suffer a high packet loss rate and a large delay, which are intolerant of safety applications. To tackle these issues, we propose a hybrid medium access control protocol for BSM dissemination in vehicular networks. Its partially centralized and partially distributed characteristic not only can effectively suppress the collisions but keep compatibility with IEEE 802.11p. In addition, the integration of Physical-Layer Network Coding and Random Linear Network Coding strengthens the reliability and efficiency. In the protocol, both V2V and V2I communications are involved. Then, comprehensive simulations have been conducted to evaluate its performance. Simulation results indicate that, compared with existing schemes, the proposed protocol can significantly improve the packet delivery ratio by a range between 20% and 300% in both sparse and dense networks. In addition, it can ensure the delivery latency meet the stringent requirement of safety application in ITS.

Table 3.1: List of Notations in Chapter 3.

Notations	Description
R	The communication range of RSU
r	The communication range of vehicle
S, $\square$	The set of vehicles, the set of PNC pairs, respectively
v_x, $\Re$	A vehicle x, and the RSU, respectively
E	The set of edges in communication graph
$d(v_i, v_j)$	The distance between v_i and v_j
$PDR(i)$	The packet delivery ratio for v_i
N	The total number of vehicles in RoI
T	The overall time spent for all vehicles to complete transmitting their BSM packets
$\chi(i)$	The total number of BSM packets received at vehicle v_i
TH	The network throughput
TH_{norm}	The normalized network throughput

T_{CCH}	The CCH interval
$v_{Relay}^{L}, v_{Relay}^{R}$	A pair of relays at the left and right side of RSU
T_{setup}	The total time spent on the *MAC setup session*
T_{poll}	The transmission time for one *poll* packet
T_{join}	The transmission time for one *join* packet
T_{coord}	The transmission time for one *coordination* packet
N_b, N_{sub}	The batch volume, the total number of data subcarriers in OFDMA
T_{SIFS}	The waiting time before sending a *join* packet
T_{DIFS}	The waiting time before sending the *PNC* session
T_{AIFS}	The waiting time before sending the *CSMA* session
$P_{coll}(n)$	The probability of a subcarrier and a batch chosen by n $(n \geq 2)$ nodes
T_{CSMA}	The time spent on the *CSMA* session
n_{CSMA}	The number of vehicles participating in the *CSMA session*
T_{BSM}	A BSM packet transmission time
$t_{bf}[i]$	A random back off time in the ith transmission
M_L, M_R	The number of BSM packets in the buffer of the left and right relay
P_{v_i}	A packet sent by vehicle v_i
P_{Relay}	A packet sent by a relay
P_{RSU}	A packet sent by the RSU
T_{PNC}	The total time spent on *PNC session*
n_{PNC}	The total number of PNC pairs
Ψ	The set of selected subcarriers
I_{x_i}	Indicator if subcarrier x_i has appeared in Ψ
$P_{(I_{x_i}=1)}$	The probability of x_i has appeared in Ψ
$E\left[N_{rp}\right]$	The expectation of repeated times for all subcarriers in Ψ
P_{veh_coll}	The proportion of vehicles colliding in subcarriers
TNP	The total number of packets sent by all vehicles and the RSU
X	The probability density function of the signal amplitude
m	The fading figure in Nakagami fading channel
ω	The average receiving power in Nakagami fading channel

3.2 System Model and Performance Metrics

This subsection delineates the system model considered in this chapter and defines three performance metrics that will be used to indicate and compare the performance of the proposed protocol.

3.2.1 System Model

We are interested in one-hop BSM packets dissemination among vehicles in a vehicular network. In particular, each vehicle is obliged to receive all BSM packets from neighbouring vehicles within a time interval (also known as the lifetime of a BSM packet). Table 3.1 lists all notations in Chapter 3.

Fig. 3.1 shows the network model for a road segment scenario and an intersection scenario. For each scenario, there are a number of moving vehicles but one static RSU. Each vehicle is equipped with an onboard unit (OBU), which is able to communicate with other OBUs and the RSU. Assume all OBUs have the same communication range. Let R and r represent the communication range of the RSU and the OBU, respectively, where $R > r > 0$. The communication range of the RSU is defined as a region of interest (ROI). In both scenarios, every vehicle disseminates its BSMs to all other vehicles in the same RoI via V2X communications. Some of the vehicles are within each other's communication range (e.g., v_1 and v_6 in Fig. 3.1 (a)), but some of them are not (e.g., v_1 and v_3 in the same figure). In addition, all vehicles in the ROI can receive packets sent by the RSU. However, the RSU may not receive any information from certain distant vehicles (say v_2 in Fig. 3.1 (a)) because it is out of the transmission range of those vehicles. Such assumptions are on the basis of fact that RSU and OBU have different transmission powers in practice. To be clearly articulated, a corresponding communication graph is explained in the next paragraph. To avoid confusion, throughout the whole chapter, OBU, vehicle and node are interchangeable terms in our discussion.

We let $S = \{v_1, v_2, ..., v_N\}$ and $\Re$ denote the set of all N vehicles in the ROI and the RSU, respectively. We further assume that a vehicle's sensing range is $2r$, and N vehicles in the ROI follow a Poisson point process distribution and the density of vehicles is α vehicles per kilometre. In addition, $d(x, y)$ is the Euclidean distance between any two points x and y on the road, where $x, y \in S \cup \Re$. We define a hybrid communication graph HCG to characterize the topology of the vehicular network, as follows:

Definition: $HCG = (V, E)$ is a communication graph with node set $V = S \cup \Re$ and edge set $E = E_1 \cup E_2 \cup E_3 \cup E_4$. For any two vehicles $v_1, v_2 \in S$, E_1 and E_2 contains bidirected edge (v_i, v_j) if $d(v_i, v_j) \leq r$ and $d(v_i, v_j) > r$, respectively. For $\forall v_x, v_y \in S$, E_3 includes bidirected edge $(v_x, \Re)$ if $(v_x, \Re) \leq r$, while E_4 comprises directed edge $(v_y, \Re)$ if and only if r $< d(v_y, \Re) \leq R$.

(a)
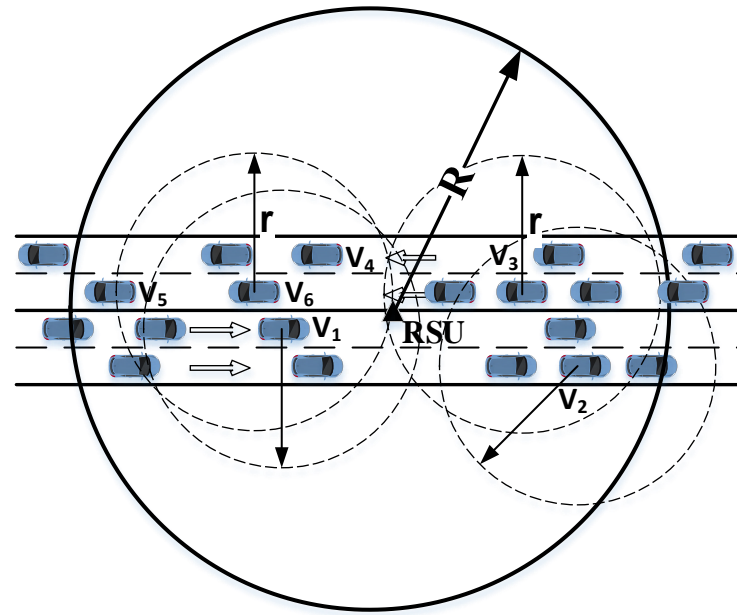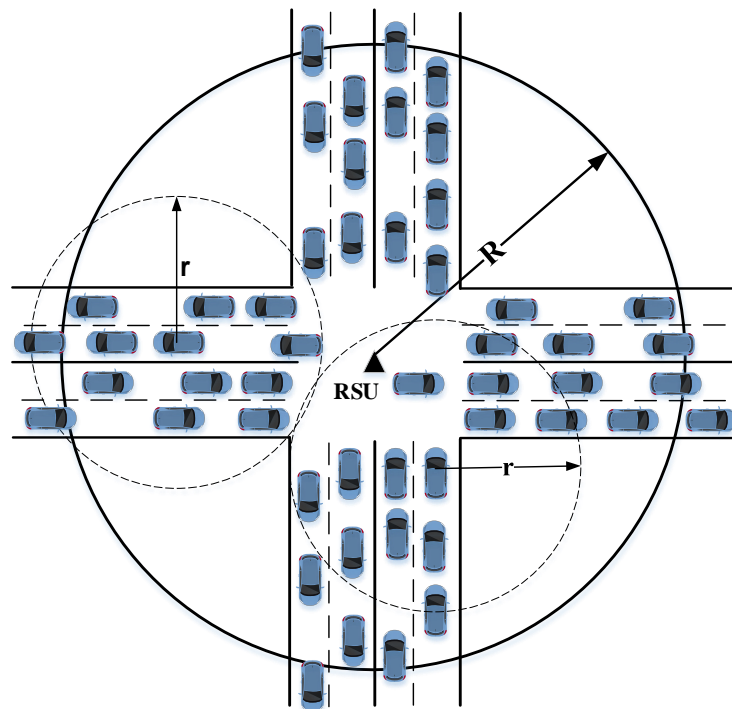
Communication range of vehicle v_i , radius is r

Communication range of RSU, radius is R

RSU node

(b)

Fig. 3.1: Network model of BSM broadcasting in vehicular networks for two typical scenarios: (a) a roadway scenario; (b) an intersection scenario.

In the *HCG*, pairwise vehicles in E_1 are able to communicate with each other directly, vehicles connected by E_2 are able to receive/send signals from/to the RSU. By contrast, vehicles involved in E_3 can only obtain signals from the RSU, but in the opposite direction, their signals cannot reach the RSU.

We assume all OBUs and the RSU can access GPS signal and have been synchronized by a mechanism shown in [67]. Besides, each vehicle generates a BSM packet at the beginning of every control channel (CCH) interval [13], and then the dissemination process is conducted during the whole interval. It is noteworthy that although vehicles may move at a high speed, the network topology can be deemed unchanged during a CCH interval. For example, for a vehicle is travelling at 100 km/h, its position change during one CCH interval of 50ms will be no more than 1.4 meters, which is not considered as significant.

In order to obtain a better performance, we consider adopting three decoders at the physical layer of the RSU: one PNC decoder, one multi-user detection (MUD) decoder and one single user successive interference cancellation (SU-SIC) based decoder [88] [120]. The PNC decoder attempts to decode a packet like $P_{v_a} \oplus P_{v_b}$ based upon the overlapped signals from two nodes, while the MUD decoder attempts to decode two individual packets, P_{v_a} and P_{v_b}, which are sent by two vehicles v_a and v_b, respectively. The SU-SIC decoder is for single-user case. At the MAC layer, both the RSU and OBUs are capable of encoding and decoding RLNC packets, as well as uncoded original packets.

3.2.2 Performance Metrics

1) Packet Delivery Ratio

We denote *PDR(i)* the packet delivery ratio for a vehicle *i* in the ROI. If the vehicle receives *n* packets during a CCH interval, we define *PDR(i) = (n+1)/N*, where *N* is the total number of generated BSM packets in the interval. If a vehicle collects all *N-1* packets, it is able to construct a complete neighbourhood map based on the information contained in those packets. Since each node has had its own BSM packet, the upper bound and lower bound of the PDR for a vehicle should be 1 and *1/N*, respectively. Different nodes may have different PDRs due to its location and channels, so we take the average PDR to evaluate the performance of the entire network.

2) Delivery Latency

Many safety applications in VANETs need to update information timely, so a large delay in BSM delivery is usually intolerable. Let T_d denote the time required to get the BSMs from vehicles in a ROI for making a neighbourhood map of a vehicle. Different number of vehicles may have different delivery latency.

3) Throughput

Throughput is usually defined as how many information bits are received by a node per time unit. With regarding to a network, the network throughput is the sum of per-node throughput over all nodes. This research investigates one-hop BSM packet dissemination in a vehicular network. Therefore, we evaluate the network throughput that exclusively involves the delivery of BSM packet for all vehicles. Let $\chi(i)$ denote total number of BSM packets received at vehicle v_i, since there are N vehicles in the network, the network throughput can be defined as

$$TH = \frac{8l\sum_{i=1}^{N}\chi(i)}{T} \tag{3.1}$$

where T is the overall time spent for all vehicles to complete transmitting their BSM packets, and l is the predefined length of a BSM packet in byte (one byte is equal to eight bits). In DSRC, safety messages are disseminated during the CCH interval (i.e., T_{CCH}). Further, we define a normalized throughput to indicate the relative efficiency of a protocol while considering safety message broadcasting among all nodes in a vehicular network, as follows:

$$TH_{norm} = \frac{\frac{8l\sum_{i=1}^{N}\chi(i)}{T}}{\frac{8N(N-1)}{T_{CCH}}} = \frac{T_{CCH}}{T}\frac{l\sum_{i=1}^{N}\chi(i)}{N(N-1)} \tag{3.2}$$

3.3 Protocol Design

The proposed MAC protocol (called NC-PNC MAC) will be explained in detail in this section. It consists of three consecutive sessions, including a *MAC setup session*, a *CSMA session* and a *PNC session*, as shown in Fig. 3.2, in which the lifetime of BSM packets is defined as the length of a CCH interval.

3.3.1 MAC Setup Session

At the very beginning of each CCH interval, the RSU broadcasts a *polling* message to invite vehicles to join in PNC session. Vehicles that successfully receive the *polling* message reply to the RSU after a short inter-frame space (SIFS) interval through an orthogonal frequency division multiple access OFDMA-based scheme [121]. Each vehicle randomly and independently selects one subcarrier out of N_{sub} subcarriers in the OFDMA. In order to reduce the collision in subcarrier selection, each vehicle randomly chooses one out of N_b transmission batches to transmit its *join* packet, the length of which is very short and only includes its ID and current location. Apparently, if two or more vehicles pick the same subcarrier and the same batch, collisions will be inevitable.

Here we use an approach of random selection to determine how to dedicate carriers to vehicles. On the one hand, the advantage of this method is that it has minimal overhead. Each vehicle can
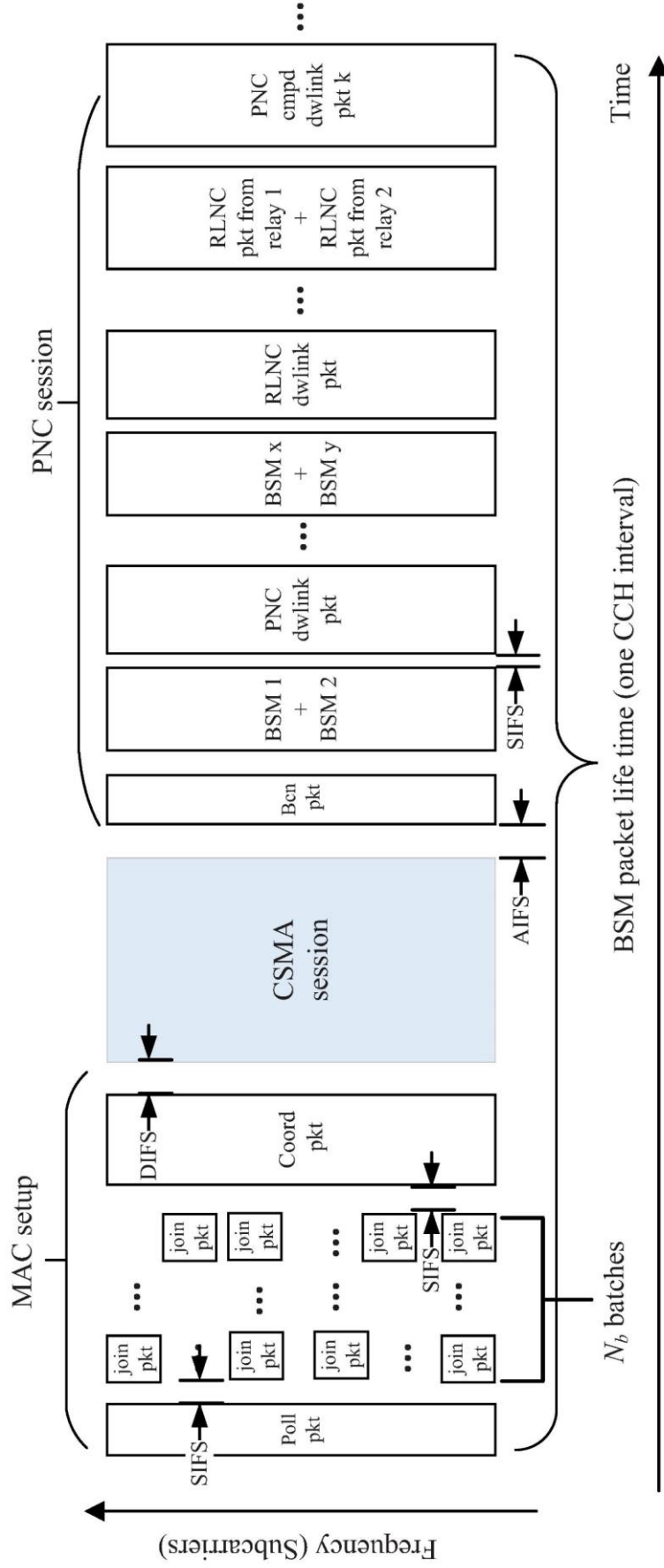
Fig. 3.2: Packet dissemination process in NC–PNC MAC protocol.

randomly adopt one carrier and one batch to send a *join* packet without any extra efforts on coordination. Many hybrid or centralized protocols like [104] and [40] have an extra period of coordination. During this coordination period, vehicles firstly broadcast a *hello* packet to show their presence and then a coordinator is elected. The coordinator can assign each vehicle a transmission time slot. Such methods waste so much time on coordination that there may be not enough time left for BSM dissemination, which may cause great delay. On the other hand, although method of random OFDMA may results in collisions in carrier selection, this problem is overcome by: 1) we can increase the number of batches to make sure the collision probability is as low as 1%[6]; 2) a *CSMA session* is reserved for those vehicles that have collisions during this OFDMA period. Those vehicles still have chance to broadcast their BSM in the subsequent session.

Since each subcarrier is orthogonal in frequency to each other, the RSU is able to know which node can take part in the *PNC session* if no transmission collision takes place for the subcarrier. Then the RSU broadcasts a *coordination* packet to notify all vehicles about which two vehicles form a PNC pair as well as the total number of PNC pairs, according to their instant locations. Here, one PNC pair consists of two vehicles that exchange their safety messages through the PNC scheme [62] during the *PNC session*. To form a PNC pair, the RSU prioritizes two vehicles at different sides of the RSU. For instance, the left-side node v_1 and the right-side node v_3 in Fig. 3.1 (a) can be a PNC pair, but v_2 and v_3 is not a wise choice because both v_2 and $v3$ are at the right side of the RSU.

Assume all PNC pairs form a set $\square$, so $\square \subseteq S$. For the roadway scenario, $\square$ can be further divided into two subsets $\square^L$ and $\square^R$, which stands for vehicles on the left and right side of the RSU, respectively. In a similar way, $\square$ can be divided into four parts ($\square^L$, $\square^R$, $\square^U$ and $\square^D$) for the intersection case. Among all PNC pairs in $\square$, the RSU designates one pair as relay nodes. The relay nodes help those nodes, which lose the opportunity to take part in the *PNC session*, to forward their safety messages. Their roles will be elaborated in the subsection of *PNC session*. In order to have the best coverage of other vehicles, a pair of relay nodes $v_{\text{Re}lay}^L$ and $v_{\text{Re}lay}^R$ must satisfy the following conditions:

$$
\begin{aligned}
v_{\text{Re}lay}^L \in \square^L \text{ and } v_{\text{Re}lay}^L = \arg\max_{v_x \in \square^L} (d(v_x, \Re)), \\
v_{\text{Re}lay}^R \in \square^R \text{ and } v_{\text{Re}lay}^R = \arg\max_{v_y \in \square^R} (d(v_y, \Re)).
\end{aligned}
\tag{3.3}
$$

Proof: Without loss of generality, take the left relay node at first. On the left side of the RSU, for a vehicle $v_x \in \square^L$, since it is communicable to the RSU, so $0 \le d(v_x, \Re) \le r$. Obviously, any vehicle v_i between v_x and RSU is communicable to v_x due to $d(v_x, v_i) \le d(v_x, \Re)$. Therefore, the

---

[6] See the collision probability analysis in section 3 of Chapter 4.

most distant vehicle to the RSU in $\square^L$ (called $\tilde{v}_{\text{Re}lay}^L$) covers the most vehicles in between. On the other hand, assume $\square_{out}^L$ denotes the set of left-side vehicles of the RSU but the distance from the RSU is larger than r (i.e., not in $\square^L$). For an arbitrary vehicle $v_j \in \square_{out}^L$, $d(v_j, \tilde{v}_{\text{Re}lay}^L) \leq d(v_j, v_x)$ where $v_x \in \square^L$ yet $v_x \neq \tilde{v}_{\text{Re}lay}^L$. Therefore, the node $\tilde{v}_{\text{Re}lay}^L$ covers the most vehicles in $v_j \in \square_{out}^L$. Thus, $v_{\text{Re}lay}^L = \tilde{v}_{\text{Re}lay}^L$ is the determined left relay. The conditions for the other relay $v_{\text{Re}lay}^R$ on right sides can be proved correspondingly.

For the intersection scenario in Fig. 3.1 (b), four relays can be elected by using a similar method as descript in equation (3.3).

Since the length of the *poll* packet, *join* packet and *coordination* packet are very short (i.e., the length of a *poll* or a *join* packet is no more than twenty bytes, and the length of a *coordination* packet is less than two hundred bytes), the total time spent on the *MAC setup session* is also very short. The duration can be estimated as follows:

$$T_{setup} = T_{poll} + N_b T_{join} + T_{coord} + N_b T_{SIFS} + T_{DIFS} \tag{3.4}$$

where T_{poll}, T_{join}, and T_{coord} are the transmission time for one *poll* packet, *join* packet and *coordination* packet, respectively, N_b is the total number of batches of OFDMA uplink, and T_{SIFS} (or T_{DIFS}) is the waiting time before sending a *join* packet (or the waiting time before the next session).

3.3.2 CSMA Session

Some nodes may not be able to participate the *PNC session* after the *MAC setup session* because the RSU fails to receive their *join* packets. The failure can be induced by various of factors, including fading channels, long distance to the RSU, disability of sending a *join* packet and so on. Therefore, the RSU cannot arrange an opportunity for those vehicles in the *PNC session*. Among all factors, the dominant one is the subcarrier collision, which means some nodes select the identical data subcarrier at the same transmission batch during the OFDMA uplink stage. The probability of a subcarrier and a batch chosen by n $(n \geq 2)$ nodes at the same time is:

$$P_{coll}(n) = \binom{N}{n} \left(\frac{N_{sub} N_b - 1}{N_{sub} N_b} \right)^{N-n} \left(\frac{1}{N_{sub} N_b} \right)^n. \tag{3.5}$$

Fig. 3.3 illustrates that the collision probability of selecting one subcarrier during the OFDMA decreases as the batch volume N_b increases. In addition, the probability of four or more vehicles picking the same subcarrier is much less than that of two vehicles selecting the same subcarrier
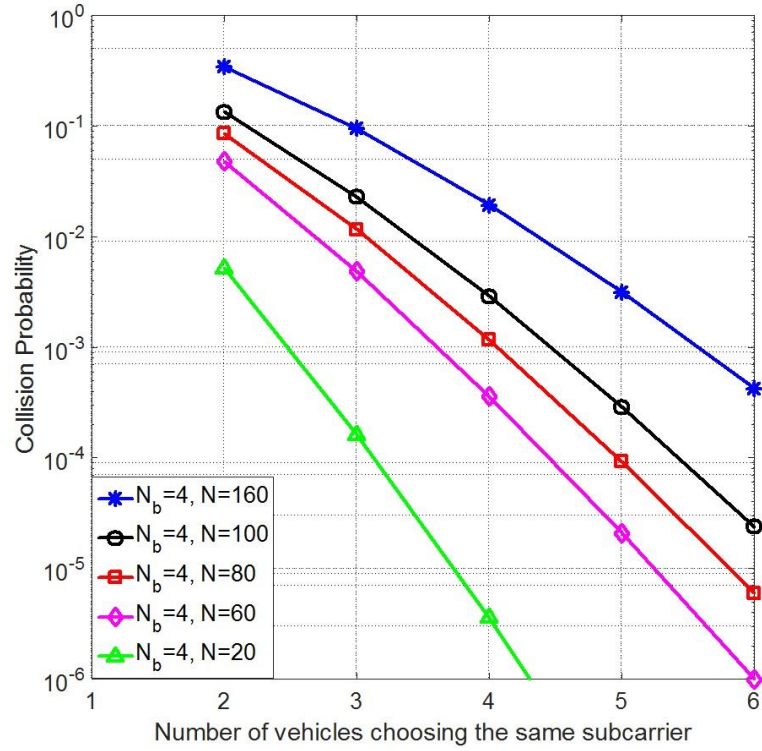
(a) $N_b = 4$
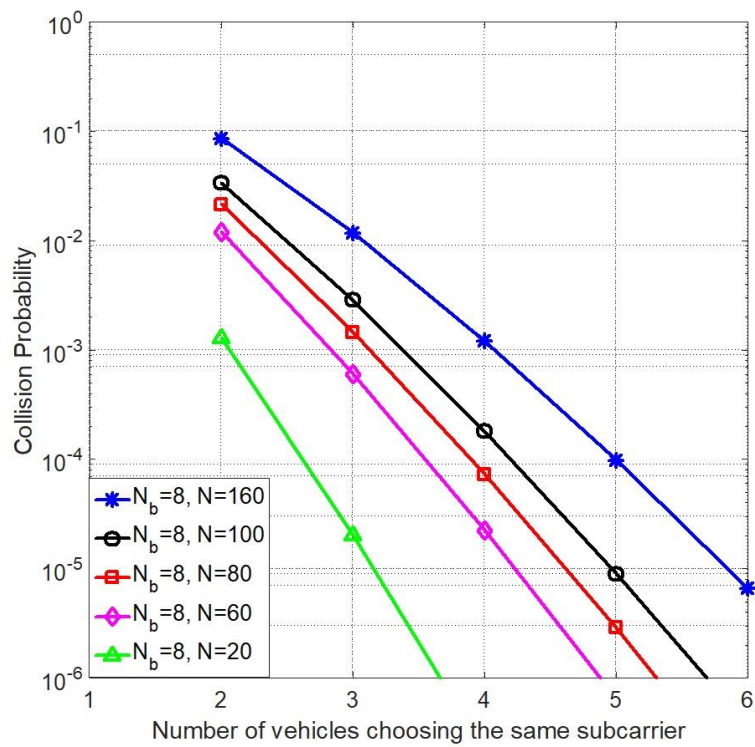
(b) $N_b = 8$

Fig. 3.3: Collision probability $P_{coll}(n)$ of selecting one subcarrier during the OFDMA up-link.

coincidentally. That is, most of OFDMA uplink transmission collisions are caused by selection collisions caused by two vehicles.

Noticeably, it might be that more than one subcarrier and one batch are repeatedly selected (i.e., it may have multiple collisions). The overall collision probability will be analysed in the following part. For all unqualified nodes, the *CSMA session* provides them with an opportunity to broadcast their BSM packets, if $T_{AIFS} > T_{DIFS} > T_{SIFS}$.

During the *CSMA session*, all participants contend for accessing channels and transmitting their safety messages by using the CSMA/CA. Vehicles in the vicinity including the relay nodes can receive these BSM packets and buffer them for further purpose of decoding the PNC packets or RLNC packets, which will be illustrated in the next subsection. The time T_{CSMA} spent on this session can be calculated by:

$$T_{CSMA} = n_{CSMA}T_{BSM} + \sum_{i=1}^{n_{CSMA}} \left(t_{bf}[i] + T_{DIFS} \right), \tag{3.6}$$

where n_{CSMA} is the number of vehicles participating in the *CSMA session*, T_{BSM} is a BSM packet transmission time, $t_{bf}[i]$ denotes a random back off time in the ith transmission.

3.3.3 PNC Session

The RSU launches the *PNC session* after the *CSMA session*. It waits for an arbitrary inter-frame space (AIFS) before broadcasting a beacon packet, which requests the first PNC pair to transmit their BSM packets. After an interval of SIFS, the first PNC pair send their BSM packets simultaneously. The RSU tries to decode the overlapped signals by utilizing the three physical-layer decoders aforementioned in Section 3.3.1. After decoding, the RSU will broadcast a downlink packet, which also notifies the next PNC pair by piggybacking their ID information. Upon receiving, the next PNC pair start the next round of BSM packet exchange, and this process repeats for all PNC pairs until the last one. For the last PNC pair, the process is slightly different from those before. The last pair comprises of two relays (or four relays at each direction for the intersection case). Each relay adopts the RLNC to encode its own BSM packet with other BSM packets buffered during the *CSMA session*. Being different from other non-relay PNC pairs, the relay nodes work in a burst mode: They consecutively conduct M rounds of exchange but with different encoding coefficients for each round. Coding coefficients are randomly generated from Galois field (GF). Here $M = \max(M_L + M_R) + 1$, where M_L and M_R is the number of BSM packets in the buffer of the left and right relay, respectively, taking into account the roadway case.

In order to distinguish different types of packets, the notation P_{v_i}, P_{Relay} and P_{RSU} means a packet sent by a vehicle v_i, a relay and the RSU, respectively. Considering the compatibility, we utilize

the same MAC header of IEEE 802.11p but assign different values in *Frame Control* (FC) field for different types. Meanwhile, to distinguish different types of packets sent by ordinary vehicles, relays or RSU, we assign different values in the *FC* field, which is shown by Fig. 3.4 and Table. 3.2.

Table 3.2: FC values for different types of signals in NC-PNC MAC.

Packet Type	FC Value
Polling signal from RSU P_{RSU_poll}	0x2001
Join signal from OBU $P_{v_i\_join}$	0x2002
Coordination signal from RSU P_{RSU_coor}	0x2003
Original BSM signal from OBU P_{v_i}	0x1000
Trigger (Beacon) signal from RSU P_{RSU_bcn}	0x2004
PNC signal from RSU P_{RSU}^{PNC}	0x1801
Compound PNC signal from RSU P_{RSU}^{comp}	0x1802
RLNC signal from RSU P_{RSU}^{RLNC}	0x1803
RLNC signal from relay P_{Relay}^{RLNC}	0x1804

Bytes:	2	4	6	6	6	2	2	0-2312	4
	FC	Dur	Addr1	Addr2	Addr3	Seq Ctrl	QoS Ctrl	Payload	FCS
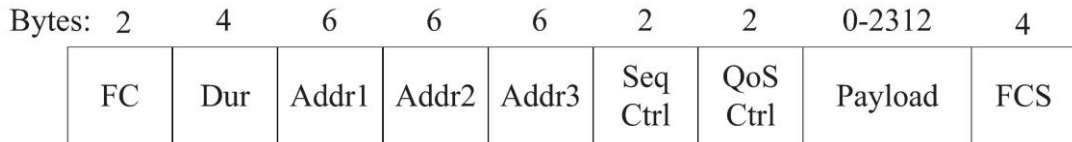
Fig. 3.4: IEEE 802.11p MAC header.

According to three physical-layer decoders in the RSU, the decoding results based upon the superimposed uplink signals would be one of the following:

1) *One lone packet*: e.g., only packet P_{v_4} from the vehicle v_4 is decoded by the MUD decoder or the SU-SIC decoder;

2) A bit-wise coded packet: e.g., $P_{v_4} \oplus P_{v_5}$ through the PNC decoder;

3) Two lone packets: e.g., both P_{v_4} and P_{v_5} through the MUD decoder;

4) No packet is obtained.

For case 2) and 3), the RSU will transmit a downlink packet such as $P_{RSU}^{PNC} = P_{v_4} \oplus P_{v_5}$. For case 1), it will buffer a lone packet at first, and then transmit an encoded RLNC packet $P_{RSU}^{RLNC} = \sum_i h_i P_{v_i}$, where P_{v_i} is a previously buffered lone packet and h_i is a random coefficient generated in GF field. In case 4), the RSU will also send an encoded packet by encoding the buffered lone packets but with different coefficients in case 1). To ensure vehicles can decode all lone packets, we conceive a lower triangular matrix for all h_i. That is, when the RSU obtains a lone packet at the first time, it just forwards it to all vehicles without encoding. Then, at the second time, it encodes the two packets (one is the packet stored at the first time) and broadcasts the encoded packet. Similarly, at the tth time when the RSU decodes a lone packet, it encodes all t packets and broadcasts the encoded packet for downlink.

As pointed out above, relay nodes generate and transmit M distinct uplink packets. As a case in point, if v_1 and v_3 are selected as relay nodes in Fig. 3.1, the kth ($1 \le k \le M$) two compound uplink packets generated at two relay nodes are:

$$
\begin{aligned}
P_{\text{Re}lay}^{L}(k) &= \sum_{i=1}^{M_L} d_{ki} P_{v_i} \\
P_{\text{Re}lay}^{R}(k) &= \sum_{j=1}^{M_R} c_{kj} P_{v_j}
\end{aligned}
\tag{3.7}
$$

respectively, where d_{ki} (or c_{kj}) are random coefficients at node v_1 (or v_3), and P_{v_i} (P_{v_j}) are its own packet as well as packets stored during the *CSMA session*. Based on the two RLNC uplink packets shown by (3.6), the PNC decoder of the RSU may generate a downlink packet also called a compound downlink packet as follows:

$$
P_{RSU}^{comp}(k) = P_{\text{Re}lay}^{L}(k) \oplus P_{\text{Re}lay}^{R}(k) = \left(\sum_{i=1}^{M_L} d_{ki} P_{v_i} \right) \oplus \left(\sum_{j=1}^{M_R} c_{kj} P_{v_j} \right).
\tag{3.8}
$$

After receiving a downlink packet, each PNC pair are able to obtain their desired information by XORing the downlink packet with their own packets. Notably, nodes that have collected sufficient number of compound downlink packets can also obtain all individual packets $P_{v_i} \forall i$ ($P_{v_j} \forall j$) by carrying out the Gaussian Elimination.
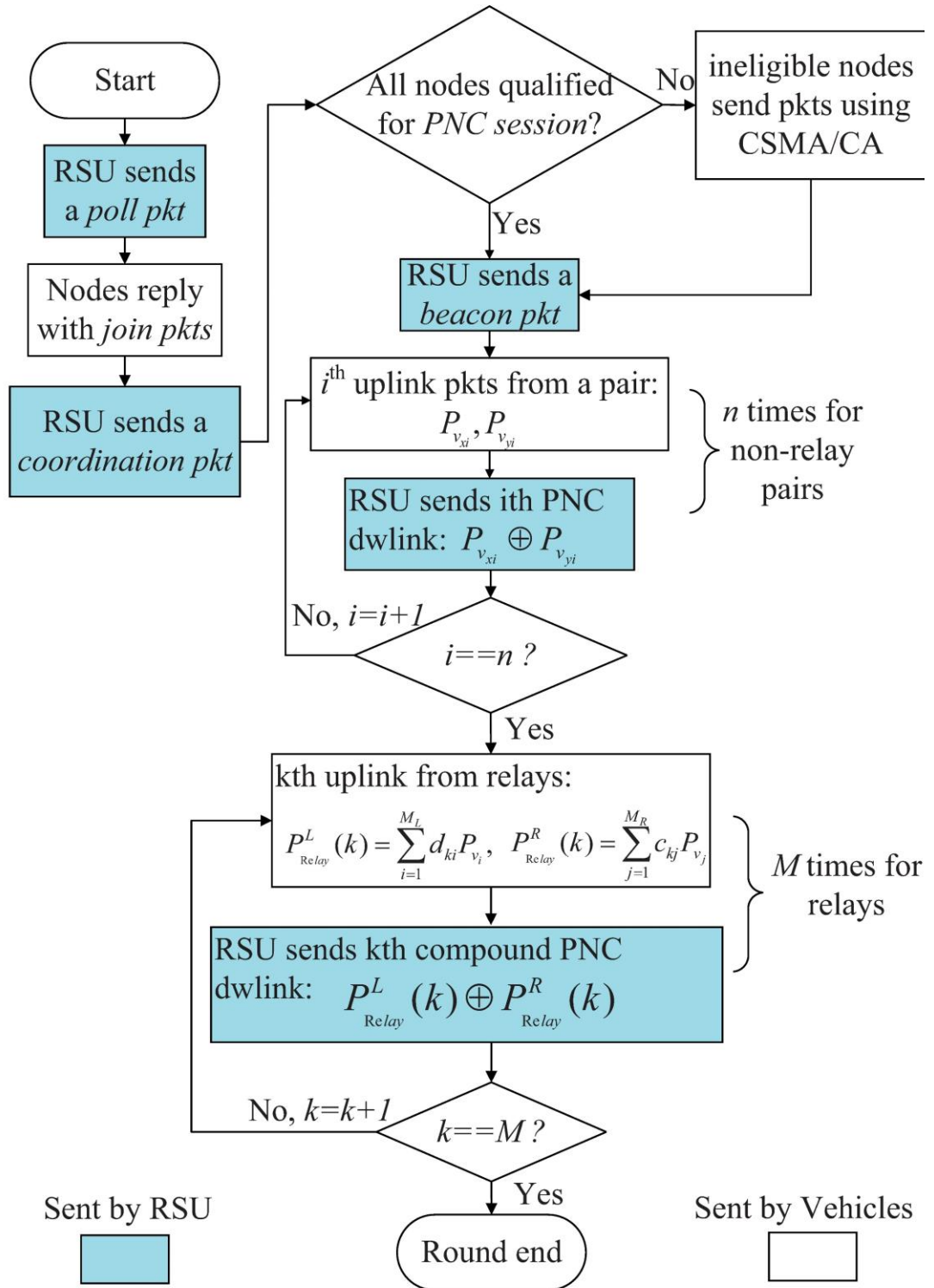
Fig. 3.5: Applied methodologies in the NC-PNC MAC.

An interesting and remarkable phenomenon is that some other vehicles also possibly restore original packets when receiving downlink packets that belong to other PNC pairs if they can overhear the corresponding uplink packets. Moreover, for a relay node, since it has the best coverage, most of the surrounding vehicles get benefits from decoding compound downlink packets, since those nodes can overhear the compound uplink from the relay. This characteristic is helpful to disseminate BSM packets. On the other hand, some vehicles may not overhear all uplink packets, so they cannot restore the original packets even though they have received downlink packets from the RSU. This issue will be tackled by our extended multiple relay scheme, which will be articulated in Chapter 4.

The total time spent on *PNC session* is:

$$
\begin{aligned}
T_{PNC} &= (n_{PNC} - 1)\left(T_{up} + T_{down}\right) + \sum_{i=1}^{M}\left(T_{up} + T_{down}\right) + 2T_{SIFS}\left(M + n_{PNC} - 1\right) + T_{AIFS} \\
&= 2\left(M + n_{PNC} - 1\right)\left(T_{BSM} + T_{SIFS}\right) + T_{AIFS}.
\end{aligned}
\tag{3.9}
$$

where $T_{up} = T_{down} = T_{BSM}$ are transmission time for one uplink packet or downlink packet, and n_{PNC} is the total number of PNC pairs.

The proposed MAC involves a series of methodologies. For the first session and the second session, it applies the OFDMA and the CSMA/CA, respectively. Both of them are widely used in many existing networks, such as LTE cellular networks and WiFi networks. Therefore, we highlight the ones adopted in the *PNC session*. As depicted by Fig. 3.5, during each uplink, a pair of nodes or relays transmit their BSMs independently and simultaneously, then the RSU broadcasts a downlink packet by employing PNC. The non-relay nodes send original BSMs only once for uplink, while the relays transmit encoded packets (by using RLNC) for uplink multiple times.

3.3.4 Collision Probability for Subcarrier Selection

As aforementioned, when each vehicle randomly and independently chooses one batch and one subcarrier to transmit its *join* packet, it may lead to transmission collisions. In this section, we will firstly derive the proportion of vehicles that involves in carrier collisions.

In order to figure out how many vehicles involved in the subcarrier collision, we firstly calculate the repeated times of selected subcarriers. The whole process can be equivalent with the case that N vehicles randomly pick up subcarriers out of $S = N_b N_{sub}$ subcarriers, where N_b is the batch volume and N_{sub} is the number of data carriers at the physical layer. Apparently, N subcarriers will be selected (including the repeated ones). Let Ψ denote the set of selected subcarriers and x_i is the ith subcarrier in this set, where $x_i \in \Psi$ and $1 \le i \le N$. We define an indicator I_{x_i} as follows:

$$I_{x_i} = \begin{cases} 1, \text{if } x_i \text{ has appeared in } \Psi \\ \quad 0, \text{otherwise} \end{cases} \tag{3.10}$$

The probability for $I_{x_i} = 0$ and $I_{x_i} = 1$ are

$$
\begin{aligned}
P_{(I_{x_i}=0)} &= \left(\frac{S-1}{S}\right)^{i-1}, \\
P_{(I_{x_i}=1)} &= 1 - \left(\frac{S-1}{S}\right)^{i-1}.
\end{aligned}
\tag{3.11}
$$

Therefore, the expectation of repeated times for all subcarriers in Ψ is:

$$E\left[N_{rp}\right] = E\left[\sum_{i=1}^{N} I_{x_i}\right] = \sum_{i=1}^{n} P_{(I_{x_i}=1)} = N - S\left[1 - (1 - \frac{1}{S})^N\right]. \tag{3.12}$$

In addition, the probability of choosing one certain subcarrier out of S subcarriers only once is $\binom{N}{1}\left(\frac{S-1}{S}\right)^{N-1}\frac{1}{S}$, and the probability of a certain subcarrier never chosen is $\binom{N}{0}\left(\frac{S-1}{S}\right)^{N}$.

Therefore, the proportion of vehicles colliding in subcarriers is

$$
\begin{aligned}
P_{veh\_coll} &= \frac{S\left[1 - \binom{N}{1}\frac{1}{S}\left(\frac{S-1}{S}\right)^{N-1} - \binom{N}{0}\left(\frac{S-1}{S}\right)^{N}\right] + E\left[N_{sub\_repeat}\right]}{N} \\
&= 1 - (1 - \frac{1}{N_b N_{sub}})^{N-1}.
\end{aligned}
\tag{3.13}
$$

3.3.5 Communication Complexity

We will examine the communication complexity of the proposed NC-PNC MAC. Generally, a protocol's communication complexity means the number of packets transmitted in function of the total number of nodes of a network. It can be deemed as an evaluation of a protocol's complexity and efficiency.

Assume N vehicles in the vehicular network and let *TNP* be the total number of packets sent by all vehicles and the RSU, so *TNP* is equal to the sum of packets in each session, i.e., $TNP = TNP_1 + TNP_2 + TNP_3$ (there are three sessions in the protocol: *MAC setup session, CSMA session and PNC session*).

During the first session, vehicles send their join packets following the polling packet. Therefore, $TNP_1 \leq N + 2$ because N join packets are sent at most.

Based on Equation (3.13), the number of vehicles that transmit their BSM packets during the CSMA *session* is $\lceil NP_{veh\_coll} \rceil$. Therefore, $TNP_2 = p_{csma}^t \lceil NP_{veh\_coll} \rceil \leq \lceil N - N(1 - \frac{1}{N_b N_{sub}})^{N-1} \rceil$,

where p_{csma}^{t} is the probability that a node transmits without collision during the *CSMA session* and has been derived in [48].

During the last session, the remaining $\left\lfloor N(1-\dfrac{1}{N_b N_{sub}})^{N-1} \right\rfloor$ vehicles will exchange their packets by using PNC. Among those vehicles except relays, each vehicle will transmit only one uplink packet, while every relay node broadcast multiple uplink RLNC packets. As mentioned in the manuscript, the relay nodes encode and forward packets from collided vehicles and remote vehicles. The former part has $\left\lceil NP_{veh\_coll} \right\rceil$ vehicles. For the latter, since vehicles distribute randomly and independently, the number of vehicles can be covered by relays are approximately $\left\lceil N\dfrac{r}{R-r} \right\rceil$.

For all occasions, the RSU will broadcast the same amount of downlink packets as uplink packets. Thus, we have

$$TNP_3 = 2\left(\left\lfloor N\left(1-P_{veh\_coll}\right) \right\rfloor + \left\lceil NP_{veh\_coll} \right\rceil + \left\lceil N\frac{r}{R-r} \right\rceil + n_r \right) \le 2N\frac{2R-r}{R-r} + 2n_r + 2, \quad (3.14)$$

where n_r denotes the number of relays ($n_r = 2$ for the roadway case, $n_r = 4$ for the intersection case). Finally, the upper bound of total number of transmissions for each round of message exchange is

$$TNP \le 2N\frac{2R-r}{R-r} - N(1-\frac{1}{N_b N_{sub}})^{N-1} + 2n_r + 5 \le 2N\frac{2R-r}{R-r} + 2n_r + 5 \quad (3.15)$$

Obviously, the communication complexity of NC-PNC MAC is linear and can be expressed as $O(N)$. The conclusion will be validated in the simulations in the following subsection.

Table 3.3: Key Physical and MAC Layer Parameters in Simulation.

Parameter	Value
Channel Frequency	5.9 GHz
Transmission Power	RSU: 45dBm; OBU: 30dBm to 40dBm
Path Loss Exponent / GF size	3.5 / 256
Number of Vehicles N/ Number of batches N_b	20 to 160 / 4 (N < 80) or 8 (N ⩾ 80)
Data Rate / BSM Packet Size	3 Mbps to 27 Mbps / 200 Bytes
Vehicle velocity / N_{sub}/ CW	10 to 30 m/s / 48 / 63
SIFS/DIFS/AIFS	16us/32us/48us

3.4 Simulation results

In this part, we first present the simulation setup for our proposed NC-PNC MAC protocol. The simulation tool we use is NS-3 [63]. Then we use simulation data to evaluate its performance and compared it with benchmarks selected from existing schemes in other relevant studies.

3.4.1 Simulation Setup

The simulation is set up according to the system model in Section 3.2. The key physical and MAC layer parameters are listed in Table 3.3. The dissemination of BSM packets experiences Nakagami fading. The probability density function of the signal amplitude X is subject to

$$f_X(x) = \frac{2m^m x^{2m-1}}{\Gamma(m)\omega^m} e^{\frac{-m}{\omega}x^2} \tag{3.16}$$

where we assume fading figure m is 1.5 (for distance less than 80m) and 0.8 (for distance larger than 80m), according to empirical measurements [122]. In addition, a so-called log-distance path loss model is added. In the simulation, vehicles distribute randomly on each lane and move with a constant speed. We run the simulation 500 times. For each time, the whole process depicted by Fig. 3.2 is continuously conducted 100 rounds, and vehicles have different initial positions and moving speed.

In order to validate the effectiveness and efficiency of the proposed protocol, we also choose several other MAC protocols as benchmarks with the same configuration. These protocols are IEEE 802.11p, which utilizes CSMA/CA to access channels, NC Relaying scheme [46], in which both RSU and vehicles are able to encode and forward the message they received, and RSU-NC [100], in which RSU carries out RLNC scheme to relay packets while vehicles still adhere to CSMA/CA.

The communication range can be changed by adjusting transmission power. The definition of a communication range is that vehicles can receive the transmitted packet more than 95% probability within this range. According to this, in our simulation, the communication range is 100 m, 150 m, 200m and 300 m, corresponding to the transmission power of 30 dBm, 35 dBm, 40 dBm and 45 dBm, respectively.

Two mobility models are used in the simulations. For the roadway scenario shown in Fig. 3.1 (a), vehicles travel on a section of a road at a constant speed. By adopting the constant speed model we simulate a scenario where vehicles move on a highway. For the intersection scenario shown in Fig. 3.1 (b), a realistic model is adopted. Vehicles slow down or even stop when they approach the intersection, in which a roundabout is used to ensure the safety. After passing the intersection, they may accelerate and leave the area.

3.4.2 Batch Volume Selection in OFDMA Uplink

It is necessary to be aware of the probability of subcarrier collision while specifying an appropriate value for N_b in simulations. The probability of vehicles involving in carrier collisions are given in equation (3.13). To validate the theoretical analysis of the probability, simulations are conducted. According the PHY of DSRC, the number of data subcarrier is 48. Thus, we take N_{sub} =48 in both simulations and analysis. Fig.3.6 shows the trend of proportions of vehicles involved in subcarrier collisions. Apparently, more vehicles and fewer uplink batch N_b will cause more collisions, which conforms to our expectation. In addition, it is evident that the analytical model precisely predicts the collision proportions as any two relevant curves are overlapped.

To keep the collision probability on a low level and according to Fig. 3.6, we need to keep N_b as large as possible. However, this strategy will expand the *MAC setup session*, thus enlarging the delivery latency substantially. Therefore, to keep balance between collision probability and time consumption, we set $N_b = 4$ if the number of vehicle is less than 80, else $N_b = 8$ in the simulation. Fig. 3.7 reveals the effect of such strategy. It illustrates that the time spent on the *MAC setup session* almost doubles when the number of vehicles increases from below 80 to above 80.
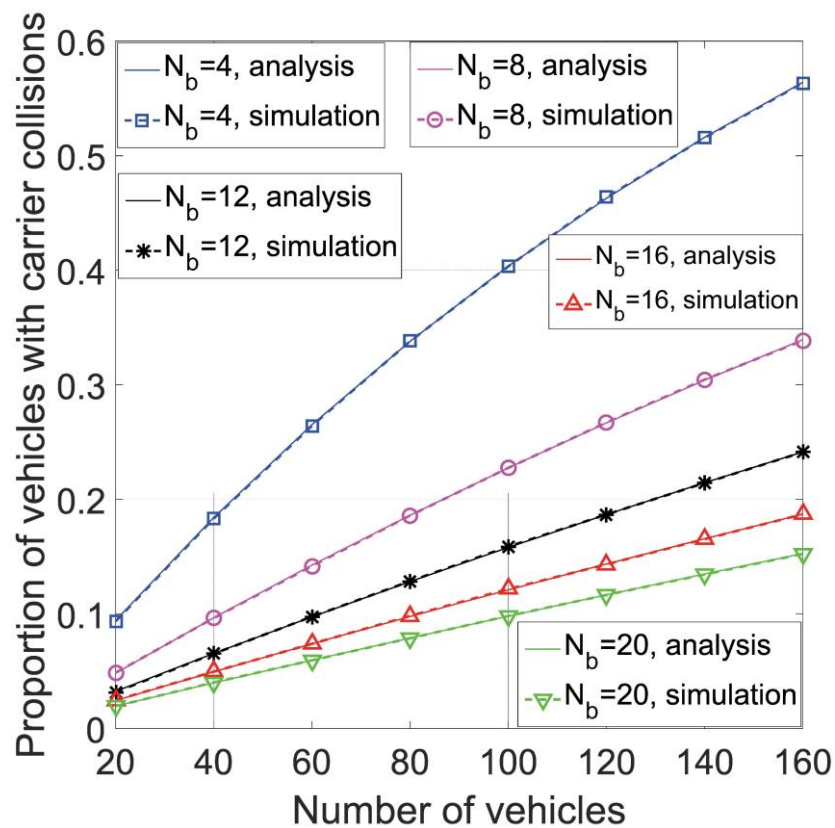

Fig. 3.6: Proportion of vehicles involved in subcarrier collisions.

3.4.3 Simulation Results and Discussions

As mentioned before, BSM packets contain real-time safety information. Each BSM packet has a limited lifetime and it should be disseminated within a certain period. Apparently, the proposed protocol

consumes different amount of time as the number of vehicles varies. Fig. 3.7 illustrates the average time consumed (e.g., $T_{setup} + T_{CSMA} + T_{PNC}$) for two scenarios with two typical data rates. The latency increases linearly as the number of vehicles increases, which is substantiated by the communication complexity in Section 3.3.5. It can be up to 95 ms (or 99 ms) in the roadway scenario (or the intersection scenario) for 160 vehicles with a 6 Mbps data rate. Remarkably, under the same condition (i.e., the same data rate and the same number of vehicles), the latency of the intersection case is larger than that of the roadway case, because there are one more pair of relays in the intersection, which need more time to exchange compound packets shown in (3.7) and (3.8).

The PDR performance of the proposed NC-PNC MAC is evaluated in Fig. 3.8 with respect to the proportion $r/R = 1/3$ and data rate = 6Mbps. In order to be fair, the three benchmarks spend the same time period of the NC-PNC MAC. Compared with three benchmarks, the NC-PNC MAC significantly improve the PDR performance in both scenarios as well as different networks with varied vehicle density. Unlike benchmarks, it can maintain a relative high PDR (no less than 0.8) even when the number of vehicles reaches 80. By contrast, the PDR curves of others plunge as the number of vehicles increases. The benefit firstly stems from the property of the NC-PNC MAC, which effectively suppresses collisions, because BSM transmissions mainly take place during the collision-free *PNC session* and only a small part of vehicles involves in the *CSMA session*. In addition, by virtue of relays and the RSU, remote nodes and nodes with transmission collisions can also broadcast their safety messages by integrating RLNC and PNC. However, the collision rate in other schemes is inevitably high, especially for dense vehicular networks. Thus, massive packets are lost, and a high PDR cannot be ensured.

To see how the proportion of two communication ranges r and R affects the PDR performance, we compare the PDR for different proportions, as shown in Fig. 3.9. The simulation results show that with the increase of r/R, a better PDR performance can be reached. The reason is that when the proportion goes up, more edges are included in the set E_1 and E_3 in *HCG*. As a result, more vehicles can communicate with each other directly and may take part into the *PNC session*, which in turn lead to a larger PDR.

Data rate is another key factor that can impose on PDR performance in vehicular networks. Generally, a vehicular network with dense vehicles may need more time to complete a round of dissemination. To avoid exceeding the lifetime of the safety messages, higher data rate should be considered for those networks. At physical layer, different data rates imply applying different

coding rates and modulations, which have impacts on packet error rate at reception. The curves in Fig. 3.10 is the PDR performance for a network adopting various typical data rates specified in [13]. Lower data rates result in a better PDR performance, which meets our expectation. More importantly, despite with a high data rate of 12 Mbps, compared with other schemes using a lower data rate of 6 Mbps, the proposed MAC has a much better PDR performance than IEEE 802.11p and even maintains the same level as the NC based scheme [46] (see Fig. 3.8).

We further evaluate the overall throughput for the entire network, as the network throughput can embody the efficiency of data exchange among different nodes. Fig. 3.11 sketches the network throughput in absolute values. In both scenarios, the proposed NC-PNC MAC outperforms other three counterparts, which means the MAC works more competently and efficiently for BSM dissemination among vehicles in the RoI. In addition, the throughput curve of NC-PNC MAC increases linearly against the number of vehicles goes up and the gap between our protocol and any other in benchmarks enlarges as the density of vehicles increases. Apart from the absolute throughput, a normalized one is also provided in Fig. 3.12. The normalized throughput is a relative value that stands for how much the real throughput is better than the DSRC standard. Again, we observe that the NC-PNC MAC has the largest normalized throughput among all schemes. A normalized value larger than 1 means a protocol spends less time than a CCH interval completing BSM dissemination in the network. The value descends gradually as the vehicle volume increases because it takes more time in a denser network, which meets our expectation.

The impact of travelling speed on PDR performance is shown in Fig. 3.13. We increase the moving speed from 10m/s to 30m/s and plot three curves under the same condition of r/R=1/3 and data rate = 6Mbps. There is no significant difference among three curves. Therefore, from all figures listed above, we can safely draw a conclusion that even if vehicles have a high moving speed up to 30m/s, the PDR performance of the proposed NC-PNC MAC in VANETs still keeps on the same level of a low-speed case. The results are consistent with those from [35]. To understand the above phenomenon, we need to examine the physical layer of DSRC [13]. The design of physical layer in DSRC has considered the features of high-speed mobile communications in VANETs. On one hand, it applies OFDM scheme and its specially designed preamble can overcome the issues caused by Doppler shift. On the other hand, the subcarrier frequency spacing (e.g., 156 KHz) in OFDM is much larger than the Doppler spread (e.g., 0.58 KHz to 1.1 KHz), according to a study [135]. Such large subcarrier spacing can absorb the impact of Doppler spread induced by vehicle-level mobility. Therefore, the influence of mobility on PDR turns to be negligible.
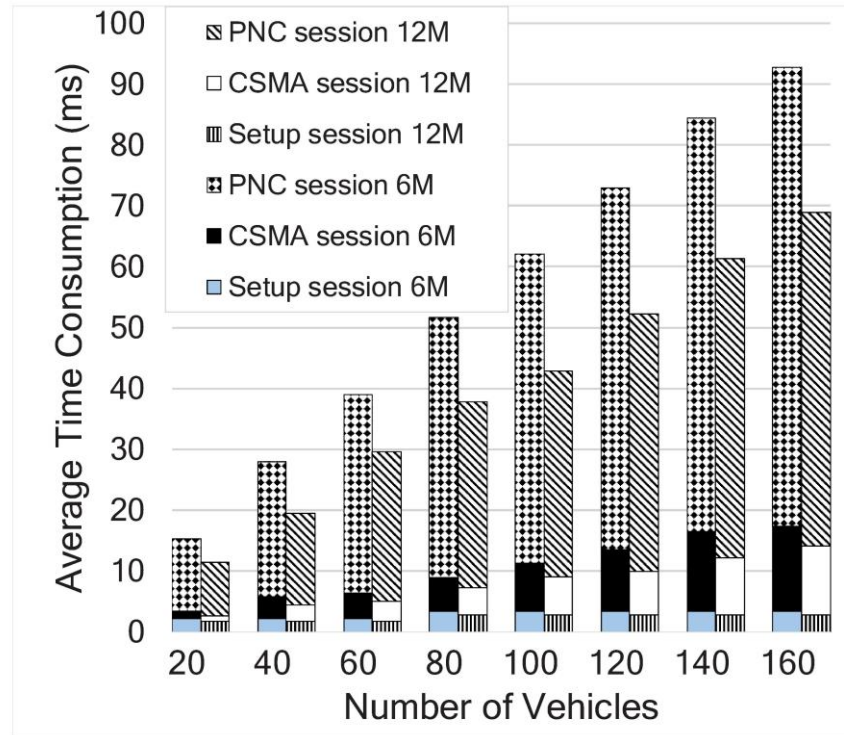
(a)
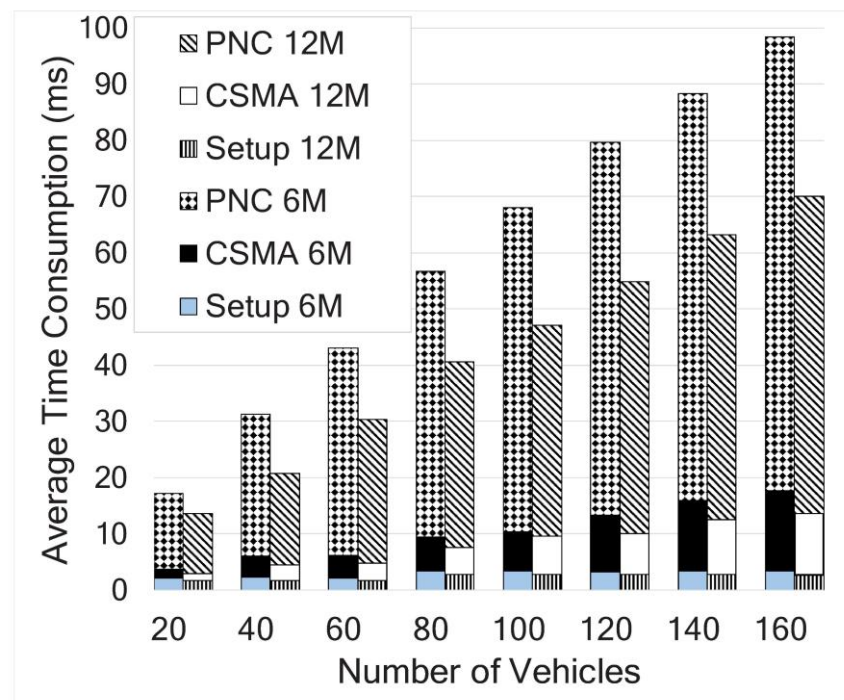
(b)

Fig. 3.7: Average time consumed of each session with different number of vehicles in: (a) the roadway scenario; (b) the intersection scenario.
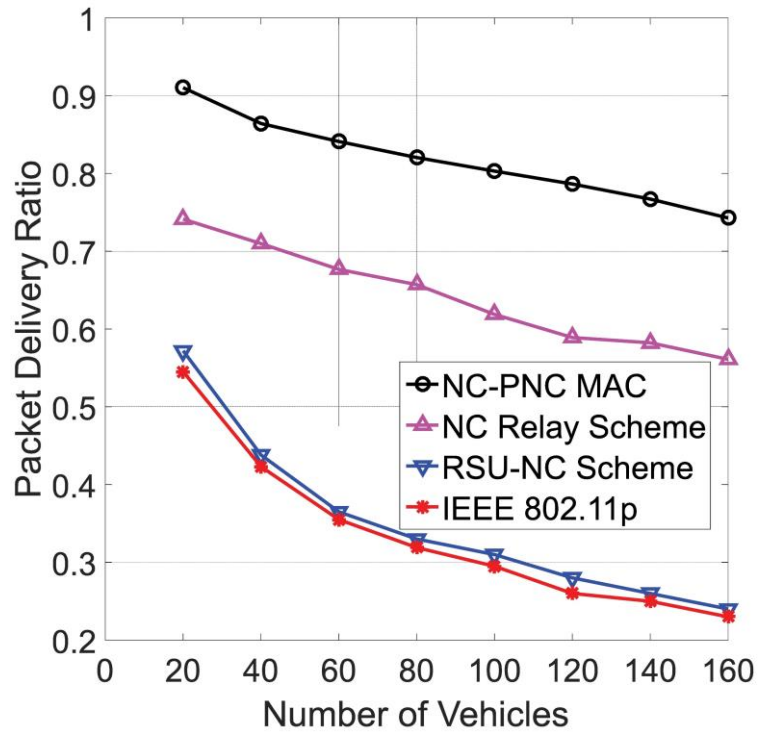
(a)
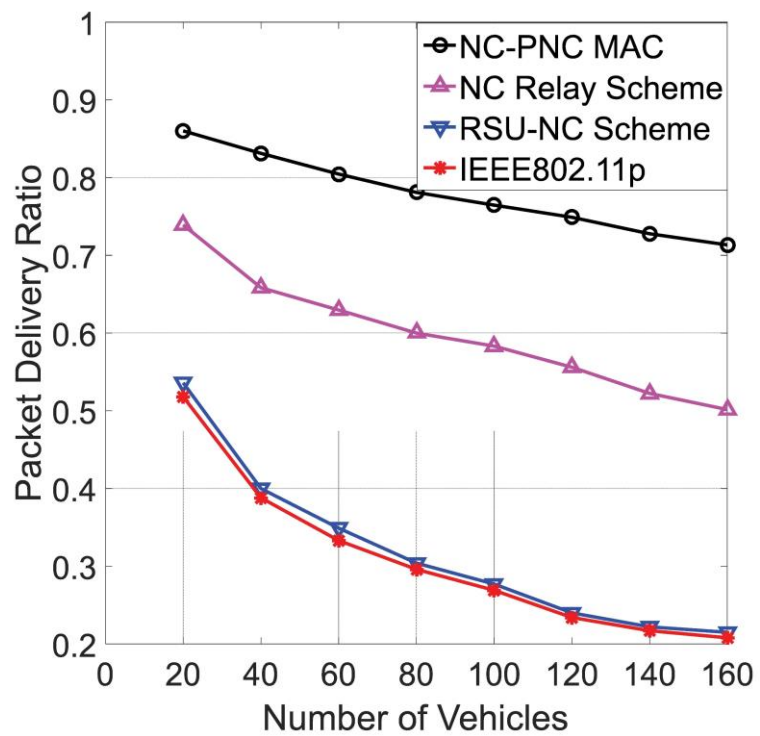
(b)

Fig. 3.8: PDR comparison among NC-PNC MAC and other existing schemes for: (a) the roadway scenario; (b) the intersection scenario.
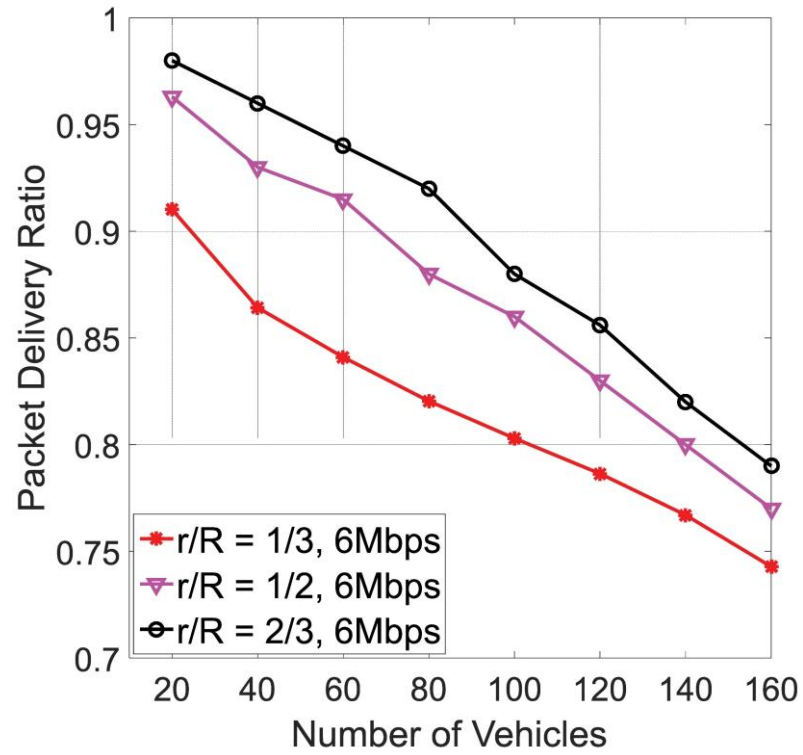
(a)
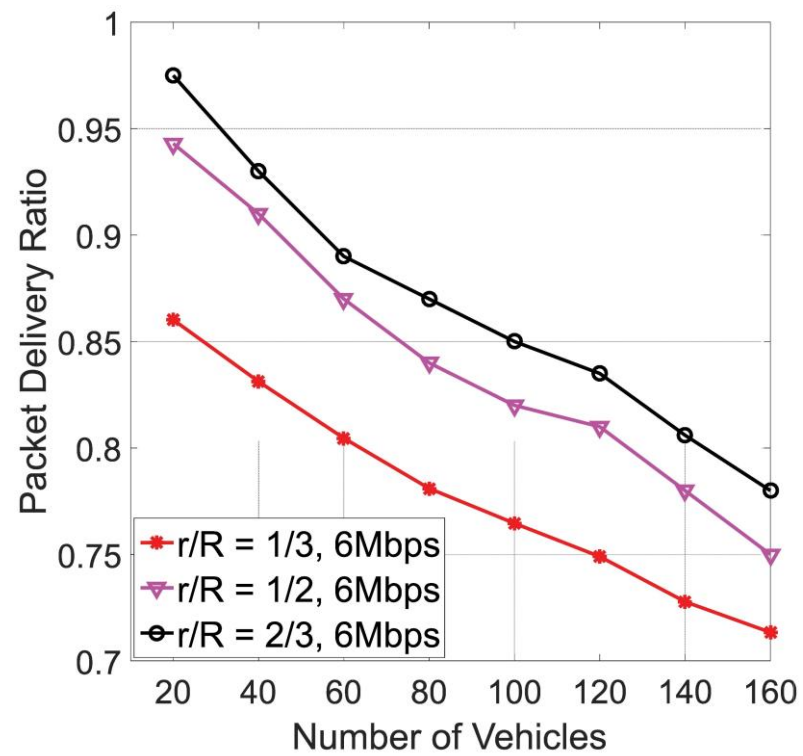
(b)

Fig. 3.9: PDR performance for different proportions of two communication ranges in: (a) the roadway scenario; (b) the intersection scenario.
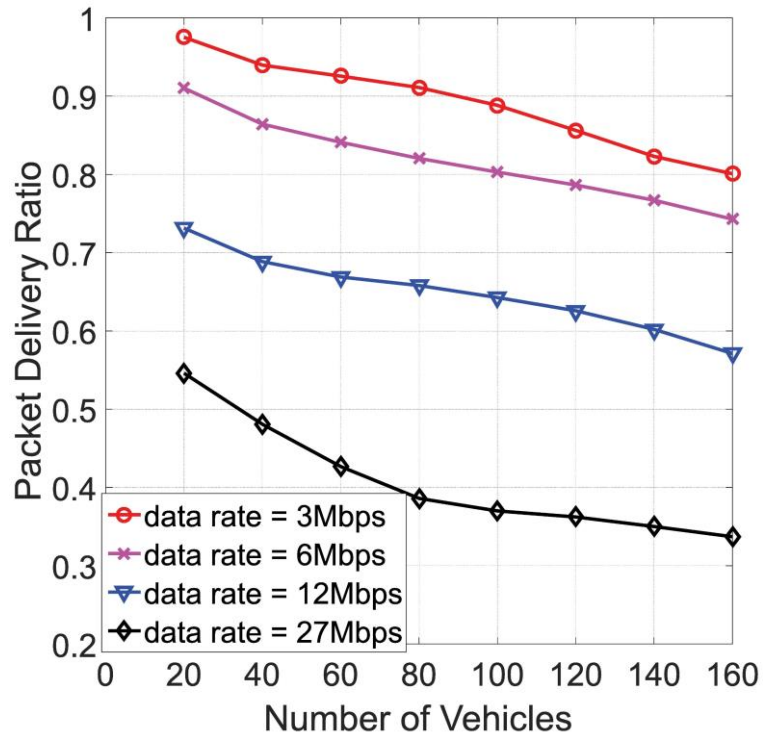
(a)
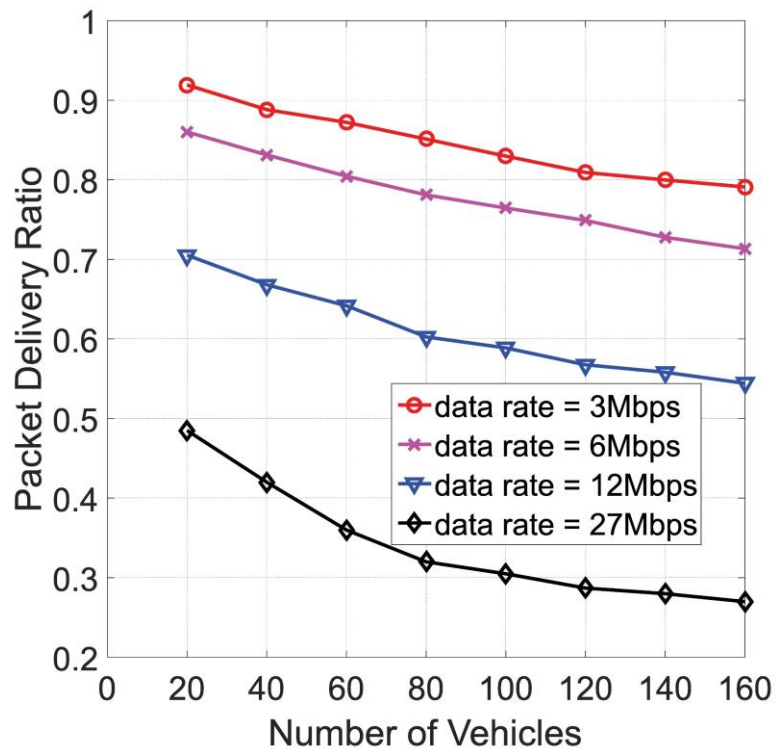
(b)

Fig. 3.10: PDR performance for different data rates in: (a) the roadway scenario; (b) the inter-section scenario (r/R=1/3).
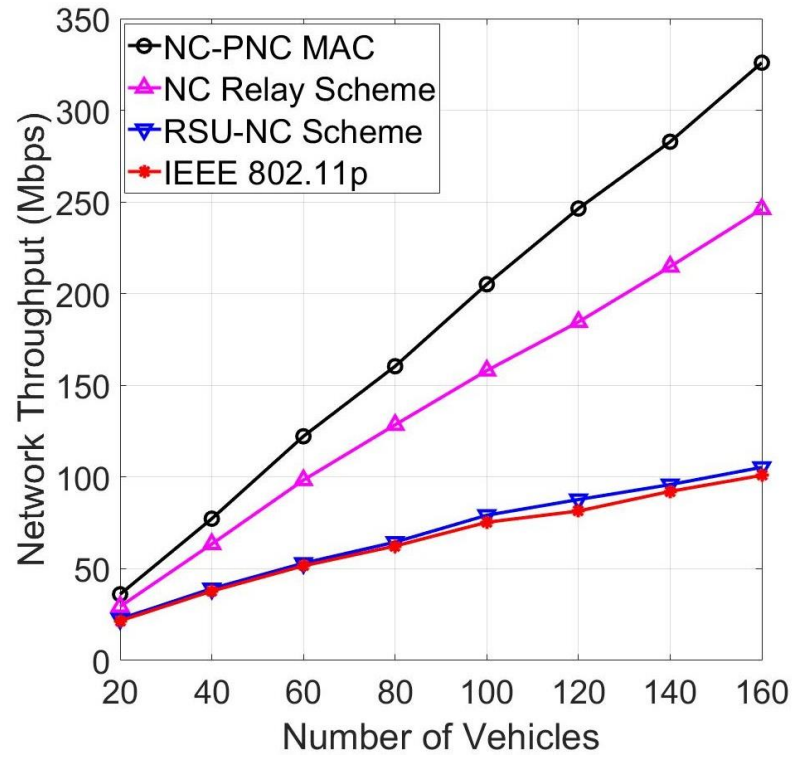
(a)
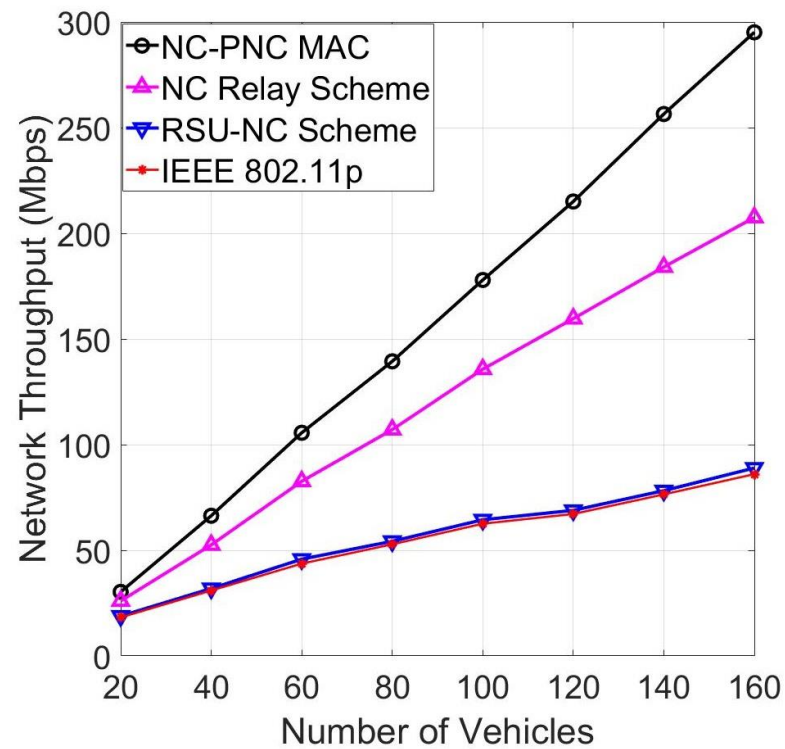
(b)

Fig. 3.11: Network throughput comparison among NC-PNC MAC and other existing schemes for: (a) the roadway scenario; (b) the intersection scenario.
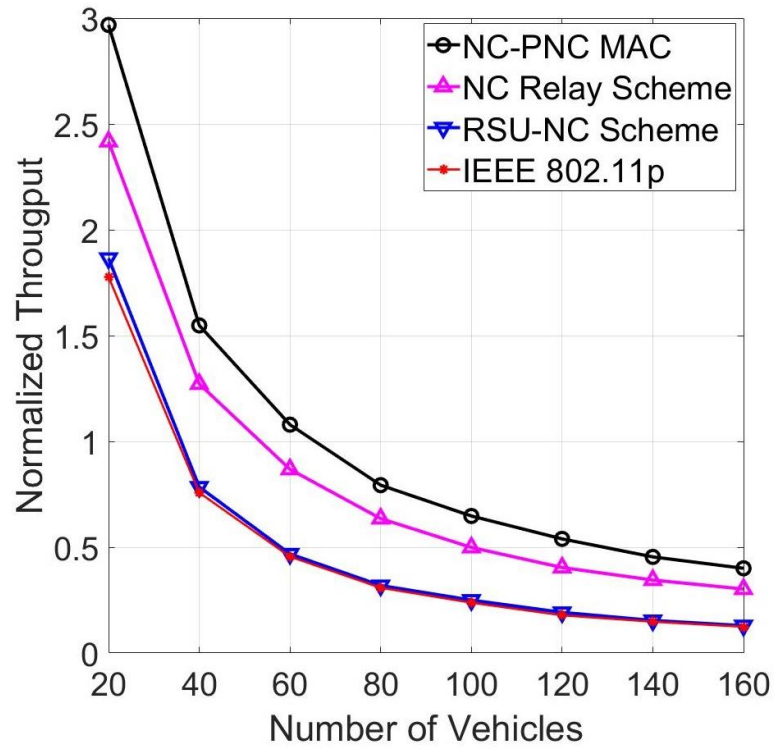
(a)
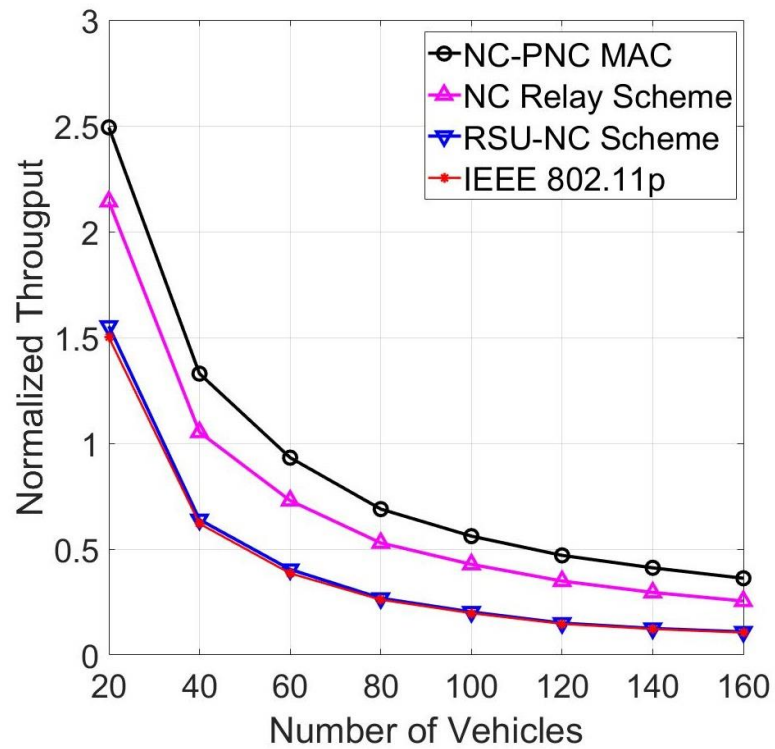
(b)

Fig. 3.12: Normalized throughput comparison for: (a) the roadway scenario; (b) the intersection scenario.
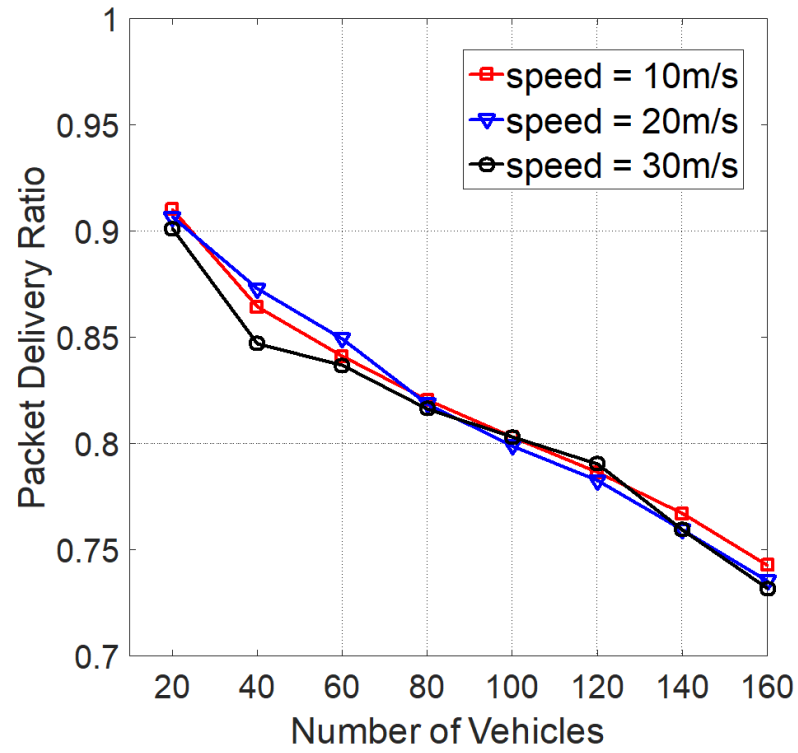
(a)
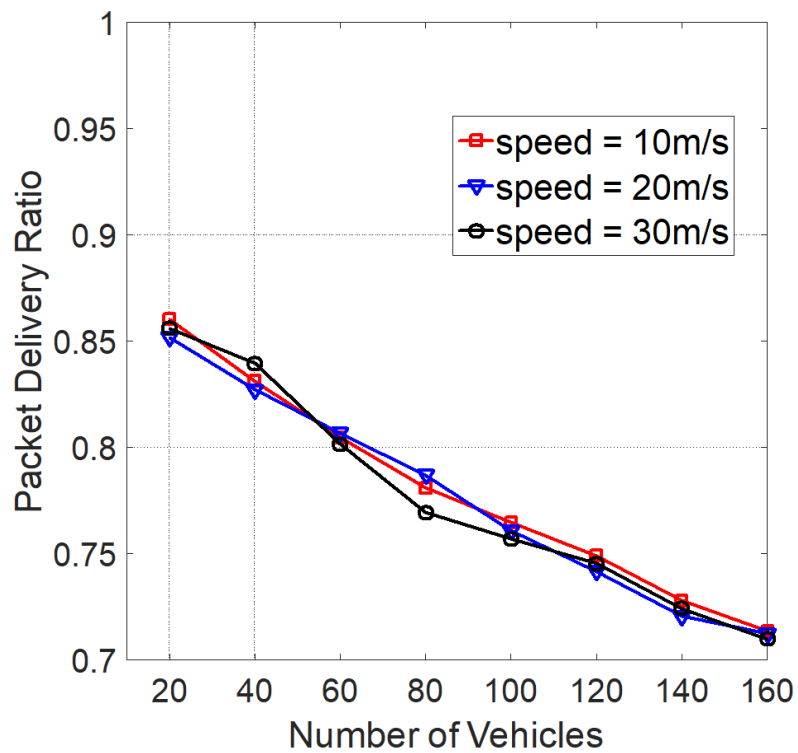
(b)

Fig. 3.13: The impact of speed on PDR from simulation with r/R=1/3 and data rate = 6Mbps: (a) the roadway scenario; (b) the intersection scenario.

3.5 Summary

This project is motivated by unsolved issues in basic safety messages dissemination in vehicular networks. We proposed a novel hybrid MAC protocol to tackle the existing issues. It consists of two centralized sessions and one distributed session. The BSMs are mainly broadcast over the centralized *PNC session* while a few remnant vehicles broadcast BSMs during the *CSMA session*, which is also reserved for legacy vehicles applying the standard of IEEE 802.11p. Such characteristic is able to effectively suppress the transmission collisions and keep the compatibility with DSRC. In addition, the joint effect of PNC and RLNC has been fully exploited during the one-hop dissemination via the V2V and V2I communications. Moreover, we theoretically analyse the subcarrier collision probability, as well as the communication complexity of the protocol. The analytical results are validated by simulations implemented in NS-3. Both the analytical results and simulation results show the proposed MAC outperforms its counterparts and has a better scalability and reliability regarding different traffic densities while maintaining a linear communication complexity. Such advantages provide a promising solution for BSM interchanging among vehicles in ITS.

Chapter 4 Performance Analysis and Enhancement for A MAC Protocol

4.1 Introduction

In this Chapter, an extended study of the NC-PNC MAC protocol proposed in last chapter is carried out. The hybrid MAC protocol, which is advantageous to other existing schemes, has been analysed only through simulations. However, its performance is still unknown on a wide range of circumstances due to lack of a theoretical model. Predicated on such observation, we propose a theoretical model to investigate its performance and provide more sights on the protocol. We firstly examine the total number of transmissions during one broadcast period in a vehicular network implementing the protocol, and then derive a model to analyse packet PDR for the network. From both the analytical model and simulations, tuneable parameters are identified and dominant factors influencing the PDR are revealed. In addition, two distinctive strategies are formulated to enhance the network performance. One strategy is to optimize the parameters of the MAC protocol, whereas the other is to designate vehicles as extra relay nodes to improve the packets reception. In both enhancement methods, the PDR performance can be enhanced by 10% to 30% under the constraint of the delivery latency.

Table 4.1: List of Notations in Chapter 4.

Notations	Description
R	The communication range of RSU
r	The communication range of vehicle
S	The set of vehicles
v_x, $\Re$	A vehicle x, and the RSU, respectively
E	The set of edges in communication graph
$d(v_i, v_j)$	The distance between v_i and v_j
$PDR(i)$	The packet delivery ratio for v_i
N	The total number of vehicles in RoI
TNT	The total number of transmissions
Y	The probability density function of the signal amplitude
m	The fading figure in Nakagami fading channel
ω	The average receiving power in Nakagami fading channel
p_e	Channel erasure probability over Nakagami fading channels

P_{tr}	Transmission power
β	Path loss exponent
N_s	The number of symbols in a packet
p_e^{PNC}	Channel erasure probability for PNC decoding
N_{sub}	The number of data subcarriers
P_{coll_occ}	The probability of the collision occurrence in OFDMA period
P_{veh_coll}	The overall proportion of vehicles colliding in subcarrier selection
α	The number of vehicles per kilometre
N_{in}^{con}	The number of vehicles that are disqualified to take part in the *PNC session* due to subcarrier collisions
N_{out}^{con}	The number of ineligible vehicles due to long distance
N_{node}	The number of non-relay nodes that are eligible for *PNC session*
P_{t-in}^{CSMA}	The probability of a successful transmission for N_{in}^{con}
P_{t-out}^{CSMA}	The probability of a successful transmission for N_{out}^{con}
N_{relay}	The number of packets relays received
PDR	The average *PDR* of the network
PDR_{CSMA}	PDR during the *CSMA* session
PDR_{PNC}	PDR during the *PNC* session
$RX_1(v_i)$	The number of vehicles falling into the communication range of v_i.
N_{node}^{in}	The number of eligible vehicles involved in E_3
N_{node}^{out}	The number of eligible vehicles involved in E_4
RX_{PNC}	The number of neighbours in a vehicle's coverage
PDR_{PNC1}^{node}	The network PDR regarding the non-relay nodes N_{node}^{in}
PDR_{PNC2}^{node}	The network PDR regarding the non-relay nodes N_{node}^{out}
N_{tx1}^{relay}	The number of vehicles belonging to E_1
N_{tx2}^{relay}	The number of vehicles belonging to E_2
P_{tx}^{relay}	The probability of successful transmission to the relay
PDR_{PNC}^{relay}	*PDR* contributed by the relay nodes

4.2 Problem Formulation

In this part, some assumptions for modelling are made and network model is stated. A concise retrospect of the MAC proposed in Chapter 3 is followed by definitions of performance metrics. The list of notations in this chapter is included in Table 4.1.

4.2.1 Assumptions and Network Model

The vehicular network considered in this study is depicted by Fig. 3.1, where vehicles move on a section of a roadway or pass through an intersection with a roundabout, while exchanging their basic safety messages. For each vehicle, BSM packets are generated and transmitted periodically via an on-board unit rigged on it.

A roadside unit (RSU) locates on the road and it can communicate with OBUs. Both OBUs and the RSU can access GPS and their clocks are synchronized. The effective transmission radius of an OBU and the RSU are r and R, respectively, where generally $R > r > 0$. Besides, a vehicle's sensing range is $2r$. We define the communication range of the RSU as the region of interest (RoI). We assume that there are N vehicles in the RoI and they follow a Poisson point process distribution. The density of vehicles is α vehicles per kilometre, so $N=2R\alpha$. We let $S=\{v_1, v_2, ..., v_N\}$ and $\mathfrak{R}$ denote the set of N vehicles in the RoI and the RSU, respectively. In addition, $d(x,y)$ is the Euclidean distance between any two nodes x and y on the road, where $x, y \in S \bigcup \mathfrak{R}$. A hybrid communication graph HCG is defined to characterize the topology of the vehicular network, as follows:

Definition: $HCG = G(V, E)$ is a communication graph with a node set $V = S \bigcup \mathfrak{R}$ and an edge set $E = E_1 \bigcup E_2 \bigcup E_3 \bigcup E_4$. For any two vehicles $v_i, v_j \in S$, the set E_1 contains bidirected edge (v_i, v_j) if $d(v_i, v_j) \leq r$, while the edge (v_i, v_j) belongs to E_2 if $d(v_i, v_j) > r$. In addition, E_3 includes all bidirected edges $\left(v_m, \mathfrak{R}\right)$ if $d\left(v_m, \mathfrak{R}\right) \leq r$, while E_4 comprises the directed edge $d\left(v_n, \mathfrak{R}\right) > r$ which only allows the direction from the RSU $\mathfrak{R}$ to v_n, if and only if $r < d\left(v_n, \mathfrak{R}\right) \leq R$. Here $\left(v_m, v_n\right) \in S$.

In the *HCG*, pairwise vehicles in E_1 are able to communicate with each other directly. A vehicle associated with E_3 and the RSU are communicable to each other. By contrast, vehicles involved in E_4 can receive signals from the RSU, but in the opposite direction, the RSU cannot obtain signals sent by those vehicles.
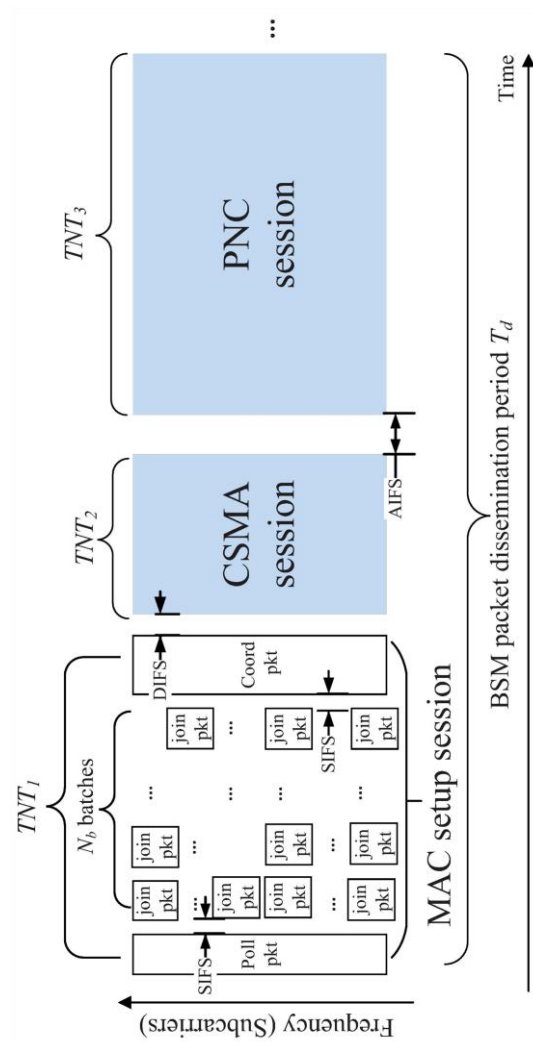
Fig. 4.1: Three sessions in NC-PNC MAC protocol and its main parameters.

4.2.2 Features of the hybrid MAC Protocol

The following paragraphs provide a retrospect of the NC-PNC MAC and list key its features. The hybrid protocol elaborated in Chapter 3 consists of three sessions, including *MAC setup session*, *CSMA session* and *PNC session*, in chronological order. During the first session the RSU invites vehicles in the RoI to participate in the upcoming *PNC session* for exchanging their safety messages. The *CSMA session* is reserved for those vehicles that cannot participate in the *PNC session* due to various reasons, involving subcarrier collisions, long distance to the RSU, etc. the dissemination of BSM packets mainly takes place in the last session.

As shown in Fig. 4.1, at the beginning of the *MAC setup session*, the RSU broadcasts a *polling* message to invite vehicles to join. Vehicles that successfully receive the *polling* message reply to the RSU after a short inter-frame space (SIFS) interval by applying a scheme called orthogonal frequency-division multiple access (OFDMA). More specifically, each vehicle randomly and independently selects one subcarrier and one batch to transmit its *join* packet, and there are N_b

batches totally in the OFDMA. Apparently, this random OFDMA uplink transmission may incur subcarrier collisions if two or more vehicles choose the same subcarrier and the same batch. Once a collision happens, the RSU cannot obtain the ID information of those vehicles. As a result, the RSU cannot arrange a chance for them to take part in the *PNC session*. In the end, the RSU broadcasts a *coordination* packet to inform vehicles how to exchange BSMs in the last session.

Vehicles that lose opportunities of joining the *PNC session* take advantage of *CSMA session* to send safety messages. Finally, eligible vehicles exchange their packets pair by pair via the RSU, by making use of PNC. Definitely, the RSU should have the functionality of executing the PNC decoding algorithm. In addition, one pair of vehicles designated as relays also participate the *PNC session*, by integrating RLNC with PNC.

4.2.3 Performance Metrics

1) Total Number of Transmissions

The total number of transmissions is defined as all transmissions carried out by all nodes in *V* over a dissemination interval, regardless of BSM packets or control packets. It is usually used to evaluate the communication complexity of a protocol. The NC-PNC MAC has three sessions. Therefore, the total number of transmissions can be expressed by $TNT=TNT_1+TNT_2+TNT_3$, where the three items at the right side represent the number of transmissions in three sessions respectively.

2) Packet Delivery Ratio

The PDR can be used to evaluate the capability and effectiveness of a MAC protocol in packet dissemination. If a vehicle v_i receives n BSM packets (messages) during one dissemination period, $PDR(v_i) = \dfrac{n}{N-1}$ will represent its packet delivery ratio. Obviously, if we do not count the vehicle's own BSM (i.e., $0 \leq n \leq N-1$), the upper bound and the lower bound of PDR for a vehicle should be 1 and 0, respectively. Different nodes may have different PDRs due to individual reception of safety messages, so we average all PDRs to evaluate the performance of the entire network.

3) Delivery Latency

Many safety applications in VANETs need to update information timely, so a large delay of BSM delivery is usually unacceptable. Let T_d denote the delivery latency, which means the time spent on completing all three sessions. Different vehicle volumes in a vehicular network may have different delivery latencies.

4) Network Throughput

The throughput of a network reflects the capability of a network in interchanging information among different nodes. One of the key factors that influence the capability is protocols. To evaluate the potential of the enhanced strategies, the performance index of network throughput is adopted. It has the identical definition in Chapter 3, as shown by equations (3.1) and (3.2).

4.3 System Modelling and Performance Analysis

This subsection provides mathematical analysis for collision probability during the *MAC setup session* and the PDR performance.

4.3.1 Channel Erasure Probability

It has been shown that Nakagami distribution with proper parameters would be a realistic channel model [123] for VANETs. We assume that all channels in the network experience Nakagami fading and keep stable during one packet duration. The probability density function of the reception power *Y* based upon this model is represented as

$$f_Y(y) = \frac{m^m y^{m-1}}{\Gamma(m)\omega^m} e^{\frac{-my}{\omega}},$$ (4.1)

where ω is the average received power and *m* is the fading figure. The average received power $\omega = P_{tr}d^{-\beta}$, in which P_{tr}, *d* and β are transmission power, distance between the transmitter and the receiver and path loss exponent respectively. According to an empirical measurement [122], *m* is 1.5 (for distance less than 80m) or 0.8 (for distance larger than 80m). In addition, a typical value of 3 for β is adopted here.

For block fading channels, the erasure probability p_e [124] for the point-to-point case is

$$p_e = \left(1 - \int_0^\infty \left(1 - Q\left(\sqrt{ky}\right)\right)^{N_s}\right) f_Y(y) dy,$$ (4.2)

where $Q(x) = \frac{1}{\sqrt{2\pi}} \int_x^\infty e^{-u^2/2} du$ denotes the Gaussian *Q* function, *k* is the number of bits per symbol, and N_s is the number of symbols in a packet. For simplicity, we consider an approximation of p_e provided in [124]:

$$p_e \approx \gamma^{-(t+1)} \left(\frac{2}{k}\right)^{t+1} \frac{aN_s}{2(t+1)\sqrt{\pi}} \Gamma\left(t + \frac{3}{2}, \frac{k\gamma_{th}}{2}\right),$$ (4.3)

in which *t=m-1*, $\gamma_{th} = \frac{2}{k}\left(erfc^{-1}\left(\frac{2}{N_s}\right)\right)^2$, $a = \frac{m^m}{\Gamma(m)}$ denotes the average signal to noise ratio (SNR). As each BSM has a fixed length in DSRC, N_s becomes a constant actually. Therefore, for a specific data rate (i.e., *k*), p_e turns to be a function of distance *d*. In the following analysis, we

deem $p_e = 0$ if a receiver locates within the communication range of a transmitter. Otherwise, we adopt the average erasure probability over a communication range of D as below

$$p_e = \frac{1}{D} \int_0^D p_e(x) dx \qquad (4.4)$$

On the other hand, we assume the erasure probability for the RSU decoding a PNC packet based on two superimposed signals from two vehicles is p_e^{PNC}. Generally, $p_e \leq p_e^{PNC}$ under the same condition. However, applying some advanced decoding algorithms [103] can ensure the bit error rate (BER) for PNC case as close as that of the point-to-point case. Therefore, we take $p_e \approx p_e^{PNC}$ in the subsequent sections.

4.3.2 Collision Probability in Subcarrier Selection

As aforementioned, when each vehicle randomly and independently chooses one batch and one subcarrier to transmit its *join* packet, it may lead to transmission collisions. In this section, we will derive the collision occurrence probability and the proportion of vehicles that involves in subcarrier collisions.

Assume there are N_{sub} available subcarriers for each batch, this problem is equivalent that each vehicle opts for one subcarrier out of $N_b N_{sub}$ subcarriers at once. Let $S = N_b N_{sub}$, and apparently there are $\binom{S}{N}$ cases without collisions. When more than one vehicle selects the same subcarrier out of S subcarriers, it will result in a collision. Therefore, the probability of the collision occurrence is

$$P_{coll\_occ} = 1 - \frac{\binom{S}{N} N!}{S^N}. \qquad (4.5)$$

From the analysis of transmission collisions in OFDMA uplink stage in Chapter 3, the overall proportion of vehicles colliding in subcarrier selection is

$$P_{veh\_coll} = 1 - \left(1 - \frac{1}{N_b N_{sub}}\right)^{N-1}. \qquad (4.6)$$

The above analysis is validated by simulations carried out in Matlab. Fig. 4.2 (a) shows the collision occurrence probability with $N_{sub} = 48$, which is the number of data subcarriers defined in DSRC. The probability rises up sharply as the number of vehicles N increases. When the number of vehicles in a VANET is more than 60, it is prone to causing subcarrier collisions. In Fig. 4.2 (b), it demonstrates how the number of vehicles and batch volume affect the proportion of vehicles with carrier collisions. More vehicles and fewer transmission batches will lead to more subcarrier collisions, which conforms to our expectation. Straying from our intuition, the number of
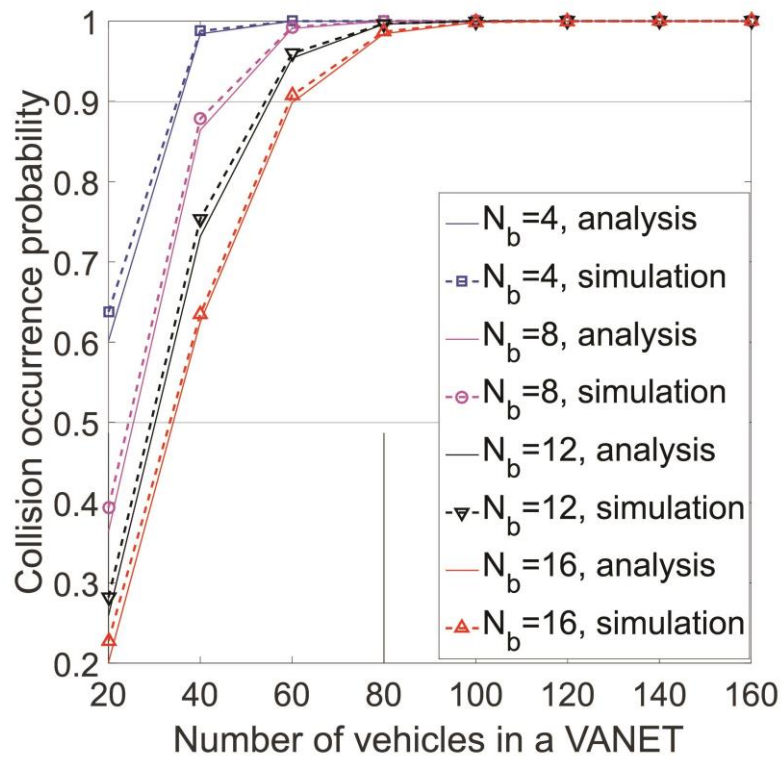
(a)
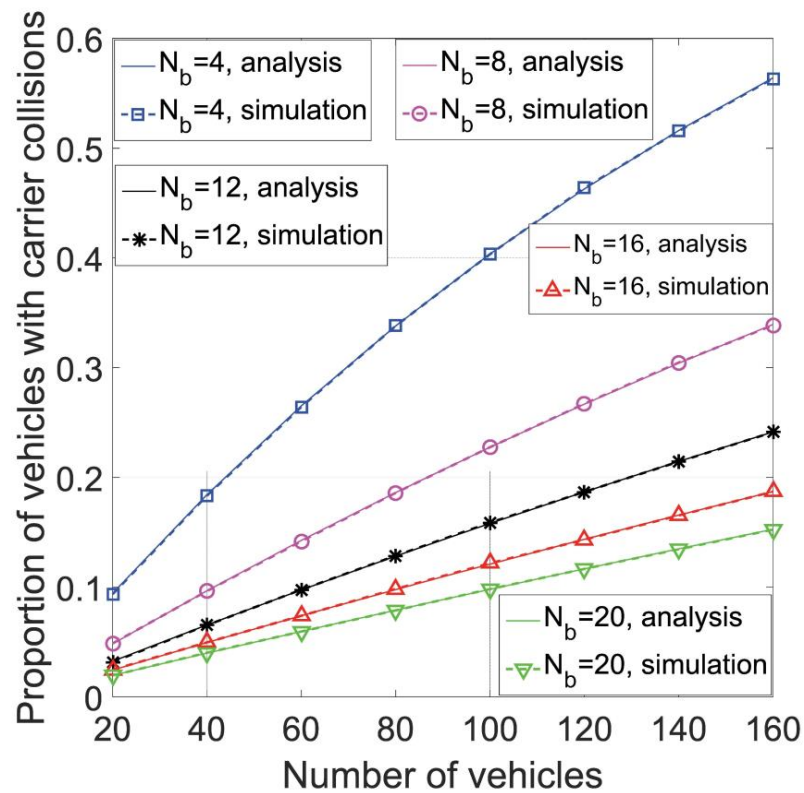
(b)

Fig. 4.2: (a) Probability of collision occurrence; (b) proportion of vehicles in subcarrier collisions.

ineligible vehicles for the *PNC session* is not rare in a dense network. For instance, assume $N = 80$ and $N_b=8$, which means although 80 vehicles have 384 choices to send their *join* packets, it almost inevitably has collisions and the proportion is about 0.2 (i.e., about 16 vehicles collide in subcarrier and are disqualified to participate in the *PNC session*).

4.3.3 Total Number of Transmissions

As sketched in Fig. 4.1, each vehicle in the RoI would send a *join* packet to the RSU in the first session. By adding a *poll* packet and a *coordination* packet from the RSU, we can easily get $TNT_1=N+2$.

During the *CSMA session*, vehicles that are ineligible for the *PNC session* access the channel and broadcast BSMs by means of CSMA/CA. The ineligibility, on one hand, stems from subcarrier collisions during the OFDMA in the first session, and on the other hand, due to large distance between some vehicles and the RSU (i.e., vehicles associated with the edge set E_4). According to the property of Poisson process, the probability of k vehicles involved in the E_3 is

$$P(k,2r) = \frac{(2\alpha)^k}{k!} e^{-2\alpha r}. \tag{4.7}$$

The expected number of vehicles in this range is

$$E[K_{in}] = \left\lceil \sum_{k=0}^{\infty} kP(k,2r) \right\rceil = \lceil 2\alpha r \rceil. \tag{4.8}$$

Among those vehicles, $N_{in}^{con} = \lceil 2\alpha r P_{veh\_coll} \rceil$ vehicles are disqualified to take part in the *PNC session* due to subcarrier collisions. Nevertheless, their counterparts involved in E_4 that might have one or both issues mentioned above lose the opportunity. Likewise, the total number of vehicles and the ineligible vehicles of this type is $E[K_{out}] = \lceil 2\alpha(R-r) \rceil$ and $N_{out}^{con} = \lceil 2\alpha(R-r)\left(1-(1-P_{veh\_coll})(1-p_e)\right) \rceil$, respectively, where p_e is the channel erasure probability. Since all the ineligible vehicles would broadcast a BSM during the second session. Thus, the total number of transmissions in this session is

$$TNT_2 = N_{in}^{con} + N_{in}^{out} = \lceil 2\alpha r P_{veh\_coll} \rceil + \lceil 2\alpha(R-r)\left(1-(1-P_{veh\_coll})(1-p_e)\right) \rceil. \tag{4.9}$$

All the eligible nodes exchange their safety messages applying physical layer network coding in the last session. A number of non-relay nodes and a pair of relay nodes constitute them. Obviously, the number of non-relay nodes is

$$N_{node} = 2\lfloor \alpha r\left(1-P_{veh\_coll}\right) \rfloor - 2 + 2\lfloor \alpha(R-r)\left(1-P_{veh\_coll}\right)\left(1-p_e\right) \rfloor. \tag{4.10}$$
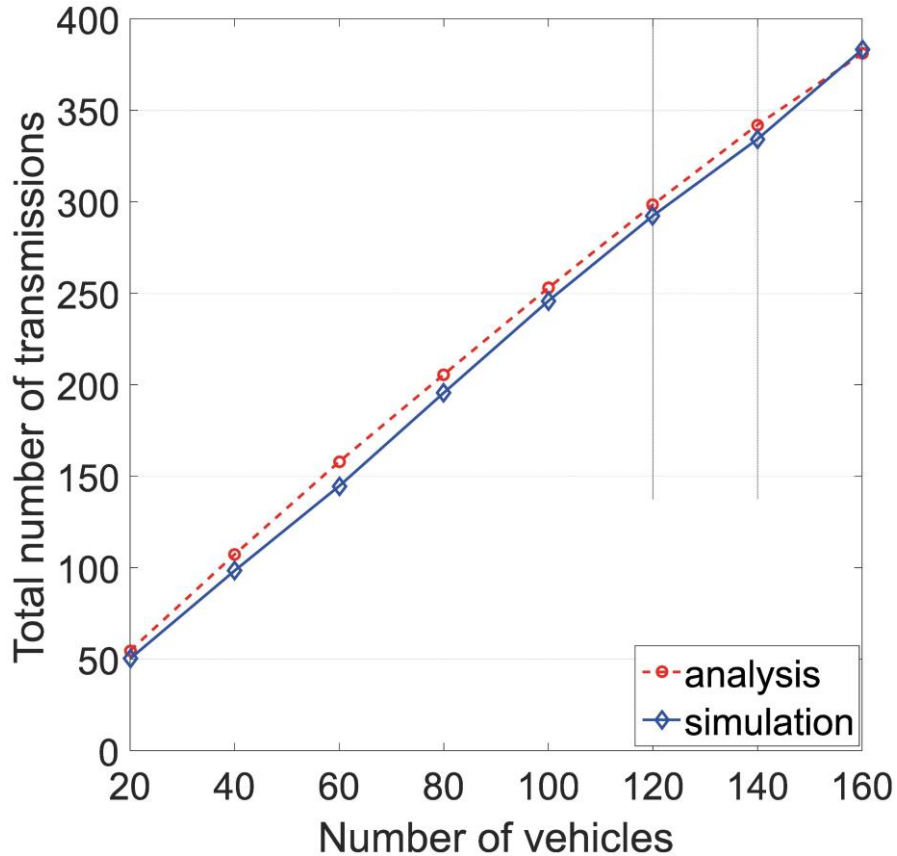
Fig. 4.3: Total number of transmissions in one CCH interval.

The relay nodes encode and transmit multiple packets that are overheard and buffered during the *CSMA session*. Since the CSMA/CA may also incur transmission collisions, according to [48], the probability of a successful transmission for N_{in}^{con} nodes and N_{out}^{con} nodes is (remember the sensing range is *2r*)

$$P_{t-in}^{CSMA} = \left(1 - \frac{1}{CW+1}\right)^{P_{veh\_coll} \min\left(\frac{2R+3r}{2}\alpha, 4\alpha r\right)-1} \quad \text{and} \quad P_{t-out}^{CSMA} = \left(1 - \frac{1}{CW+1}\right)^{P_{veh\_coll} \min\left(\frac{R+3r}{2}\alpha, 4\alpha r\right)-1}, \quad (4.11)$$

respectively, where *CW* is the contention window ranging between CW_{min} (15) and CW_{max} (1023). Therefore, the number of packets relays received (adding their own packets) is

$$N_{relay} = \left\lceil N_{in}^{con} P_{t-in}^{CSMA} + N_{out}^{con} P_{t-out}^{CSMA} (1-p_e) \right\rceil + 2. \quad (4.12)$$

Considering for each pair of uplink packets either from the relays or the non-relay nodes, the RSU will broadcast a downlink PNC packet after decoding, we can derive the total number of trans-missions in the *PNC session* is $TNT_3 = \frac{3}{2}\left(N_{node} + N_{relay}\right)$.

Fig. 4.3 delineates the analytical results and the simulation results with respect to the total number of transmissions *TNT*. It has a linear relationship with the number of vehicles in the RoI, which is

consistent with the equations above. Therefore, the communication complexity of the protocol can be regarded as *O(N)*. The simulation is conducted in NS-3 [63], and the setup and parameters are shown in Section 4.4.

4.3.4 PDR Analysis

In order to derive the PDR, the roadway scenario is considered at first. The average PDR of the network can be expressed by

$$PDR = \frac{\sum_{i=1}^{N} RCV(i)}{N(N-1)}, \tag{4.13}$$

where *RCV(i)* is the total number of received BSM packets of v_i. The BSM broadcast only occurs in the *CSMA session* and the *PNC session*. As a consequence, the average PDR is the summation of the average PDR of the two sessions, as below

$$PDR = PDR_{CSMA} + PDR_{PNC}. \tag{4.14}$$

During the *CSMA session*, only an interference-free transmission may lead to a successful reception, as transmission collisions cannot be eliminated even if applying the CSMA/CA. According to the analysis in the last subsection, the number of vehicles involved in E_4 that would transmit BSMs is N_{out}^{con} and the probability of a successful transmission from $P_{t-out}^{CSMA}(v_i)$. Therefore, taking into account all transmissions from vehicles in this set, the average PDR of the network is

$$PDR_1^{csma} = \frac{\sum_{i=1}^{N_{out}^{con}} \left(P_{t-out}^{CSMA}(v_i)RX_1(v_i) + (1-p_e)\left(N - RX_1(v_i)\right) \right)}{N(N-1)}$$

$$= \frac{N_{out}^{con} P_{t-out}^{CSMA} \left(E[RX_1] + (1-p_e)(N - E[RX_1]) \right)}{N(N-1)}, \tag{4.15}$$

in which

$$E[RX_1] = \left\lceil \min\left(\frac{\alpha(R+r)}{2} - 1, 2\alpha r - 1 \right) \right\rceil \tag{4.16}$$

denotes the expectation of $RX_1(v_i) = \left\lceil \min\left(\alpha(r + R - d(v_i, \Re)) - 1, 2\alpha r - 1 \right) \right\rceil$, which means the number of vehicles falling into the communication range of v_i. On the other hand, for vehicles $0 < d(v_i, \Re) \le r$, based upon (4.8) and (4.11), the PDR contributed by this part can be acquired similarly:

$$PDR_2^{csma} = \frac{N_{in}^{con} P_{t-in}^{CSMA} \left(E[RX_2] + (1-p_e)(N - E[RX_2]) \right)}{N(N-1)}, \tag{4.17}$$

$E[RX_2] = \left\lceil \min\left(\frac{\alpha}{2}(2R+r)-1, 2\alpha r-1 \right) \right\rceil$. The summation of PDR_1^{csma} and PDR_2^{csma} would lead to the

PDR of the second session PDR_{CSMA}.

For the *PNC session*, let consider the non-relay nodes at first. The total number of those vehicles is N_{node}, which can be further divided into two parts, N_{node}^{in} and N_{node}^{out}. The former comes from eligible vehicles involved in E_3, while the latter is the number of their counterparts in E_4. From (4.10), we have

$$N_{node}^{in} = 2\left\lfloor \alpha r(1 - P_{veh\_coll)}) \right\rfloor - 2 \text{ and}$$
$$N_{node}^{out} = 2\left\lfloor \alpha(R-r)(1 - P_{veh\_coll})(1 - p_e) \right\rfloor \tag{4.18}$$

Suppose a non-relay node v_i, the amount of neighbours in its coverage is $RX_{PNC} = \left\lceil \min\left(\alpha(r + R - d(v_i, \Re)) - 1, 2\alpha r - 1 \right) \right\rceil$. Those nodes can overhear the uplink packets. Consequently, they can recover the original packets after receiving the corresponding downlink PNC packets from the RSU. By using the expectation of RX_{PNC}, the network PDR regarding the non-relay nodes can be expressed by (4.19) and (4.20), as follows:

$$PDR_{PNC1}^{node} = \frac{N_{node}^{in}}{N(N-1)}\left(\left\lceil \min\left(\alpha(R+\frac{r}{2})-1, 2\alpha r-1 \right) \right\rceil + \left(N - \left\lceil \min(\alpha(R+\frac{r}{2}), 2\alpha r) \right\rceil \right)(1-p_e) \right) \tag{4.19}$$

$$PDR_{PNC2}^{node} = \frac{N_{node}^{out}}{N(N-1)}\left(\left\lceil \min\left(\frac{\alpha}{2}(R+r)-1, 2\alpha r-1 \right) \right\rceil + \left(N - \left\lceil \min(\frac{\alpha}{2}(R+r), 2\alpha r) \right\rceil \right)(1-p_e) \right) \tag{4.20}$$

Vehicles on the left side that have received the left relay's uplink packets are able to restore the packets encoded by the right relay, and vice versa for the right-side vehicles. On either side, vehicles sending BSMs to a relay can be divided into two groups that belong to E_1 and E_2 respectively. The number of vehicles in two sets is denoted by N_{tx1}^{relay} and N_{tx2}^{relay} respectively, where

$$N_{tx1}^{relay} = \left\lceil \alpha r P_{veh\_coll} + \min\left(\alpha r, \alpha(R-r) \right)\left(1 - (1 - P_{veh\_coll})(1 - p_e) \right) \right\rceil,$$
$$N_{tx2}^{relay} = \left\lfloor \max\left(0, \alpha(R-2r) \right)\left(1 - \left(1 - P_{veh\_coll} \right)(1 - p_e) \right) \right\rfloor. \tag{4.21}$$

Among those nodes, the probability of successful transmission to the relay is

$$P_{tx}^{relay} = \left(1 - \frac{1}{CW+1} \right)^{N_{in}^{con} + \min\left(2\alpha r, \alpha(R-r) \right)p_{out} - 1} \tag{4.22}$$

where $p_{out} = 1 - (1 - P_{veh\_coll})(1 - p_e)$. Since packets from N_{tx2}^{relay} vehicles might be received with the probability $1 - p_e$, we have

$$PDR_{PNC}^{relay} = \frac{1}{N(N-1)} P_{tx}^{relay} \left(N_{tx}^{relay} + N_{tx2}^{relay}(1 - p_e) \right)\left(R_x^{relay} + (1 - p_e)(N - R_x^{relay}) \right), \quad (4.23)$$

where $R_x^{relay} = \lceil \min(2\alpha r, R\alpha) \rceil$ is the number of nodes in a relay's coverage. By adding the two parts of PDR from non-relay nodes (i.e., (4.19) and (4.20)) and the one from relays (i.e., (4.23)), we can get the PDR for the *PNC session*

$$PDR_{PNC} = PDR_{PNC1}^{node} + PDR_{PNC2}^{node} + PDR_{PNC1}^{relay}. \quad (4.24)$$

By substituting 4.24) and $PDR_{CSMA} = PDR_1^{csma} + PDR_2^{csma}$ with relevant variables in (4.14), the average PDR of the entire network can be derived. Likewise, the overall PDR performance of the intersection scenario can be obtained.

On the basis of (4.13) to (4.24), we plot the PDR performance against various vehicle volumes for both the roadway and the intersection scenario[7] where *r = 100 m* and *R = 300 m*, as shown by Fig. 4.4. In addition, by changing N_s and *k* in (4.3), the corresponding p_e for different data rates can be calculated. The figure also demonstrates the PDRs for three typical data rates of DSRC. Under the same condition, lower data rate will lead to better PDR performance. Furthermore, to validate the theoretical analysis presented above, simulations are conducted in NS-3 under the same configuration (the simulation setup will be elaborated later in Section 4.4.1). The analytical results follow tightly the simulation ones, which approve the PDR performance of the proposed protocol. In all situations, the theoretical results are slightly better than the corresponding simulation results because we adopt $p_e^{PNC} = p_e$ in the model. However, in the reality, $p_e^{PNC} < p_e$ but their gap is very small.

4.3.5 Discussions About the Analytical Model

The average PDR performance of the whole network has been derived in the above section 4.3.4, based on the analysis of channel erasure probability, the probability of collisions taking place in the OFDMA uplink and the total number of transmissions. As shown in the equations from (4.13) to (4.24), the derivation of the PDR is based on calculation of probability (e.g., packet reception probability). Such analytical model significantly distinguishes from the models based on the Markov Chain, which is widely adopted in paper [45], [46] and [100]. The main reason is that the proposed NC-PNC MAC is a hybrid MAC that contains both centralized and distributed session,

---

[7] The PDR analysis for the intersection situation is very similar to the roadway situation, so we omit the derivation in order to avoid redundancy.

whereas the Markov Chain is applicable to distributed MAC, such as IEEE 802.11p. In fact, the theoretical model proposed in this chapter can also be used in other hybrid MAC like [104]. Furthermore, the correlation and state of the packet transmission is not considered in our analysis because this model is for the scenario of BSM broadcasting, where BSMs are independently and periodically transmitted in each vehicle, and all BSMs generated from different vehicles are independent. Therefore, the ignorance of the correlation relationship and the state of the packet transmission will not affect the analytical results.

4.4 Strategies for Performance Boost

We will show two different strategies to enhance the performance of the hybrid MAC protocol. One is to optimize the parameters of the MAC and the other is to add extra relays.

4.4.1 Parameter Optimization

In this section, we firstly try to identify the tuneable parameters in the system and maximize the PDR without any constraint. Then we build a simulation model to confirm the performance enhancement results with the consideration of latency constraint.

1) Tuneable Parameters and Their Influence on PDR

From the PDR-related equations from (4.15) to (4.24), the PDR mainly depends on a number of parameters, including communication ranges (i.e., r and R), traffic density α, successful transmission probability P_t^{CSMA} during the *CSMA session*, erasure probability p_e, subcarrier collision probability P_{veh_coll} and so on. However, among those parameters, the vehicle density α on a road segment is contingent on traffic situations, while the communication ranges, which are mainly subject to transmission power of the corresponding radio devices, cannot be tuned frequently and arbitrarily due to limited number of fixed levels of transmission power in DSRC [13]. According to (4.3), once the channel model is determined, p_e is inversely proportional to data rate (i.e., the variable k in (4.3)). Actually, the PDR is a monotonic function of data rate. A higher data rate will lead to lower PDR, which is also substantiated in Fig. 4.4. By contrast, the PDR has a more complicated relationship with the directly adjustable P_{veh_coll}, which is only determined by the variable N_b, as both the total number of vehicle N in the RoI and the amount of data carrier N_{sub} are constant, based on (4.6).

Therefore, to find the maximum PDR, let $\dfrac{\partial PDR(\square)}{\partial P_{veh\_coll}} = 0$, the corresponding collision proportion of the maximum PDR can be obtained. Unfortunately, the closed-form expression is hard to be solved, because the partial derivative equation contains transcendental functions. Here we use
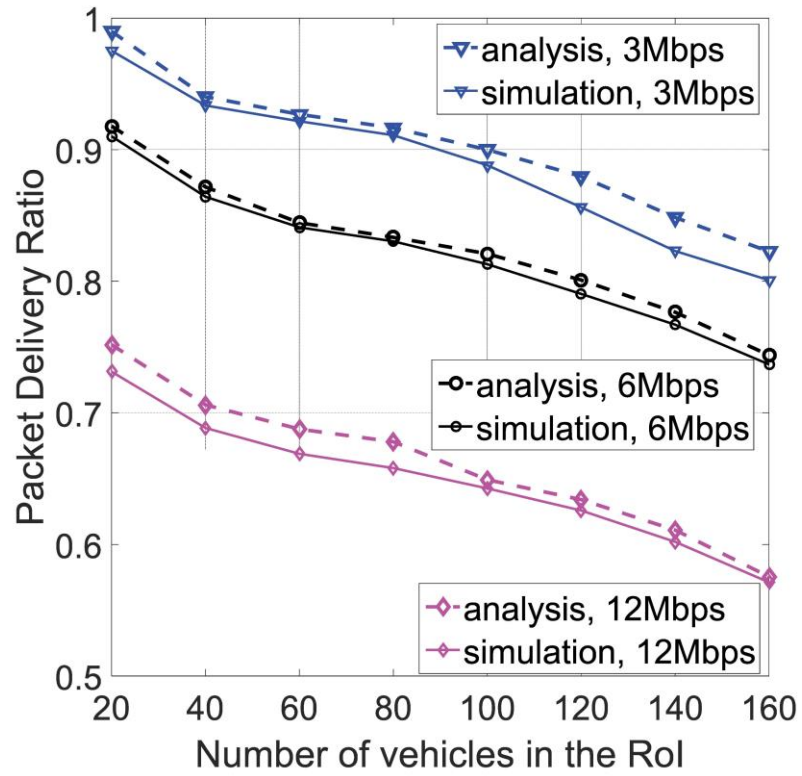
(a)
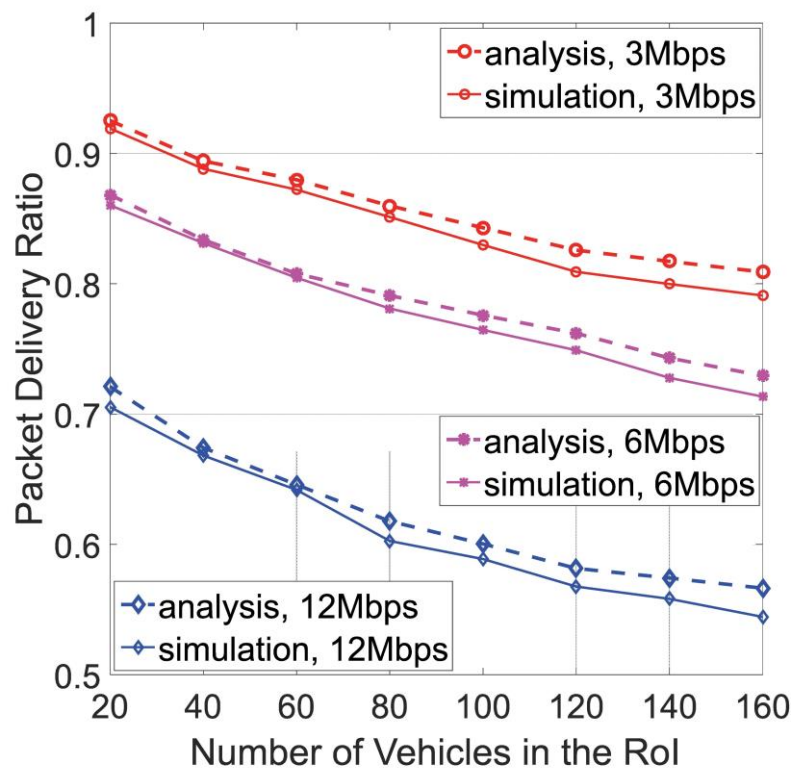
(b)

Fig. 4.4: Analytical results vs simulation results for the average PDR performance under the different data rates in: (a) the roadway scenario; (b) the intersection scenario.

Matlab to calculate the approximate numerical roots (e.g., the method adopted to acquire the roots is *bisection* method). After that, by inversely use (4.6), the corresponding N_b is given by:

$$N_b = \frac{1}{N_{sub}} \cdot \frac{1}{1 - \left(1 - P_{veh\_coll}\right)^{\frac{1}{N-1}}} \tag{4.25}$$

Finally, the numerical results of the maximum PDR and the relevant values of N_b and P_{veh_coll} are shown in Table 4.2.

2) Simulation Setup

Table 4.2: The maximum PDR and the corresponding values of P_{veh_coll} and N_b.

N	20	40	60	80	100	120	160
P_{veh_coll}	0.091	0.094	0.098	0.097	0.098	0.1	0.099
N_b	6	9	12	16	20	24	32
PDR	0.95	0.9	0.86	0.82	0.8	0.75	0.67

Table 4.3: Key PHY and MAC Layer Parameters.

Parameter	Value
Channel Frequency / CW	5.9 GHz / 511
Transmission Power	RSU: 45 dBm, OBU: 30 dBm
Path Loss Exponent / Antenna Gain	3 / 2 dB
Number of Vehicles / N_{sub}	200 to 160 / 48
BSM Packet Size / Data Rate	200 Bytes / 3 Mbps, 6 Mbps, 12 Mbps
Vehicle Velocity	10 to 30 m/s (36 to 108 km/h)
SIFS / DIFS / AIFS	16 us / 32 us / 48 us
Road Length / Number of Lanes	2 km / 4

All the best PDRs listed in Table. 4.2 are obtained mathematically and without time constraint. Considering the requirement of delivery latency in vehicular networks, some of the results may be invalid. To verify the results, a simulation model is built up according to the network model in Section II. We adopt the Nakagami channel model for all communication channels, as shown in (4.1). In addition, a so-called log-distance path loss model is also added on all these channels. All key simulation parameters are listed in Table 4.3. All relevant simulations are conducted in NS-

3. For each case, it consists of 2000 trials, and each trial means running the whole process shown by Fig. 4.1.

Before maximizing the PDR by simulation, Table. 4.4 shows the elected N_b and the corresponding P_{veh_coll} in simulations. Due to limited space, results for other vehicle volumes can be calculated similarly by applying (4.6).

Table 4.4: Selected N_b for different vehicle volumes.

N	N_b, P_{veh_coll}					
20	16, 0.0245	12, 0.0325	8, 0.0483	4, 0.094	2, 0.18	1, 0.33
40	24, 0.0333	16, 0.0495	8, 0.0967	4, 0.184	2, 0.33	1, 0.56
60	36, 0.036	20, 0.06	12, 0.0974	6, 0.185	3, 0.337	2, 0.46
80	40, 0.0403	28, 0.057	16, 0.098	8, 0.186	4, 0.338	2, 0.56
100	36, 0.055	20, 0.098	8, 0.227	6, 0.29	4, 0.4	2, 0.64
120	40, 0.06	24, 0.098	12, 0.187	7, 0.298	5, 0.392	3, 0.56
160	54, 0.0595	30, 0.104	14, 0.21	10, 0.282	6, 0.425	4, 0.56

3) Enhancement Results and Discussion

Based on the configuration described in the above paragraphs, we simulate the BSM packets dissemination and figure out the maximum PDR for vehicular networks with different vehicle volumes. As shown in Fig. 4.5 (a), for each vehicle volume, the PDR curve has a maximum value at a particular batch volume N_b. Compared with the original performance (see Fig. 3.8 (a) in Chapter 3), the PDR can be boosted up by 10% to 30%, if an appropriate N_b is predetermined. However, the condition (i.e., the parameter N_b) of the best PDR performance for different vehicle volumes is not necessarily the same. For instance, when the number of vehicles is 40, the curve peaks at $N_b = 8$. By contrast, a network with 80 vehicles reaches its highest point only if $N_b = 28$. Nevertheless, a common feature among them is that all corresponding P_{veh_coll} of the maximum PDR is around 0.1. Moreover, the simulation results of maximizing PDR are basically consistent with the analytical results listed in Table. 4.2.

Because the delivery latency is a significant metric in VANETs, Fig. 4.5(b) presents the average delivery latency T_d as a function of N_b as well. Comparing the curves vertically, networks with more vehicles consume more time. Horizontally, for a particular N, a larger N_b means more batches for vehicles to choose and more time needed in the *MAC setup session*. Thus, the total
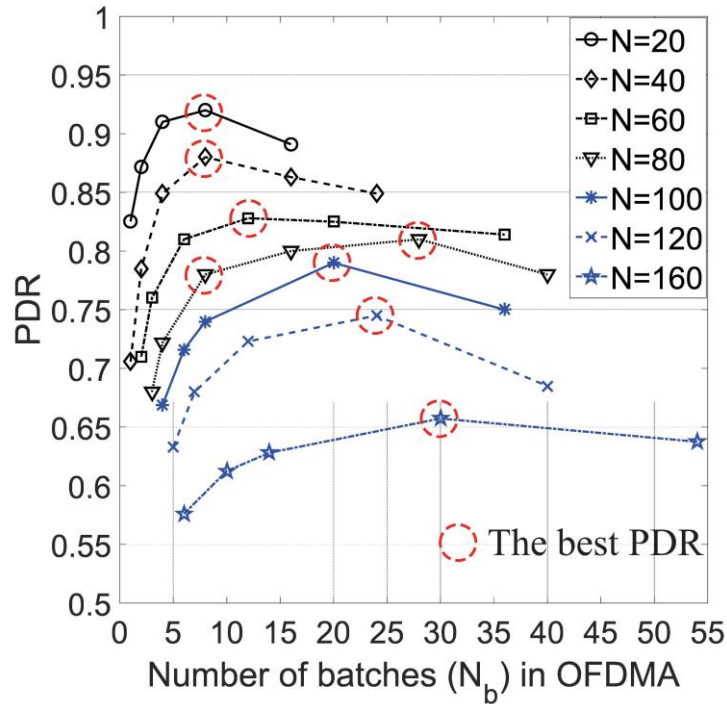
(a)
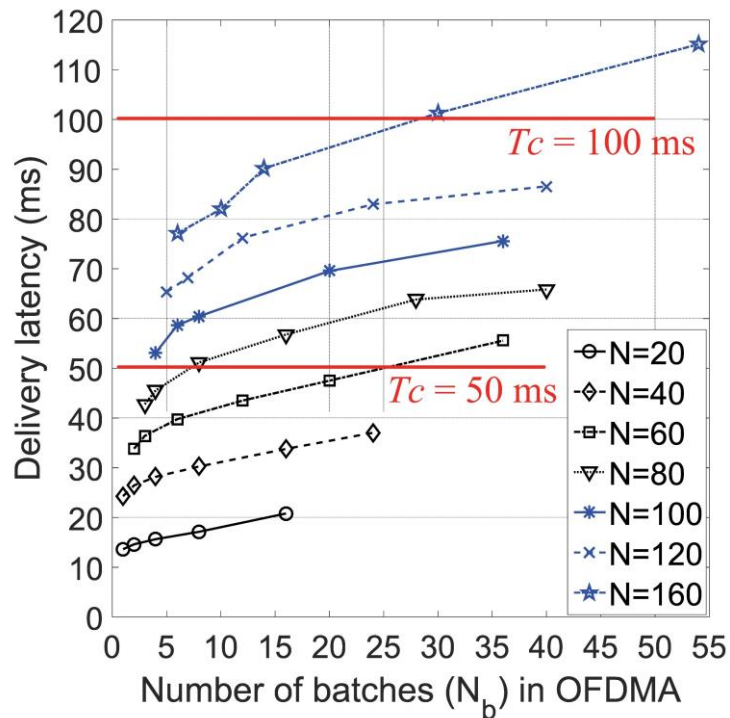
(b)

Fig. 4.5: (a) PDR performance for vehicular networks with different batch volumes (data rate 6 Mbps, r/R=1/3); (b) Delivery latency T_d for vehicular networks with different batch volumes (data rate 6 Mbps, r/R=1/3). To easily determine the best PDR under a time constraint T_c, each pair of curves with the same number of vehicles in the above two figures have the same set of batch volumes N_b. When $N \geq 100$, the minimum T_d exceeds 50 ms.

consumed time increases gradually as the N_b goes up, but the PDR curves do not have this attribute.

Table 4.5: The best PDR and corresponding N_b under time constraints.

	$T_c = 50$ ms		$T_c = 100$ ms	
N	N_b	PDR	N_b	PDR
20	8	0.93	8	0.93
40	8	0.88	8	0.88
60	12	0.83	12	0.84
80	8	0.78	28	0.81
100	N. A.	N. A.	20	0.78
120	N. A.	N. A.	24	0.74
160	N. A.	N. A.	30	0.66

More essentially, a comprehensive consideration is necessary while making a network attain the best PDR. Since most safety applications in vehicular networks have stringent requirement on delivery latency, we may need to determine the best PDR under time constraint. Here we set two time constraints $T_c = 50$ ms and $T_c = 100$ ms, according to safety applications in DSRC. As a result, the best PDR of a vehicular network is the one that not only has the maximum value among all PDR candidates, but ensures the corresponding T_d is no more than a pre-set T_c. As a case in point, assume $N = 80$ and $T_c = 50$ ms, based on Fig. 4.5 (b), the three leftmost data points of the curve meet the requirement of $T_d < 50$ ms. The relevant values of N_b of the three points are 2, 4 and 8. Since Fig. 4.5 (a) and Fig. 4.5 (b) have the same coordinates of N_b for each pair of curves with the same N, we can acquire three PDRs from the three leftmost data points of the curve (for $N = 80$) in Fig. 4.5 (a). After a simple comparison, the best PDR and its associated N_b in this example are 0.78 and 8, respectively. If we still consider the case with $N = 80$ but set $T_c = 100$ ms, in 4.5 (b) we can easily observe that all of the delivery latencies are less than 100 ms. Consequently, the peak of the entire curve for $N = 80$ in Fig. 4.5 (a) represents the best PDR (i.e., 0.81 in this case) and its corresponding N_b is 28. Repeating this process for every vehicle volume in the network, we can get all best PDRs and their corresponding N_b under the two time

constraints, as shown in Table 4.5 (the data rate is 6 Mbps). Similar conclusions can be drawn for other time constraints and data rates.

In fact, according to the transmission power of the RSU, the radius R of the RoI is 300 meters. Confined within this range, the probability of the traffic density on a typical bidirectional four-lane road section that has no more than 160 vehicles per kilometre is larger than 95%, according to a relevant study [125] Therefore, a latency constraint with a period of 100 ms can ensure vast majority of VANETs achieve their maximum PDRs.

4.4.2 NC-PNC MAC with Multiple Relays

Distinguishing from some distributed protocols like IEEE802.11p, the NC-PNC MAC is a hybrid protocol with both centralized parts (*MAC setup session* and *PNC session*) and distributed part (*CSMA session*). Therefore, after the *PNC session*, channels enter an idle state until the next round if the actual consumed time is less than one CCH interval. On the other hand, although the proposed protocol has a much better PDR performance than several benchmarks, the average PDR still does not reach as close as 100%, based upon the observation in Fig. 3.8. There are many factors accounting for this phenomenon, such as decoding failure at the RSU or OBUs because of fading channels, insufficient packets collected to decode a compound packet and so on. However, the dominant factor is that some remote nodes cannot obtain desired packets even if they have received downlink PNC packets from RSU, because they fail to overhear the uplink packets. For instance, in Fig. 3.1 (a), the vehicle v_5 is out of the transmission range of v_4. If v_4 takes part in the *PNC session*, v_5 possibly does not receive the uplink packet P_{v4}. Thus, even if the node v_5 can receive a downlink packet $P_{v4} \oplus P_{vx}$ from the RSU, it still is not able to retrieve the target packet P_{vx}, which is a safety message from a certain node v_x at the other side of the RSU.

Based upon the discussion above, there are two strategies to deal with the problem. The first one is to extend the *PNC session* by blindly reassigning new PNC pairs. Let assume node v_6 and node v_x become a PNC pair, node v_5 can decode P_{vx} with a high probability after receiving $P_{v6} \oplus P_{vx}$ from the RSU if it has overheard uplink packet P_{v6} previously. However, this strategy cannot guarantee that those distant nodes like v_5 can always decode the target information from downlink packets. In addition, intentionally shuffling PNC pairs to ensure a high decoding probability is not easy and needs massive calculations at RSU.

By contrast, the second strategy proposed is able to solve the issue more effectively. In this strategy, extra relays are assigned (called auxiliary relays) along with relays set previously (called primary relays). To make a distinction, we denote this strategy NC-PNC-MR MAC. Both primary and auxiliary relays apply RLNC to encode and forward BSM packet but with distinguished

purposes. Primary relays only serve to relay packets received during the *CSMA session*, while auxiliary relays intend to relay BSM packets from vehicles in the vicinity of RSU to distant vehicles (i.e., inside vehicles close to the rim of the larger solid circle in Fig. 3.1).

The RSU selects one auxiliary relay v_{Relay}^{aux} at each side, according to the location information contained in *join* packets sent during the first setup session. Therefore, for the roadway scenario, one at left side and the other at the right side of the RSU are selected. Certainly, four auxiliary relays are selected for the intersection case. We apply the following conditions to determine a left-side auxiliary relay:

$$v_{Relay}^{aux-L} \in \square^L \text{ and } {}_{Relay}^{aux-L} = \arg\max_{v_x \in (\square^L \backslash v_{Relay}^L)} \left(d\left(v_x, \Re \right) \right). \tag{4.26}$$

The remaining auxiliary relays can be identified in a similar way. Once both the primary relays and the auxiliary relays are determined, the RSU announces them in the *coordination* packet.

An auxiliary relay node does not necessarily help encode and forward all overheard uplink safety messages for the purpose of keeping efficiency. As aforementioned, it only relays the packets from vehicles close to the RSU. Therefore, we define a forwarding range $d_{Relay}^{aux} = R/3$, which means that for any vehicle $v_i \in \square$, if $d(v_i, \Re) < d_{Relay}^{aux}$, their packets will be forwarded by a corresponding relay node v_{Relay}^{aux}.

In order to evaluate the performance of the NC-PNC-MR MAC, simulations are conducted in NS-3, for both roadway and intersection scenarios. The PDR performance and average consumed time are shown in Fig. 4.6. From the left figure, we can see that two PDR curves of the multiple relay scheme increase about 15%, compared with the NC-PNC MAC. The PDR is no less than 0.9 when the number of vehicles is below 80 and can ensure a PDR of 0.8 even the number of vehicles reaches 160. At the same time, the consumed time (i.e., average delivery latency) increases approximately 10% to 15%.

Finally, we further make a broad comparison for the normalized throughput among five MAC protocols for both the roadway and the intersection scenario, depicted in Fig. 4.7. It is observed that NC-PNC-MR have much higher throughput than that of the *NC relay scheme*, *RSU-NC scheme* and DSRC standard, but it is less efficient than the NC-PNC MAC (about 1% to 5% less in sparse network if $N < 80$). The reason is that multiple relays spend extra time in broadcast network coded packets than single relay. However, the downgrade of the efficiency is not significant. Generally, the enhanced NC-PNC MR scheme have higher reliability and efficiency for safety information dissemination in vehicular networks, for both sparse and dense networks.
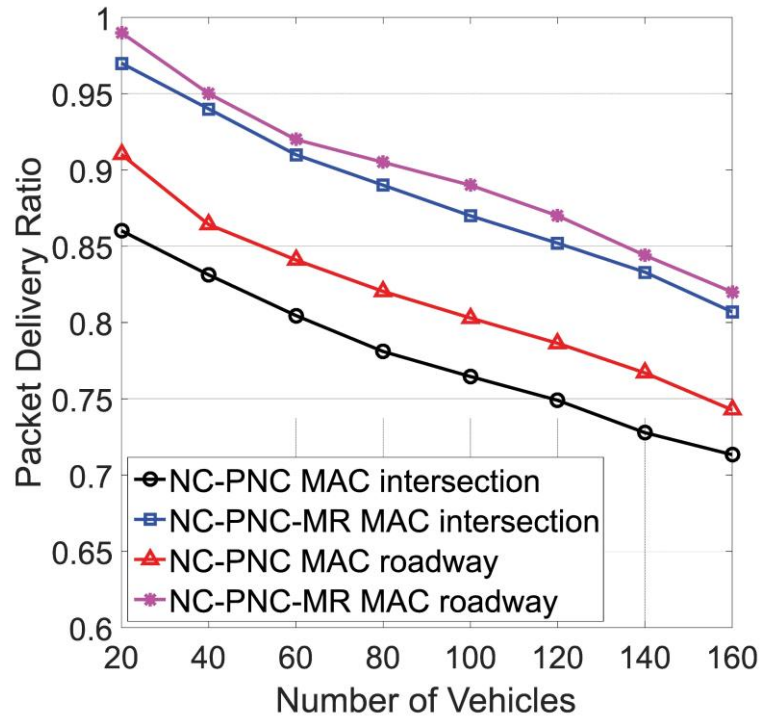
(a)
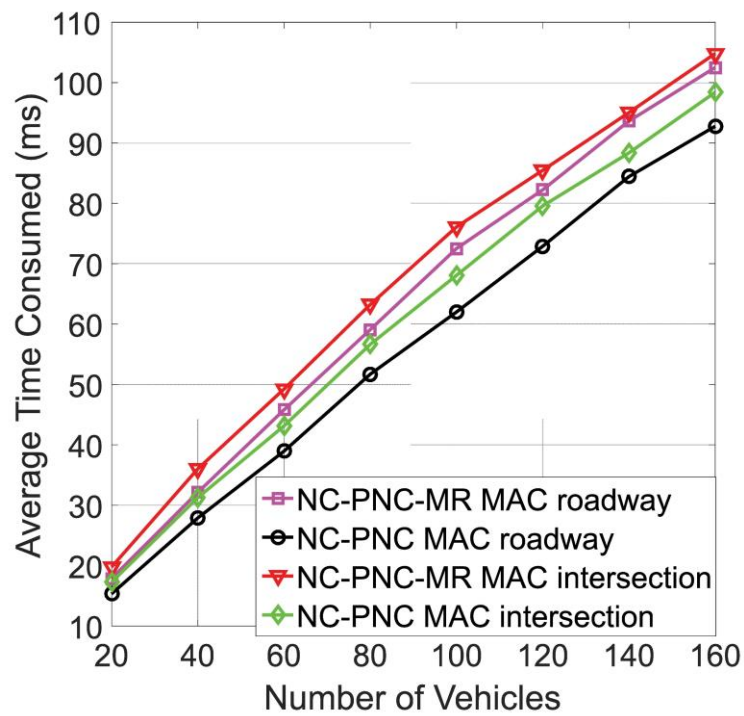
(b)

Fig. 4.6: Performance evaluation for NC-PNC-MR MAC with different number of vehicles (*r/R*=1/3, data rate = 6 Mbps) in: (a) PDR performance; (b)average consumed time.
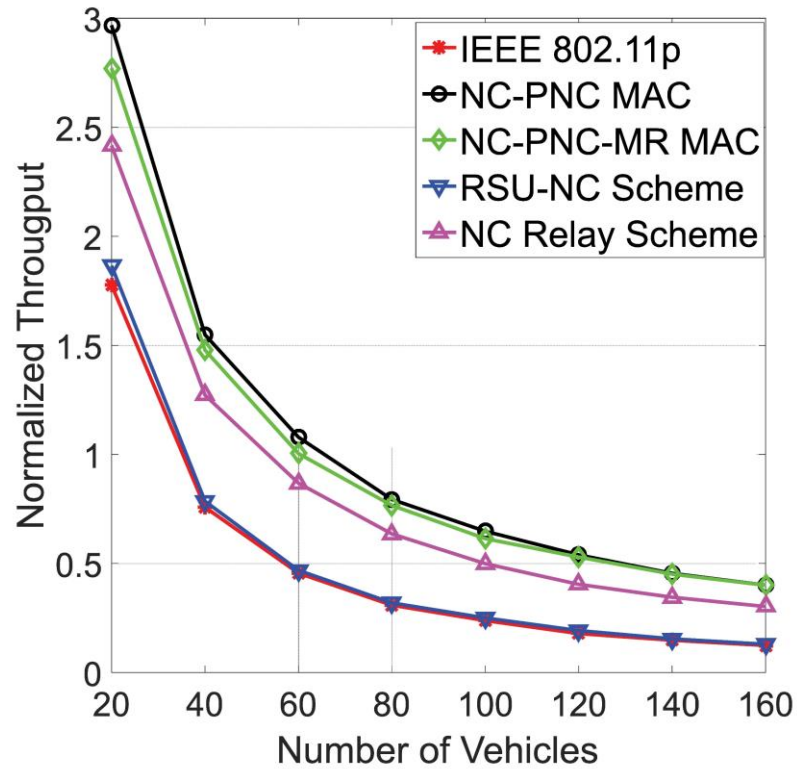
(a)
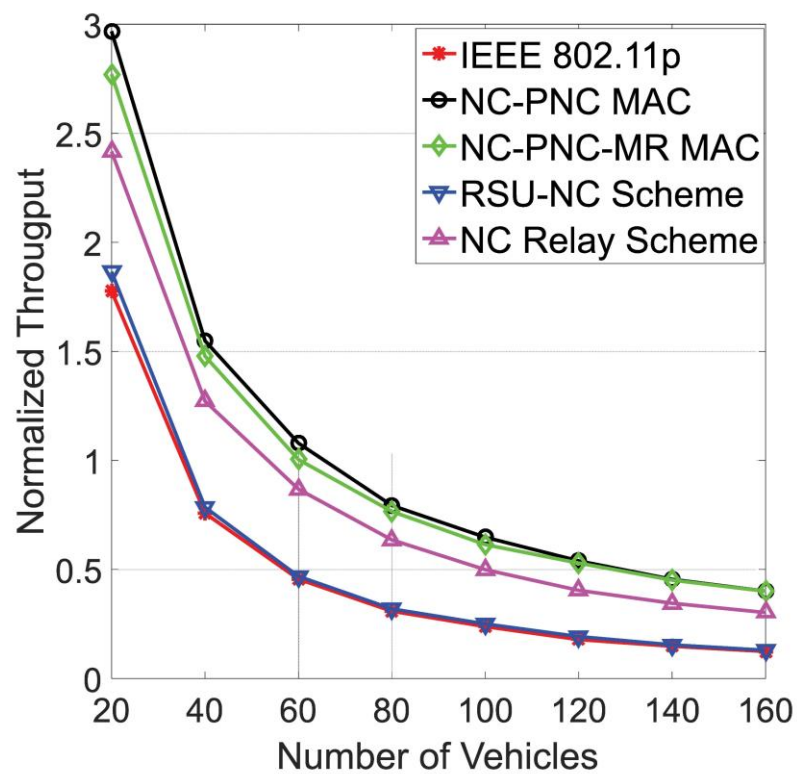
(b)

Fig. 4.7: Normalized throughput comparison among different schemes (r/R=1/3, data rate=6 Mbps) in: (a) the roadway scenario; (b) intersection scenario.
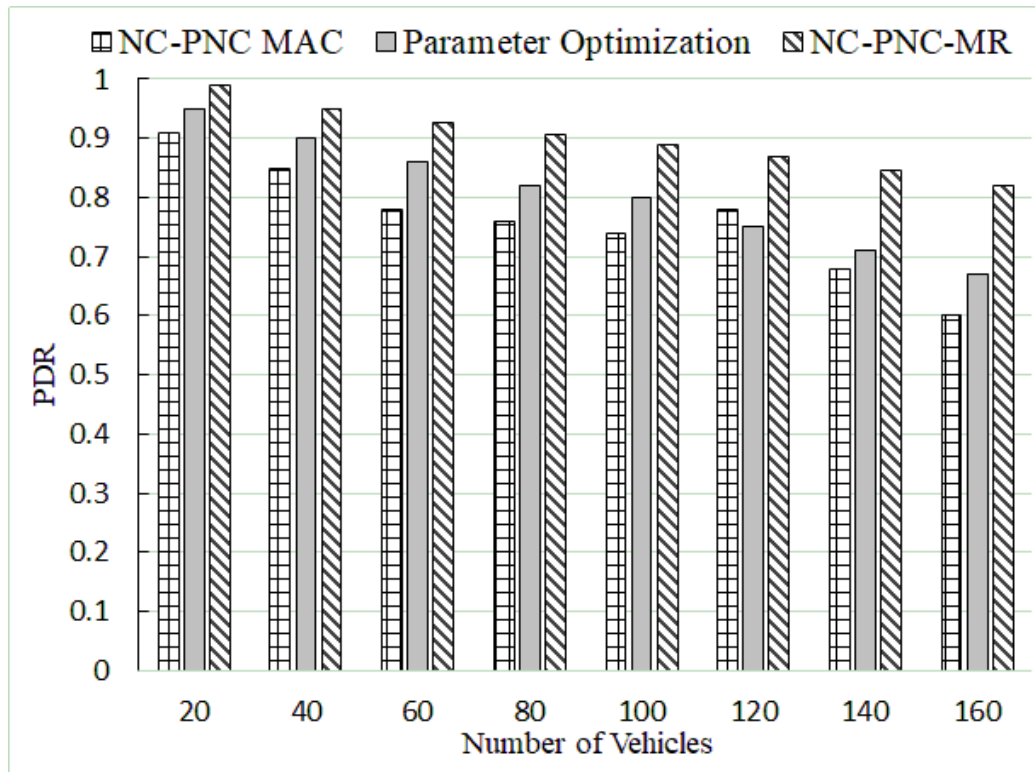
(a)
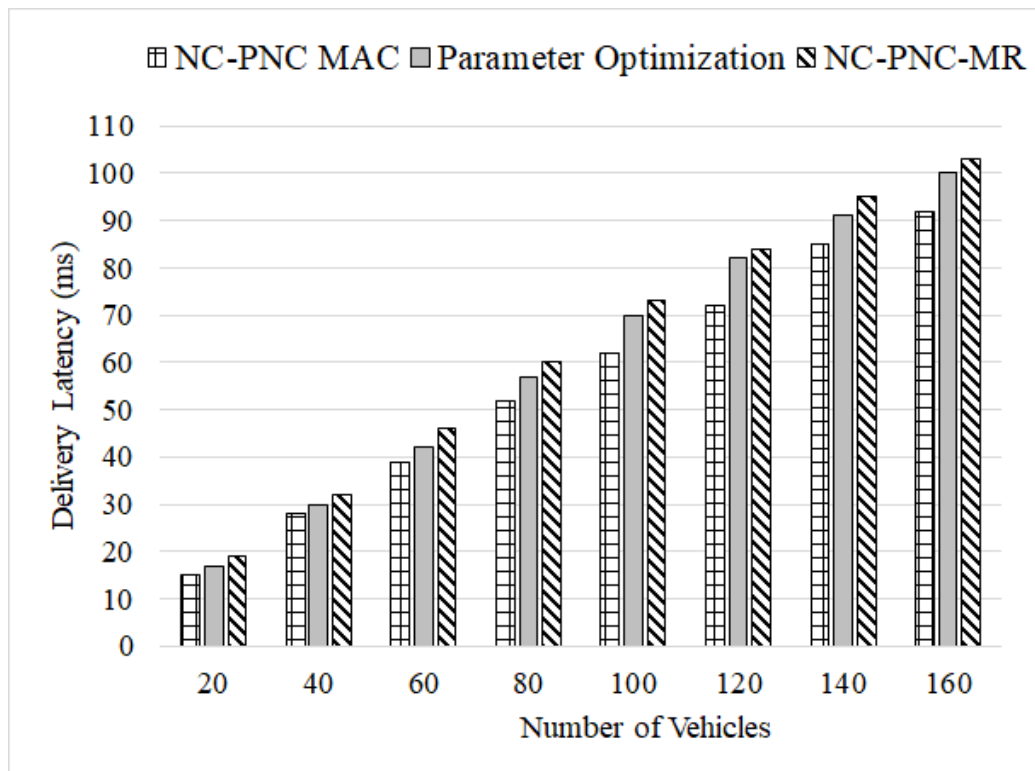
(b)

Fig. 4.8: Comparison between two performance enhancement strategies (*r/R*=1/3, data rate=6 Mbps) in: (a) enhancement in PDR performance; (b) cost of the enhancement in time consumption.

4.4.3 Comparison Between Two Enhanced Strategies and Discussions

In the above two subsections, two upgraded strategies have been proposed and evaluated. Both of the strategies can boost the PDR performance of the vehicular network, thereby contributing to improve the reliability of safety message broadcasting. The following parts will examine and compare the two enhanced schemes and shed more light on their features.

In order to illustrate which strategy has better PDR performance, we plot a bar chart to show the PDR for the original NC-PNC MAC, the parameter-optimized scheme discussed in 4.4.1 and multiple-relay scheme (NC-PNC-MR) described in 4.4.2, as shown in Fig. 4.8 (a). From the figure, the NC-PNC-MR scheme has the largest packet delivery ratio with the same configuration (i.e., data rate is 6 Mbps and $r/R=1/3$) for all traffic densities. This advantage is enlarged in dense networks. The performance difference between NC-PNC-MR and parameter-optimization one increases from 4% to 20% as the number of vehicles increases from 20 to 160. The relative superiority of NC-PNC-MR proves that it can better handle the BSM dissemination in dense vehicular networks than others because the auxiliary relays broadcast network-coded packets to vehicles that are remote from the main relays. The above observation provides us with an inspiration for deployment of NC-PNC MAC. In some areas with less vehicles (say rural areas), the parameter-optimized scheme or even the NC-PNC MAC is excellent enough. By contrast, in urban areas, NC-PNC-MR may be more suitable.

On the other side, from the Fig. 4.8 (b), it is not hard to find that the NC-PNC-MR, though has the best PDR performance, also consumes the most quantity of time, which may incur larger delivery latency or even exceeds the lifetime of BSM packets (i.e., 100 ms). This is unacceptable for safety messages as a late reception may not prevent road accidents. However, the NC-PNC-MR scheme demands more computational resources than that of the parameter-optimization scheme, because the auxiliary relays need to execute the RLNC encoding process shown in equation (3.7) and recipient nodes also need to implement decoding process. The parameter-optimized approach requires the same resources of the single-relay NC-PNC MAC. The overhead of extra time consumption stems from more transmission batches during OFDMA uplink period. In short, the two enhanced approaches have better performance at the cost of either larger delivery latency or more computational resources.

4.5 Summary

This chapter provides more insights on the hybrid MAC protocol, the NC-PNC MAC, as well as attempts to enhance its reliability for BSM dissemination in vehicular networks by means of two distinct strategies. At first, it mathematically analyses the protocol, including the total number of transmissions and the average packet delivery ratio in one broadcast interval. The analytical results prove that the protocol shows a linear communication complexity as the total number of

transmissions in a dissemination interval grows linearly against the vehicle volume. The analytical model has been validated by extensive simulations carried out in NS-3. Furthermore, based upon the theoretical analysis, an adjustable parameter N_b (i.e., the number of uplink batches) that affects how vehicles join the data exchange sessions is pinpointed, and the maximum PDR is acquired accordingly by assigning an appropriate value of N_b. Then taking into account the time constraint on safety message dissemination in reality, the results are reconsidered before indicating the best PDR performance for vehicular networks with different traffic densities. Besides the parameter-optimization strategy, a multi-relay scheme is conceived based on the features of the protocol and observations in the simulation. The PDR performance can be improved by designating extra relays (called auxiliary relays), which forward network-coded packets to distant vehicles. Finally, the individual advantages of two upgraded schemes are compared and the trade-off between the PDR and the extra costs (delivery latency and computation resources) are discussed.

Chapter 5 A Fuzzy-Logic Based Resource Allocation Algorithm in 5G V2X

5.1 Introduction

This chapter spotlights V2X communications in 5G cellular networks, which has drawn much attention in recent years. Differing with V2X communications supported in DSRC, C-V2X communications in 5G enable more advanced services included in the latest standard released by the Third Generation Partnership Project (3GPP). Those services, on the one hand, fulfil more exciting functions visualized in ITS; on the other hand, however, consume much more spectrum and time resources, as well as have more stringent requirements. To guarantee the quality of the services, making full use of the limited resources is necessary. Therefore, resource allocation plays a crucial role to exchange information among vehicles, infrastructure, and other devices. To investigate the resource allocation in C-V2X and its influence on network performance, we firstly develop a straightforward resource allocation scheme derived from the standard and a location-aware strategy. A network model for V2X communications is built in urban areas, and typical safety and non-safety services are considered in the network. Simulation results reveal that although both the proposed resource allocation schemes are able to avoid transmission collisions and inter-vehicle interference, they cannot provide guaranteed services, especially for the enhanced V2X services. Consequently, a self-adaptive fuzzy-logic based algorithm is proposed to allocate resources in a more intelligent way. Compared with the counterparts, the proposed fuzzy algorithm can effectively improve the resource utilization and satisfy the requirements of V2X services. Table 5.1 list all notations used in Chapter 5.

5.2 System Model

This subsection will describe a cellular network as the study objective and discuss types of V2X services considered in the network.

5.2.1 Network Model

We aim to investigate how to allocate resources for V2X communications in a 5G cellular network that provides various UEs (including vehicles, RSUs, smart phones) with basic safety services, enhanced safety services and infotainment-related services.

As depicted in Fig. 5.1, different types of UEs (RSU is deemed as a static UE) and an eNB in the network model. All UEs fall into the coverage of the eNB. Each RSU covers a zone at a predefined hotspot. Those UEs are exchanging information via sidelink and working in mode 3. The eNB, on the other hand, are dynamically dedicating resources to UEs. A UE should firstly send a request message to the eNB via the uplink. As long as receiving a reply message that indicates which

Table 5.1: List of Notations in Chapter 5.

Notations	Description
r, S	Coding rate, Packet size
N_{RB}^{sub}	The number of RBs in a subchannel
L_{subCH}	the number of contiguously allocated subchannels
N_{subf}	The number of subframes
RIV	Resource indication value
n_{subCH}^{start}	The beginning subchannel index
N_{subCH}	The total number of subchannels
$numsubfr$	The number of subframes needed for a transmission
$numsubch$	The number of subchannels needed for a transmission
$curSubfr$	The index of current subframe
$curSubch$	The index of current subchannel
$subfr\_tx$	The subframe index for a scheduled transmission
$subch\_tx$	The subchannel index for a scheduled transmission
P	Transmission period for a certain application
w	the sequential number of the current subframe in the whole transmission period P
P_r, P_t	The receiving power, The transmission power
G_l	The antenna gain
λ	The wave length
d	The distance between transmitter and receiver
d_0	The reference distance
PL_0	The path loss at the reference distance d_0
χ	A zero-mean Gaussian distributed random variable
R	The transmission radius of the vehicle
d_i	The distance between a transmitter and the ith interfering node
$\mu_{\tilde{A}}(x)$	The output membership function
x^*	The x coordinate of the centroid of the shape
ω	The average received power in Nakagami fading channels
m	The fading figure in Nakagami fading channels

resources have been reserved for the UE from the eNB via downlink, the UE would start a transmission in accord with the resources assigned by the eNB. If the eNB fails to find available resources for a request, it will decline the request and the UE will cancel the transmission.
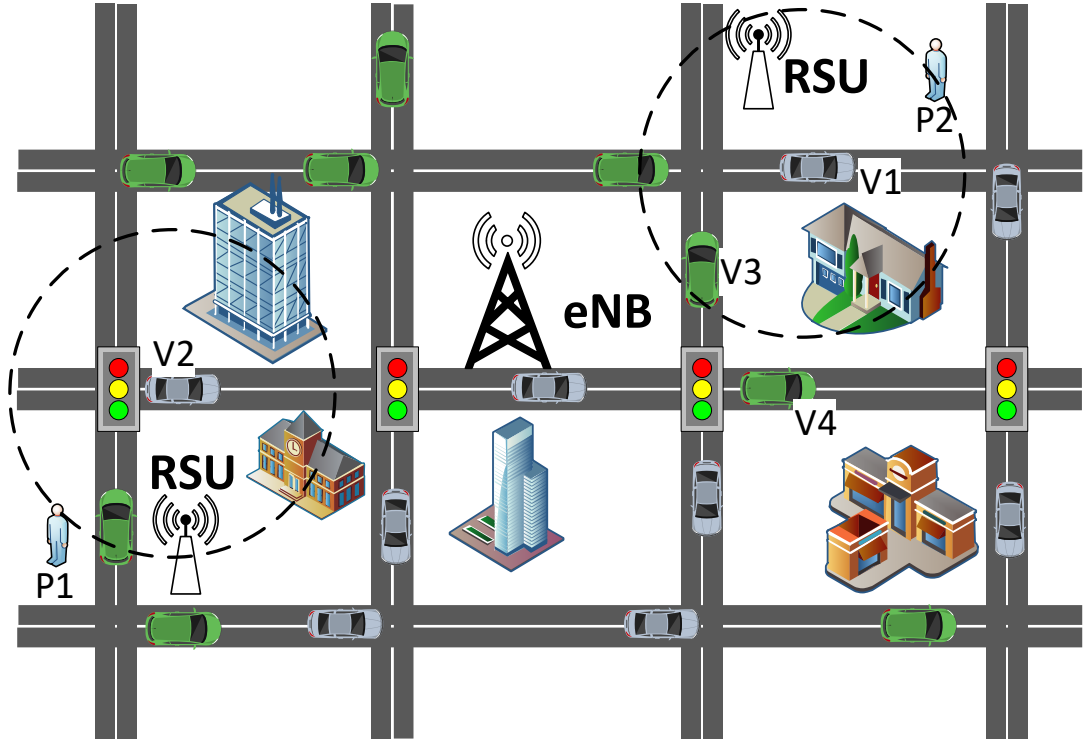
Fig. 5.1: V2X communications in a 5G cellular network in urban areas.

5.2.2 V2X Services Implemented in the Network

We consider six typical services in the system model. To clearly demonstrate the comprehensive effect impacted by various of V2X applications in a cellular network, the elected services cover both safety and non-safety related scenarios. Their features and requirements are listed in Table 5.2.

Cooperative awareness message (CAM) defined by European Telecommunications Standards Institution (ETSI) [127] is a periodic message to interchange a vehicle's instant status among its counterparts in vicinity. It resembles the BSM in DSRC. Cooperative manoeuvre is used to coordinates moving vehicles, such as platooning, lane change coordination, thus requiring higher data rate and beacon frequency than CAM. Distinguishing with the two prior types, cooperative sensing involves in triggering events rather than continuously periodic broadcast. In this case, immense amount of data generated by kinds of sensors equipped in vehicles are exchanged within a short period to prevent crashes or provide mutual awareness, for instance. In our network model, we assume vehicles broadcast such kind of data only when they arrive at an interception because it can prevent accidents in complicated traffic situations, such as zones at interceptions.

For the case of dynamic traffic control and warning, it is concerned with notifying vehicles about current traffic status and road conditions. Regarding the last two scenarios, which are both non-safety applications, the real-time one is usually required by social media applications and entertainment applications such as online chat and video stream, while the other is demanded by data downloading services like email over Internet. For the sake of easier discussion, we use CAT1, CAT2, …, CAT6 to denote six elected scenarios listed in the table, from the top to the bottom.

Table. 5.2: Type of services implemented in the V2X communications.

V2X Services	Message Type	Beacon Frequency	End-to-End Delay	Data Rate
Cooperative awareness (CAT1)	Periodic broadcast	100 ms	100 ms	5-100 Kbps
Cooperative manoeuvre (CAT2)	Periodic broadcast	10 ms	10 ms	2-5 Mbps
Cooperative sensing (CAT3)	Event-driven Broadcast	N/A	10 ms	10-25 Mbps
Dynamic traffic Control and warning (CAT4)	Periodic broadcast	500 ms	500 ms	0.5-2 Mbps
Nonsafety non-real-time content (CAT5)	Non-periodic unicast	N/A	N/A	1-5 Mbps
Nonsafety real-time content (CAT6)	Non-periodic unicast	N/A	20 ms	5-10 Mbps

5.3 Dynamic Resource Allocation Schemes in 5G V2X

In this subsection, three dynamic resource allocation schemes for mode 3 will be presented. The first one that is based on the standard is a basic method. Compared to the first method, the second one attempts to increase the network capacity by leveraging the position information of vehicles, while the third strategy adopts a fuzzy logic system to further boost the network performance.

5.3.1 A Straightforward Resource Allocation Scheme

Since V2X communications in mode 3 are assisted by the base station, each vehicle needs to be under the cellular coverage. In fact, base station is in charge of radio resource allocation, and channel and transmission parameters are configurable. In this case, data is transmitted over sub-channels that consist of a number of RBs. To change subchannel granularity, the quantity of RB in a subchannel is flexible, and the number of subchannels for different transmissions is also adjustable. Unlike mode 4, in which UEs work in a distributed way and reserve resources applying an approach called semipersistent scheduling (SPS), 3GPP standard does not specify a particular algorithm to allocate resources for UEs in mode 3. However, according to [29], the assignment

of subframes and resource blocks should be done either in a dynamic way or a SPS-based way, as follows:
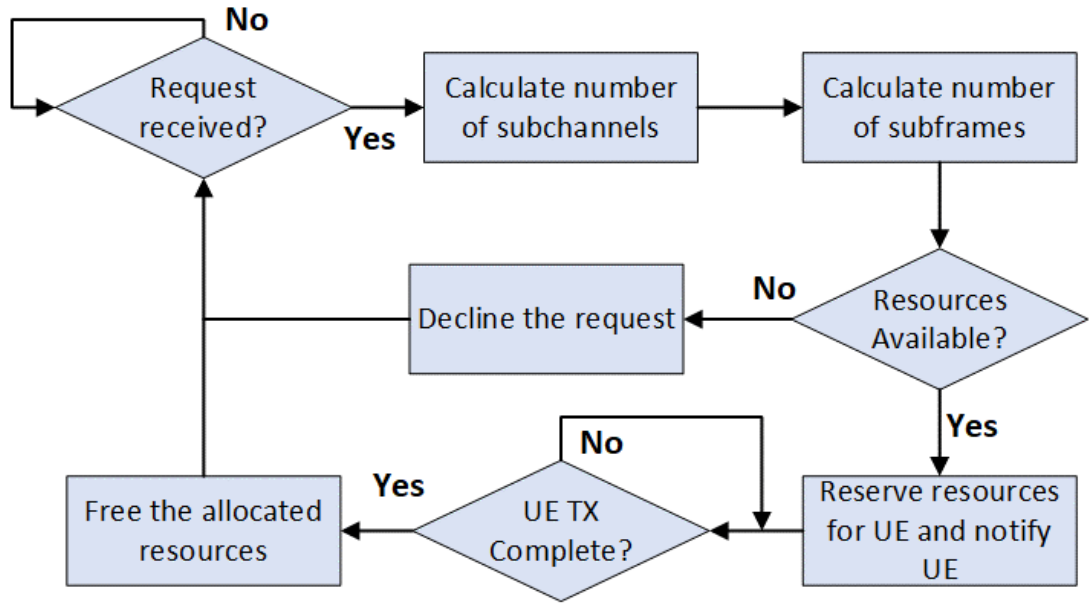
Fig. 5.2: The process of allocating resources in the naive method.

1) *Dynamic Allocation*: Vehicles and other UEs send requests to the associated eNB via uplink before each sidelink transmission and the eNB allocates resources and notify them via downlink. Suppose coding rate is r, packet size is S in bytes and the number of RBs in a subchannel is N_{RB}^{sub}, the number of contiguously allocated subchannels L_{subCH} for a transmission can be calculated by

$$L_{subCH} = \frac{8S}{12rN_{subf}N_{RB}^{sub}\log_2(M)},\tag{5.1}$$

where N_{subf} is the number of subframes shall be used and it is determined by the required data rate of a specific application, M is the constellation size. Frequency resource location is equal to resource indication value (*RIV*) that is given by

$$RIV = \begin{cases} N_{subCH}(L_{subCH}-1) + n_{subCH}^{start}, & \text{for } (L_{subCH}-1) \le \lfloor N_{subCH}/2 \rfloor \\ N_{subCH}(N_{subCH}-L_{subCH}+1) + N_{subCH}-1-n_{subCH}^{start}, & \text{other,} \end{cases}\tag{5.2}$$

where n_{subCH}^{start} is the beginning subchannel index and N_{subCH} is the total number of subchannels in the resource pool. Finally, if the SCI is transmitted on the PSCCH resource m in subframe t_n^{SL}, L_{subCH} consecutive subchannels $m, m+1, ..., m+L_{subCH}-1$ will be reserved for a requesting UE in the corresponding PSSCH in the same subframe.

2) *SPS-based scheme*: eNB allocates radio resources with a similar mechanism in mode 4. Since we mainly focus on dynamic method in mode 3 in this study, the details of SPS-based scheme and its performance evaluation are skipped, and relevant content can be found in [29-30][50].

A simple dynamic allocation method (the naive method) is based on random selection of sub-channels and subframes for each request. To explicitly show the process, a flow chart is provided in the Fig. 5.2. Once the eNB receives a request from a UE, it firstly calculates how many sub-channels and subframes needed by the UE, according to (5.1), then it searches the resource pool and attempts to allocate random resources for the UE. If it successfully locates available resources, it will notify the UE and specify which resources the UE can occupy. Otherwise, it will decline the request. The eNB may receive multiple requests from different UEs, to easily handle them, the eNB works in a first-come-first-serve mode.

The sidelink radio interface in each UE works in a half-duplex mode and VUEs cannot receive and transmit data at the same time via PC5 interface. In consequence, certain applications in V2X services, such as CAM, need to engage one or more subframes exclusively and do not allow other UEs to transmit over free subchannels during the engaged subframes. Otherwise, those UEs that are currently broadcasting messages forfeit receiving messages from their counterparts, which may cause road crashes. On the other hand, unicast related applications (i.e., CAT5 and CAT6) may allow multiple UEs to transmit simultaneously but adopting different subchannels.

5.3.2 A Location-Aware Resource Allocation

In order to obviate transmission collisions for message broadcasting, the eNB node tries to allocate different subframes for different UEs. Otherwise, all concurrent senders cannot receive each other's message even they occupy different subchannels, due to the property of half-duplex radio. For instance, for cooperative awareness message, which has the size of only 300 bytes, if we allocate 6 subchannels to it, such a message only takes up one subframe. Apparently, the remain 16 subchannels are wasted because other UEs cannot use them during the subframe. As a consequence, such strategy negatively influences the resource utilization ratio, thereby lowering the successful transmission ratio and the throughput. Relevant results will be discussed in 5.3.4.

Predicated on the above observation, we propose a distinctive resource allocation scheme called location-aware resource allocation (LARA) scheme. The key idea is to allow multiple UEs to transmit their data simultaneously without causing interference in reception. To realise this, when a UE sends a request to base station, it encloses its current location in the request packet. After receiving the request, the base station will allocate resources for the UE, which may reuse certain resources allocated to others previously or take up fresh ones. This process is conducted in accordance with both UE's location and message type. For instance, in Fig. 5.1, the two dashed circles are transmission range of vehicle *V1* and *V2* respectively. If both vehicles are broadcasting packets, they can use the same resources because they are too far to cause significant interference to their respective receivers.

Algorithm 1: Pseudo code of LARA

1: Procedure RA (*srcNod, srcAddr, dstNod, dstAddr, pkt*)
2:    *numsubfr* = calculateSubfr(*pkt*)
3:    *numsubch* = calculateSubch(*pkt*)
4:       **while** *curSubfr <= total_num_subfr*
5:        **if** *curSubch* in *curSubfr* free
6:          *subfr_tx* ⟵ *curSubfr*
7:          *subch_tx* ⟵ *curSubch*
8:        **else if** *dstAddr* is broadcast
9:          **if** *curSubfr* is broadcast
10:            *dist* ⟵ distance (*srcNod, other_src*)
11:              **if** *dist < 2*commRang*
12:                *curSubfr* ⟵ *curSubfr*+1, **Continue**
13:              **else**
14:                *subfr_tx* ⟵ *curSubfr*
15:                *subch_tx* ⟵ *curSubch*
16:                TxSchedule (*curSubfr, curSubch, pkt*)
17:          **else** *curSubfr* is unicast
18:            *dist1* ⟵ distance (*srcNod, other_dst*)
19:            *dist2* ⟵ distance (*other_src, other_dst*)
20:            **if** *dist1 > 2*dist2*
21:              *subfr_tx* ⟵ *curSubfr*
22:              *subch_tx* ⟵ *curSubch*
23:              TxSchedule (*curSubfr, curSubch, pkt*)
24:            **else**
25:              *curSubfr* ⟵ *curSubfr* + 1, **Continue**
26:        **else if** *dstAddr* is unicast
27:          *dist1* ⟵ distance (*srcNod, dstNod*)
28:          *dist2* ⟵ distance (other_*src, dstNod*)
29:          **if** *dist1 < 2*dist2*
30:            *subfr_tx* ⟵ *curSubfr*
31:            *subch_tx* ⟵ *curSubch*
32:            TxSchedule (*curSubfr, curSubch, pkt*)
33:          **else**
34:            *curSubfr* ⟵ *curSubfr*+1, **Continue**
35:        **end while**
36:      **if** Tx scheduled
37:        Send (*subfr_tx, subch_tx, numsubfr, numsubch, pkt*)
38:      **else**
39:        AbortTx (*pkt*)

Another case in point is to use different subchannels yet the same subframes. Let us still suppose *V1* is broadcasting at subframe *t* and *V4* would send a packet to *V3*, *V4* probably cannot receive the broadcast information from *V1* due to large distance between them. In this case, the based station can allow *V4* to use other free subchannels in subframe *t* rather than waiting for the next subframe. The location-aware resource allocation is described in Algorithm 1.

The LARA algorithm begins to run once the eNB receives a request sent by a UE via uplink. The variable *curSubfr* and *curSubch* are pointers to subframes and subchannels in the resource pool, respectively. They are initialized to the beginning positions of the pool. From Line 5 to Line 35, it searches resources one by one until finding free resources or occupied ones yet not resulting in much interference to the ongoing transmissions. To reuse the resources and restrain the inter-vehicle interference, A simple and effective strategy is to compare distances. If the distance between the destination node(s) (say node d_1) and the source node (say node s_1) of a planning transmission is no more than half of the distance between d_1 and another source node s_2 that is sending at the moment, we deem s_1 and s_2 will not interfere with each other. If available sources are fund, the values of the two pointers will be assigned to two new variables *subfr_tx* and *subch_tx*, which are input arguments of transmission function in Line 37. Otherwise, transmission will be aborted due to inadequate resources.

5.3.3 A self-adaptive fuzzy-logic based algorithm for Resource Allocation

1) Features of the standardized scheme and the LARA and challenges

The proposed random allocation method in 5.3.1 and the LARA in 5.3.2 can achieve almost 100% packet delivery ratio, as shown in Fig. 5.10, if inter-cell interference is not considered, because the intra-cell interference is diminished as much as possible. For example, in the randomly assigning method, two or more simultaneous broadcasts are not allowed, while in the LARA the distance between any two concurrent transmitting nodes are far larger than their communication range, thus not causing too much interference. However, the two approaches are not able to guarantee the QoS because a considerable part of requests have been declined, especially the density of the network turns larger, as depicted by Fig. 5.9. In such circumstance, the low successful transmission rate (STR)[8] means those UEs cannot exchange information with their peers.

In order to improve the STR yet keeping a high reception ratio, resources should be optimally dedicated to UEs in the cellular network. To this aim, multiple interacting factors should be considered at the same time. Otherwise, it cannot produce the best results. For example, in many wireless networks, channels are usually highly reused by multiple users. That is, concurrent links have been considered. Notwithstanding, concurrent transmissions may cause severe interference sometimes, if not well arranged. As we know, the probability of the packet reception rate depends on signal-to-interference-plus-noise ratio (SINR). In wireless channels, the factors that contribute

---

[8]STR is defined as the ratio that the total number of successful transmissions account for the total number of transmission requests over a period.
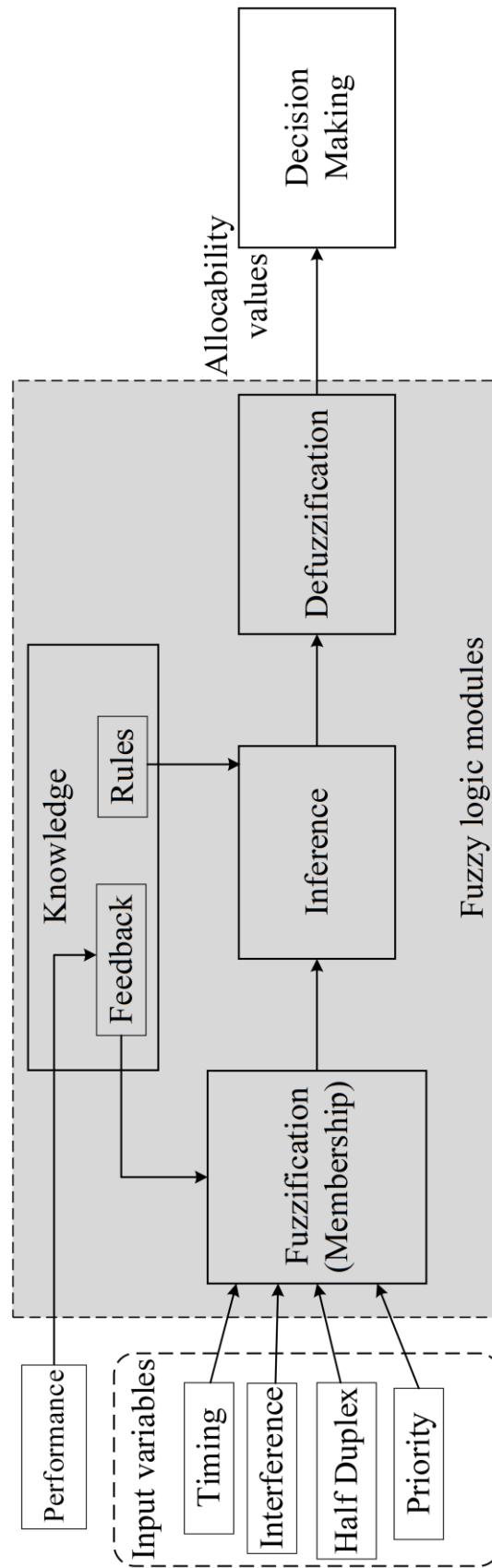
Fig. 5.3: Diagram of FUZZRA algorithm.

to the SINR are often random (or appear random), including the signal propagation and the location of transmitters and receivers. Therefore, although interference can be theoretically formulated sometimes, it is rather hard to predict and track the SINR, especially in highly mobile vehicular networks. Based on such observation, adopting the range of SINR seems to be more effective and reasonable to model the network performance. Compared with some heuristic algorithms [54] [55] in resource allocation, the proposed FUZZRA does not need accurate information of channel state, which is nearly impossible to acquire in highly dynamic mobility and complicated environment like urban areas. In addition, another advantage of fuzzy logic is that there is no training process before deploying it in a C-V2X network, compared with newly emerging algorithm based on machine learning [136].

On the other hand, aside from the interference, other factors also play a part in determining the network performance. Those factors also possess certain extent of fuzzy attribute. For example, different types of applications coexisting in the network may have different priorities, which should be considered at the same time. However, crispy-value based functions/algorithms cannot well deal with such factors. To comprehensively taking account the randomness and fuzziness of interference and other factors, an adaptive fuzzy-logic based algorithm is designed to allocate time and frequency resources more wisely.

2) Overview of the algorithm

The proposed fuzzy-logic based resource allocation (FUZZRA) specifes the best choice of resources for sidelink transmissions in a cellular network and maximize the reuse of the resources, thus improving the network performance. Fig. 5.3 presents the schematic diagram of the algorithm.

The core of the algorithm is the *fuzzy logic modules* that process the input information and output crisp values indicating allocability of certain resources. The input variables are actually four factors (i.e., timing, interference, half-duplex and service priority) that will assess the suitability of the resources for a transmitter. The definition of those factors will be discussed in the following paragraphs. Upon reception of a request from a UE, the four corresponding factors will be fuzzified by the membership functions that convert single-valued inputs into the values of a fuzzy set. The fuzzy values will be judged in the inference module according to predefined rules. Finally, the judgement that stands for the extent of a verdict will be defuzzified and numerical values showing allocability will be yielded for decision making. Furthermore, the real-time network performance, which also acts as knowledge, is fed back to the fuzzification module as a critical principle in adjusting the parameters of the membership functions. In this study, according to the feature of the inputs, the coefficients of the membership functions of the interference factor and the half-duplex factor can be adjusted, while the priority of provided services in the network can also be reconfigured accordingly. Noticeably, before each sidelink transmission, the sender

should first send a request message that contains the information of its current location and packet reception during the last transmission period.

3) Considered factors

I. Timing factor

This factor shows how urgently a message will be sent. The higher value is, the less the time left for transmission. Different types of messages have different requirement on data rate, i.e., transmission period. This factor is defined based on the observation that different applications in V2X have different requirements on data rate. A message can be transmitted at any subframes (i.e., time) but should be within the right transmission period, in order to obviate a large delay.

Table 5.3: Transmission periods and packet size for different services.

Services	Transmission period (millisecond)
CAT1	100
CAT2	10
CAT3	10
CAT4	500
CAT5	50
CAT6	10
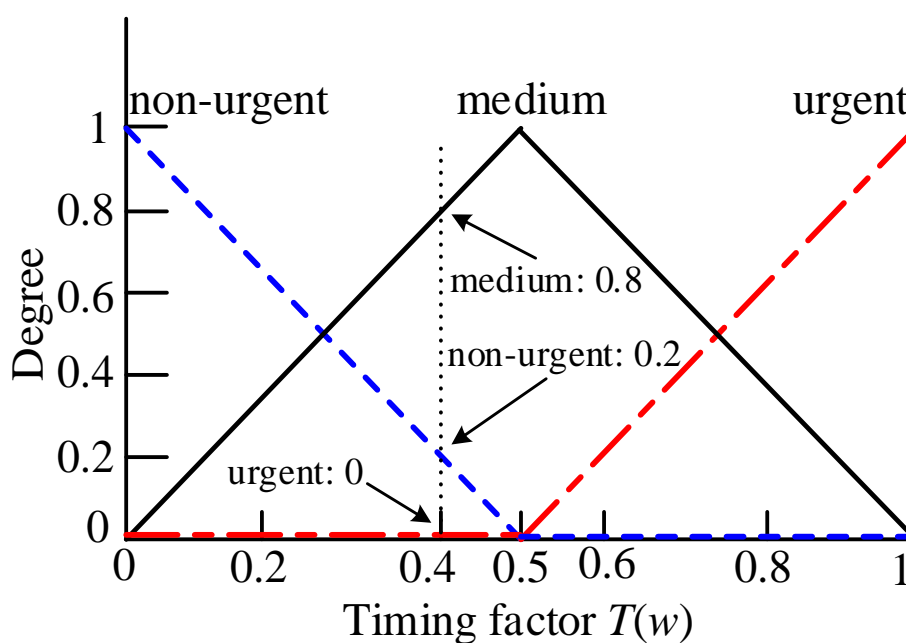
Fig. 5.4: Timing membership function and a fuzzification example.

Assume the transmission period for a certain type of message is P (i.e., P milliseconds or P sub-frames), the timing factor is calculated by:

$$T(w) = \frac{w}{P}, \quad 1 \leq w \leq P \tag{5.3}$$

where w is the sequential number of the current subframe in the whole transmission period P and it must be a positive integer. For example, if a transmission being currently scheduled situates in the ith subframe, then we let $w = i$. The w can only increase one each time if the current subframe does not work for the transmission. This can be deemed as adjournment. The values of P for different services are shown in Table 5.3, which is obtained according to data rates in Table 5.2.

II. Interference factor

Identical subchannels may be dedicated to multiple UEs at the same time, in order to improve the spectrum efficiency. This will surely cause interference to the recipient nodes owning to simultaneous transmissions. To assess the influence on a scheduling transmission accurately, real time SINR should be considered. However, among all service types, a substantial proportion of them involve in broadcasting, according to our system model and the reality of C-V2X networks. Apparently, a real-time update of SINR would pose great burden on networks. Fortunately, by adopting the fuzzy concept, we can estimate the interference level according to the distance between transmitters without feeding back the SINR.

Typically, the received power P_r for the unobstructed scenario is

$$P_r = P_t \left(\frac{\sqrt{G_l} \lambda}{4\pi d} \right)^2, \tag{5.4}$$

where P_t is the transmitted power, G_l is the antenna gain, λ is the wave length, and d is the distance between transmitter and receiver, according to Friis path loss model. The Friis model is restricted to unobstructed clear path between the transmitter and the receiver. To encompasses random shadowing effects due to signal blockage by objects like vehicles, trees, buildings, etc, we usually adopt a logarithmic-distance path loss model where the path loss PL is $PL = PL_0 + 10\gamma \log_{10}(d / d_0) + \chi$. In the equation, PL_0 is the path loss at the reference distance d_0, γ is the path loss exponent, χ is a zero-mean Gaussian distributed random variable. The equivalent non-logarithmic gain model is

$$\frac{P_r}{P_t} = d_0^\gamma 10^{-\frac{PL_0 + \chi}{10}} \frac{1}{d^\gamma}. \tag{5.5}$$
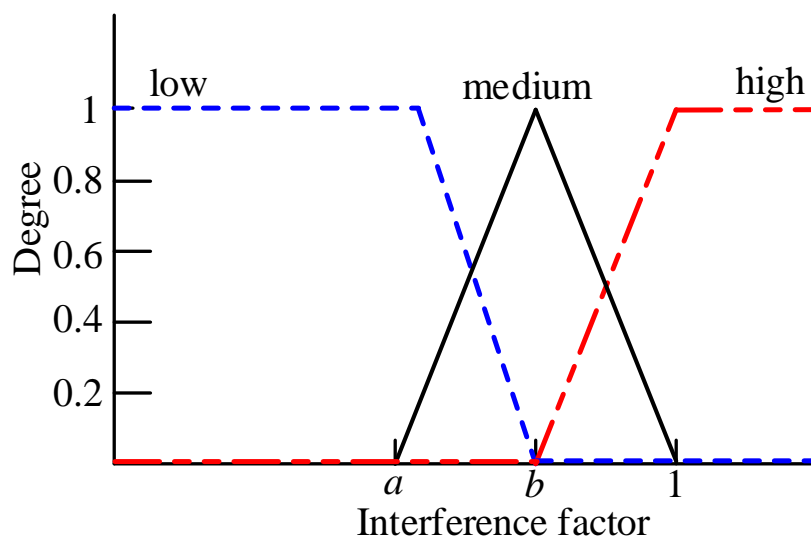
(a)
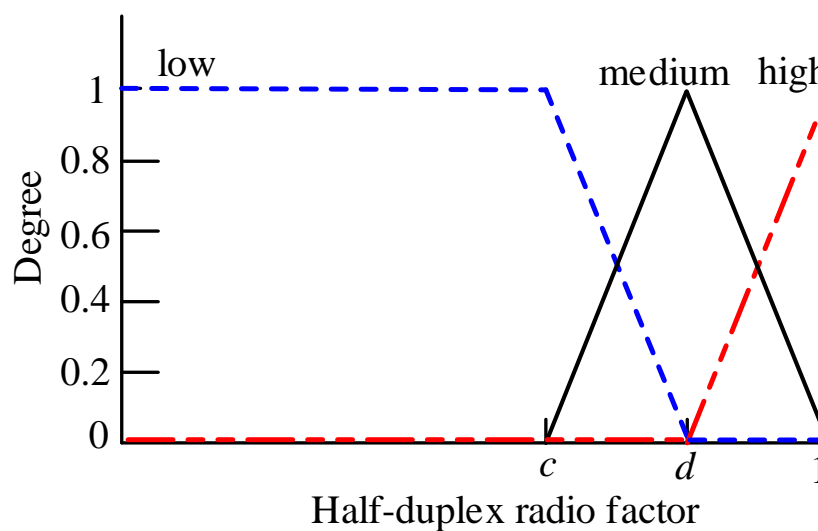
(b)

Fig. 5.5: The membership functions for (a) the interference factor and (b) the half-duplex radio factor.

Assuming all VUEs have the same transmission power, the received power is inversely proportional to the distance. That is, $P_r \propto d^{-\gamma}$ and γ depends on channel model. According to [127], the value of γ should range from 2.7 to 3.5 in urban areas, so we take $\gamma = 3$ in the definition of the interference factor.

Let R denote the transmission radius of the vehicle and d_i is the distance between a transmitter and the ith interfering node, if there are m transmitters that can cause interference, the interference factor can be defined as follows:

$$I(d_1, d_2, \ldots, d_m) = \begin{cases} +\infty, & \forall d_i \leq R \\ \dfrac{\sum_{i=1}^{m} \dfrac{1}{(d_i - R)^3}}{\dfrac{1}{R^3}} = \sum_{i=1}^{m} \dfrac{R^3}{(d_i - R)^3}, & d_i > R \end{cases} \tag{5.6}$$

The above formula reflects the relative strength between the interference and the receiving signal. A larger value of $I(d_1, d_2, \ldots, d_m)$ suggests a stronger interference caused to the receivers. For instance, if there is an interfering node within the transmission range of a node (i.e., $d_i \leq R$) that is broadcasting, a considerable percent of receiving nodes may experience failure in reception due to high interference level. By contrast, if the interfering node is far away from the sender, only the nodes locating within the overlapped area (if applicable) cannot receive the data.

III. Half-duplex radio factor

Half-duplex problem means a UE cannot receive data while transmitting at the same time even via different channels. This is confined by the attribute of the half-duplex radio. In V2X communications, if two VUEs within each other's communication range broadcast concurrently in different subchannels, vehicles around them can receive both information from them as the interference between two subchannels is negligible. However, the two sending nodes cannot have mutual reception in this situation. We call this as half-duplex problem, or mutual reception problem. Such situation diverges the original desire of certain applications, such as mutual awareness in CAM. On the other hand, if one vehicle lies outside broadcast range of another vehicle and they don't share the same resources, vehicles locates at the overlapped area of two vehicles can receive messages from both vehicles, which enhances the road safety in turn. Like interference factor, mutual reception factor is up to the received power and the distance between transmitters. Its definition is

$$M(d_{\min}) = \begin{cases} 1, & d_{\min} \leq R \\ \dfrac{\dfrac{1}{d_{\min}^3}}{\dfrac{1}{R^3}} = \dfrac{R^3}{d_{\min}^3} & d_{\min} > R \end{cases} \tag{5.7}$$

where $d_{\min} = \min(d_1, d_2, \ldots, d_n)$ represents the smallest distance between one currently sending node and n other sending nodes. From 0 to 1, the closer the value of $M(d_{\min})$ to 1, the larger the probability of suffering half-duplex problem will be.

IV. Service priority factor

As described in the 5G standard, different types of services have different priority levels. Generally, safety-related services have higher priority than those of non-safety-related ones. When the resources are limited and excessive UEs contend for transmission, high-priority services are superior to low-priority ones and they are supposed to have priority to obtain resources. In our system model, there are totally six types of services coexisting in the network. According to the service priority and the beacon frequency, the priority factor is initialized in Table 5.4.

Table 5.4: Priority factor.

Service Type	Priority
Cooperative manoeuvre (CAT2) Cooperative sensing (CAT3)	High
Cooperative awareness (CAT1) Dynamic traffic Control and warning (CAT4)	Medium
Non-safety non-real-time content (CAT5) Non-safety real-time content (CAT6)	Low

Remarkably, the above specification is not always fixed. The FUZZRA can adjust the priority of a service according to the dynamics of a network. When the transmission requests for a certain service with lower priority are largely more than that of another service with higher priority, its original priority can be promoted, for the purpose of avoiding waste of resources. Such adaptive strategy is based on the observation that transmissions for certain services like CAT3 and CAT6 take place intermittently or even some serviced can be disabled temporarily. In such situation, a dogmatic prioritization could incur large delay and low efficiency.

4) Fuzzification

In the fuzzification module, numerical values of input factors are converted to fuzzy values using fuzzy membership functions.

By using predefined linguistic variables of non-urgent, medium and urgent and their respective membership functions, the timing factor can be transformed into fuzzy value, as shown in Fig. 5.4 and equations from (5.8) to (5.10). For instance, when timing factors is 0.4, a vertical line representing this timing factor meets with curves of "non-urgent", "medium" and "urgent" at (0.4, 0.2), (0.4, 0.8) and (0.4, 0), respectively. Therefore, the fuzzy values we obtained are {non-urgent: 0.2, medium: 0.8, urgent: 0}.

The mathematical expressions of the three membership functions for the timing factor are

- the non-urgent: $f_{tn}(x) = \begin{cases} -2x+1, & x \in [0, 0.5], \\ 0, & x \in (0.5, 1], \end{cases}$ (5.8)

- the medium: $f_{tm}(x) = \begin{cases} 2x, & x \in [0, 0.5], \\ -2x+2, & x \in (0.5, 1], \end{cases}$ (5.9)

- and the urgent: $f_{tu}(x) = \begin{cases} 0, & x \in [0, 0.5] \\ 2x-1, & x \in (0.5, 1] \end{cases}$ (5.10)

The membership function of the interference factor is illustrated in Fig. 5.5 (a). The functions of the curves in the figure are:

- the low interference: $f_{IL}(x) = \begin{cases} 1, & x \in [0, a], \\ \dfrac{x-b}{a-b}, & x \in (a, b], \\ 0, & x > b \end{cases}$ (5.11)

- the medium interference: $f_{IM}(x) = \begin{cases} \dfrac{x-a}{b-a}, & x \in (a, b], \\ \dfrac{x-1}{b-1}, & x \in (b, 1], \\ 0, & other, \end{cases}$ (5.12)

- and the high interference: $f_{IH}(x) = \begin{cases} 0, & x \in [0, b], \\ \dfrac{x-b}{1-b}, & x \in (b, 1], \\ 1, & x > 1 \end{cases}$ (5.13)

In the above functions, the two parameters a and b are adjustable, in order to maximize the throughput of the network. More specifically, if a and b are tuned to be smaller, the degree of the interference factor will be inclined to enlarge the value of medium and high fuzzy value, thereby suppressing concurrent transmissions as well as alleviating the interference. In opposition, a larger a and b can encourage more nodes to transmit simultaneously via same resources but making the network subject to higher interference levels. By making use of feedbacks from nodes in the cellular network, the FUZZRA can adjust both parameters to improve the spectrum efficiency and the network throughput. The variable a and b are initialized to 0.4 and 0.7, respectively.

Similarly, the membership function for the half-duplex factor is defined in Fig. 5.5 (b), and the curves for low, medium and high cases are represented by (5.14), (5.15) and (5.16), respectively. Again, both c and d can be adjusted, and their initial values are 0.5 and 0.7, respectively.

$$f_{ML}(x) = \begin{cases} 1, & x \in [0, c], \\ \dfrac{x-d}{c-d}, & x \in (c, d], \\ 0, & x > d \end{cases}$$ (5.14)

$$f_{MM}(x) = \begin{cases} \dfrac{x-c}{d-c}, & x \in (c, d], \\ \dfrac{x-1}{d-1}, & x \in (d, 1], \\ 0, & x \in [0, c], \end{cases} \qquad (5.15)$$

$$f_{MH}(x) = \begin{cases} 0, & x \in [0, d], \\ \dfrac{x-d}{1-d}, & x \in (d, 1], \end{cases} \qquad (5.16)$$

5) Inference

Once the fuzzy values of the factors are determined, the inference module will use IF/THEN rules to induce the verdict. The linguistic variables of the verdict are defined as {Perfect, Good, Acceptable, Not Acceptable, Bad}. The rules are listed in Table 5.5. For example, in the table, Rule 5 can be expressed as follows.

IF *Timing* is Non-urgent, *Interference/Half-duplex* is Low, and *Priority* is High, **THEN** *Verdict* is Good.

In the table, interference and half-duplex radio factor are listed in the same column, because only one of them can appear at a time. That is, for resources being assigned to a currently scheduling of a transmission, those scheduled resources can cause either interference (i.e., with overlapped subchannels) or half-duplex radio (i.e., totally different subchannels) effect on the current ones.

Since there could be multiple rules being applied at the same time, the inference system adopts an unweighted Min-Max principle to obtain the results. In the principle, for each applied rule, the minimal value of the antecedent (i.e., the IF part) turns to be the final degree, while the maximal value of the consequents (i.e., the THEN part) is finally accepted when combining different rules.

To articulate how the Min-Max principle works, an example is included in Fig. 5.6. Suppose the degree of timing, interference and priority for a potential transmission are {Non-urgent: 0.2, Medium: 0.8, Urgent: 0}, {Low: 0.7, Medium: 0.3, High: 0} and {High}, respectively. In this case, these fuzzy values match the condition of rule 3, rule 6, rule 12 and rule 15. In rule 3, the degree for the non-urgent timing is 0.2, for the low interference is 0.7 and service priority is high. According to the minimal principle, we take 0.2 for the final verdict of Good. Similarly, the fuzzy value of final verdicts from rule 6, rule 12 and rule 15 are 0.2 for Acceptable, 0.7 for Perfect and 0.3 for Acceptable, respectively. In the last stage, as both rule 6 and rule 15 lead to the verdict of Acceptable, according to the maximal principle, the largest value between the two consequents is confirmed as the final value for the Acceptable.

Table 5.5: Rule base.

Rule	Timing	Interference/Half-duplex	Priority	Verdict
1	Non-urgent	Low	Low	Not Acceptable
2	Non-urgent	Low	Medium	Acceptable
3	Non-urgent	Low	High	Good
4	Non-urgent	Medium	Low	Bad
5	Non-urgent	Medium	Medium	Not Acceptable
6	Non-urgent	Medium	High	Acceptable
7	Non-urgent	High	Low	Bad
8	Non-urgent	High	Medium	Bad
9	Non-urgent	High	High	Not Acceptable
10	Medium	Low	Low	Acceptable
11	Medium	Low	Medium	Good
12	Medium	Low	High	Perfect
13	Medium	Medium	Low	Not Acceptable
14	Medium	Medium	Medium	Acceptable
15	Medium	Medium	High	Acceptable
16	Medium	High	Low	Bad
17	Medium	High	Medium	Bad
18	Medium	High	High	Not Acceptable
19	Urgent	Low	Low	Acceptable
20	Urgent	Low	Medium	Good
21	Urgent	Low	High	Perfect
22	Urgent	Medium	Low	Not Acceptable
23	Urgent	Medium	Medium	Acceptable
24	Urgent	Medium	High	Good
25	Urgent	High	Low	Bad
26	Urgent	High	Medium	Bad
27	Urgent	High	High	Not Acceptable

- Timing {Non-urgent: 0.2, Medium: 0.8, Urgent: 0}
- Interference {Low: 0.7, Medium: 0.3, High: 0}
- Priority {High}

- Rule 3: Non-urgent: 0.2, Low: 0.7, High $\longrightarrow$ Good: 0.2 = {min (0.2, 0.7)}
- Rule 6: Non-urgent: 0.2, Medium: 0.3, High $\longrightarrow$ Acceptable: 0.2 = {min (0.2, 0.3)}
- Rule 12: Medium: 0.8, Low: 0.7, High $\longrightarrow$ Perfect: 0.7 = {min(0.8, 0.7)}
- Rule 15: Medium: 0.8, Medium: 0.3, High $\longrightarrow$ Acceptable: 0.3 = {min (0.8, 0.3)}

- Perfect: 0.7
- Good: 0.2
- Acceptable: 0.3 = {max(0.2, 0.3)}
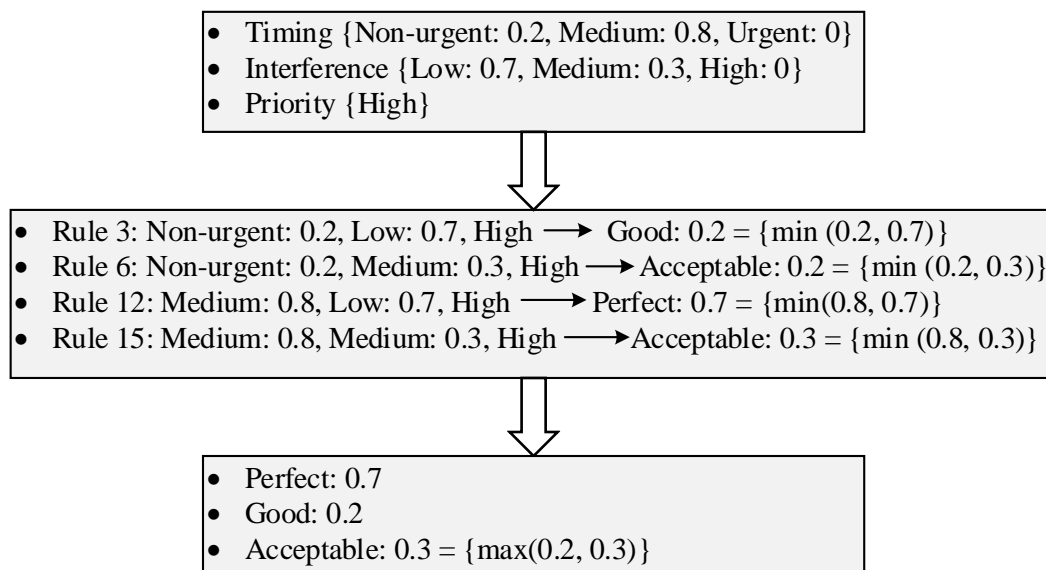
Fig. 5.6: An example of application of Min-Max principle in fuzzy rule evaluation.
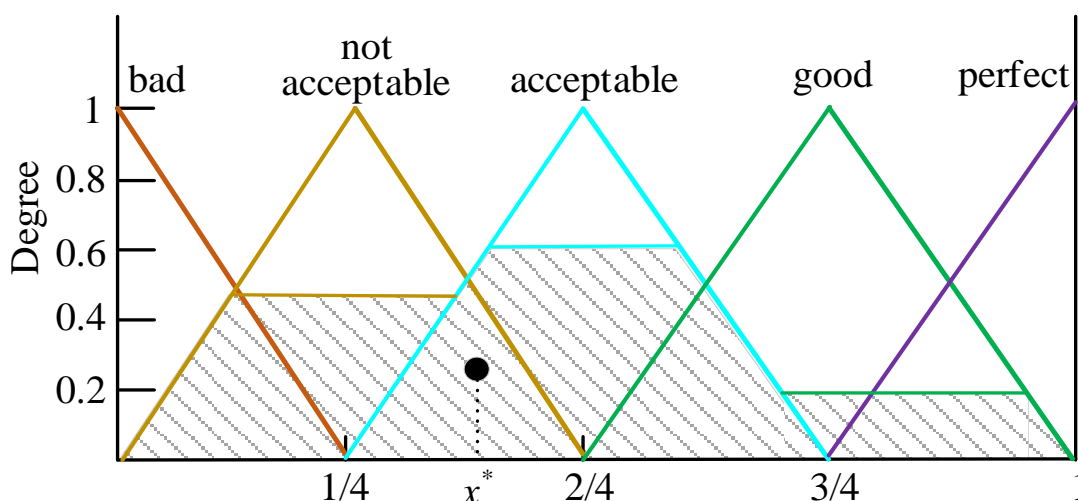
Fig. 5.7: Output membership function and the defuzzification method of COG.

6) Defuzzification and Decision Making

In defuzzification, the fuzzy values of verdicts are processed, and crisp values are produced based on an output membership function. There are different defuzzification methods with diverse characteristics and computation complexities. For example, according to the work [96], they are mainly categorized into two groups: maxima methods and distribution methods. In this study, we select the centroid method that calculates the centre of area or the centre of gravity (COG), which belongs to the latter. The output membership function is defined in Fig. 5.7. To compute the output value, we firstly use output values from fuzzification to truncate the defuzzification

functions in the figure, and then apply the disjunction principle to merge shapes and form a new shape. Finally, the following formula is utilized to calculate the x coordinate of the centroid of the shape, which is also the output of the whole fuzzification system.

$$x^* = \frac{\int x\mu_{\tilde{A}}(x)dx}{\int \mu_{\tilde{A}}(x)dx} \tag{5.17}$$

where $\mu_{\tilde{A}}(x)$ is the output membership function. In Fig 5.7, an example is provided to show the mechanism of COG. Assume the degree for the verdict "bad" and "perfect" is zero, and for "not acceptable", "acceptable" and "good" are 0.5, 0.6 and 0.2, respectively. After truncating the output membership function and applying disjunction on trapezoids, the geometric shape we obtained is the shadowed shape. By applying the equation (5.17), the final results of defuzzification can be obtained.

The *decision-making* module compares the output of the fuzzy system with a predefined value of threshold. If it is larger than the threshold, the resources will be dedicated to the requesting UE. Otherwise, other resources will be considered. If the FUZZRA cannot find appropriate resources for a request after searching the entire resource pool and the transmission time has expired, the eNB would decline the request and the transmission will not take place. As aforementioned, both the interference issue and the half-duplex issue are considered in the fuzzy system, two thresholds are predefined, and they correspond to the application of different combination of antecedents in rule base, i.e., applying timing factor, interference factor and priority factor or timing factor, half-duplex radio factor and priority factor.

5.3.4 Performance Evaluation

1) Simulation Setup

In order to evaluate the performance of C-V2X communications that apply the resource allocation strategies described above, we developed a 5G cellular network in NS-3 [63] according to the system model described in 5.2. It contains one eNB, a number of pedestrians, vehicles and RSUs. To simulate traffics in urban areas, a Manhattan grid network is built in SUMO [64], and it is connected with the cellular network created in NS-3 to form a complete communication system shown by Fig. 5.1. Vehicles and pedestrians are moving UEs on roads and footpath respectively, while RSUs play a role as static UEs. In addition, taking into account the existence of both the inter-cell interference and intra-cell interference in the reality, we simulate nine independent cells at the same time and measure the performance of the middle one (cell 9), as shown in Fig. 5.8.

Traditionally, the covered area of a cellular network is drawn as a hexagon. However, the shape of hexagon is far from the actual circumstance. In the reality, the network of roads/streets forms a grid, like typical Manhattan district. The road in adjacent cell may connect each other. However,

a hexagon cell means some of the roads may not be connected. Moreover, in the conducted simulations, the inter-cell interference is considered. The inter-cell interference usually significantly affects the vehicles moving on the roads on the borders of two cells. Hexagon cells make it hard to simulate the interference and reflect its influence. Therefore, for both the reasons of reality and simulations, a square cell is more suitable to reveal the real performance of C-V2X networks.
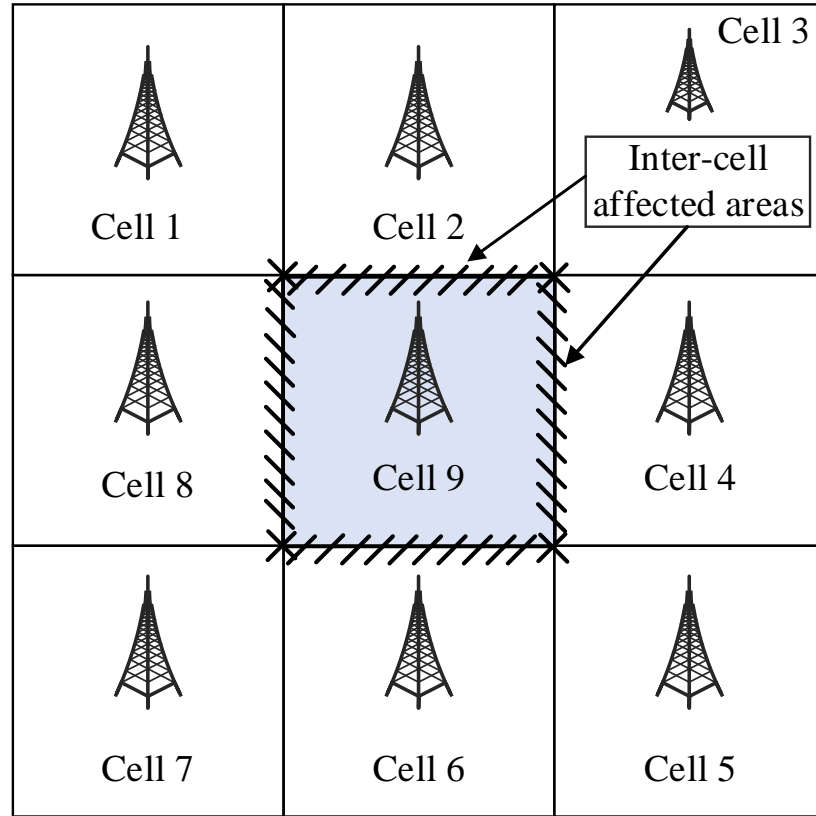
Fig. 5.8: Nine adjacent cells in the simulation model.

Vehicles broadcast the first two types of messages listed in Table 5.2 all the time to avoid accidents. The event-driven information (CAT3) is only disseminated when vehicles at interceptions and 200 packets are broadcast per vehicle per time. The CAT6 information is broadcast by RSUs. For the last two non-safety categories, we assume they are mainly associated with RSUs. Moving VUEs can directly access Internet when they fall into the coverage of RSUs. Actually, VUEs need to retrieve data from Internet only when they have the demand. To simulate it, we let P_{CAT5} and P_{CAT6} to denote the probability a UE needs to access Internet for the case CAT5 and CAT6, respectively. Pedestrians, as vulnerable road users, enable the CAM applications via cellular user equipment (CUEs, such as smart phones) to notify vehicles. Apart from CAT1, CUEs can also access services of CAT5 and CAT6 but not include services in CAT2, CAT3 and CAT4.

The Nakagami fading channels with proper parameters has been indicated as a realistic channel model in many vehicular networks. We assume that all channels in the simulation experience Nakagami fading and have the same channel gain over the whole duration of a packet. The probability density function of reception power Y can be expressed by

$$f_Y(y) = \frac{m^m y^{m-1}}{\Gamma(m)\omega^m} e^{\frac{-my}{\omega}}, \qquad (5.18)$$

where ω is the average received power and m is the fading figure. We make m equal 1.5 when the distance between sender and receive is less than 80 m or 0.8 for other cases, according to an empirical measurement [122]. In addition, for the large-scale fading, the path loss exponent between 2.7 and 3.5 is also indicated in the paper.

Table 5.6: Key Parameters in simulation.

Parameter	Value
Frequency/Band Width/Number of cells	5.9 GHz/20 MHz/9
Number of VUEs/CUEs/RSUs	200 to 1200/50/4
Transmission Range	eNB: 500 m, RSU: 200 m CUE and VUEs: 100 m
Packet Size/Coding Rate	300 to 3000 bytes/0.5
UEs Travel Velocity	Vehicle: 0 to 50 km/h Pedestrian: 0 to 10 km/h
Area Size/Grid Size	1000 m x 1000 m/10x10
Number of RBs per Subchannel / Total number of Subchannels in PSSCH	5/22
Supported Modulation	QPSK, 16QAM, 64QAM

Table 5.7: Combination of various services in simulations.

Simulation Case	Included Services
Case 1	CAT1, CAT2, CAT3, CAT4, only safety-related Services
Case 2	All services, $P_{CAT5} = P_{CAT6} = 0.1$
Case 3	CAT1, CAT3, CAT4, $P_{CAT5} = P_{CAT6} = 0.1$
Case 4	CAT1, CAT2, CAT4, $P_{CAT5} = P_{CAT6} = 0.1$

Table 5.6 lists all key simulation parameters. The PC5 interface for V2X communication works at 5.9 GHz. The resource pool consists of 100 subframes in time and 22 subchannels in frequency. To avoid large delay, a request should be approved in next T_{sf} subframes if resources can be found. The variable T_{sf} equals to beacon frequency or 100 ms for periodic or non-periodic transmissions, respectively. Packet reception can be guaranteed within the transmission range, but UEs that are out of the range may still have a certain probability to receive the transmitted information. The 3GPP standard has specified message size for different applications. The cooperative awareness only needs short packet of 300 bytes, while the packet size for both cooperative manoeuvre and non-safety applications is at least 1500 bytes. In contrast, in cooperative sensing scenario the size of transmitted packet can be up to 3000 bytes. The packet size of the event-trigger one is 1200 bytes.

Different types of message may adopt different modulations. For safety-related messages, since they are mostly broadcast and no retransmission once lost, low-order modulations are preferred. Instead, high-order modulations are more suitable for non-safety applications and high-data-rate scenarios. In the simulations, two types of non-safety related information are modulated by 64QAM while the 16QAM is adopted for the rest cases listed in Table. 5.2.

As mentioned before, eNB assigns resources to UEs according to the arrival sequence of the requests in the naive and LARA method. For some UEs, multiple requests may made for different V2X cases during the same period, so eNB deems all types of data have the same priority and treats them equally. By contrast, FUZZRA processes different requests with the consideration of their degree of urgency and service priority. Considering network congestions, retransmission is not allowed for broadcast cases.

2) Simulation results and discussions

Extensive simulations have been carried out to evaluate the network performance with the respects of successful transmission ratio (STR), packet delivery ratio (PDR), and the network throughput. To better show how different V2X services impact on the network, various combinations of the services have been considered in the simulations, as listed in Table 5.7.

Fig. 5.9 shows *STR* against number of UEs in a cellular network. the term *STR* is defined as the total number of successful transmissions divided by the total number of requests an eNB received over a period of time. With the increase of vehicle volume in a cellular network, the eNB may not find available resources for excessive transmission requests. From the figure, it is easy to observe that with the more UEs competing for resources for transmissions, *STR* descends significantly for both the naive and the LARA schemes in all cases. Moreover, a worse case is that even there are only 200 VUEs spreading over an area of 1 km^2, the *STR* is rather low (about 0.2) if all six services

are enabled (case 2) and the *naive* method is applied, not to mention the case with more VUEs. That is, more than 80% of the requests are declined due to insufficient resources, which is far to meet the requirements of many V2X applications. Although the LARA scheme can boost the *STR* somehow, compared with the naive, it is still far from satisfactory. However, the FUZZRA can maintain the *STR* in four cases at a very high level (no less than 98%) at all times. On the other hand, FUZZRA shows more robust than the other two methods, if enabling and disabling two eV2X services (cooperative manoeuvre and cooperative sensing). This is based on the observations that for the same resource allocation scheme, the gaps between case2 and case 3 or case 4 are different for three schemes but the smallest one is the FUZZRA.

In Fig. 5.10, the PDR performance is presented for both three schemes in case 2. The naive scheme has the highest PDR and it is followed by the LARA and the FUZZRA. The naive and the LARA has better PDR because the former does not have intra-cell interference and the latter has very limited intra-cell interference, so the corresponding two dashed curves are very close to 100%. This is determined by their characteristic of avoiding concurrent transmissions as much as possible in the same cell. However, the FUZZRA allows concurrent links as many as possible, in order to satisfy more requests from VUEs. Therefore, intra-cell interference inevitably appears, and it will lower the PDR. In addition, the inter-cell interference negatively causes almost the same effect on PDR for all three schemes because the resource allocation in all the adjacent cells works independently and the interference mainly affects VUEs that are close to the boundaries.

The curves for network throughput are plotted in Fig. 5.11. In case 1 and case 2, the throughput curves of the naive and the LARA fluctuate between 50 Mbps and 400 Mbps. One possible explanation for the fluctuation is that the resource allocation in naive and LARA does not prioritize the packet type, but different types have different packet sizes and data amount. As a result, if resources are mostly engaged by small-size packets, the throughput will be low. By contrast, the network throughput obtained from the fuzzy logic grows steadily from 1 Gbps to 11 Gbps, which significantly outperforms its counterparts more than 10 times. For each scheme in Fig. 5.11 (a), its relevant curves for case 1 and case 2 are very close. It proves that non-safety data does not affect the throughput substantially.

On the other hand, for the naive and the LARA, the two eV2X services have more considerable impact on the throughput than that of the FUZZRA, which can be seen based on the comparison between bottom curves in (a) and (b). Removing any one of eV2X services will greatly lower the throughput from 350 Mbps to 10 Mbps. However, such changes in provided services do not incur so large difference of the throughput if FUZZRA is adopted in the network. The benefit stems from the adaptiveness of the FUZZRA that can dynamically promote the priority of a service to a higher priority in accord with network status (say raise the priority of CAT1 from medium to high if less requests of high-priority messages). However, the naive and the LARA always treat
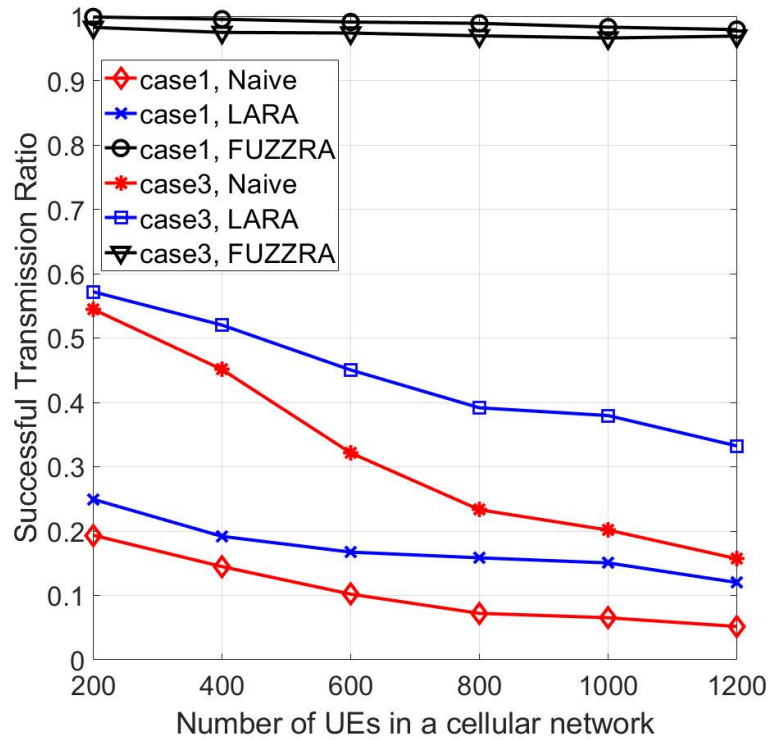
(a)
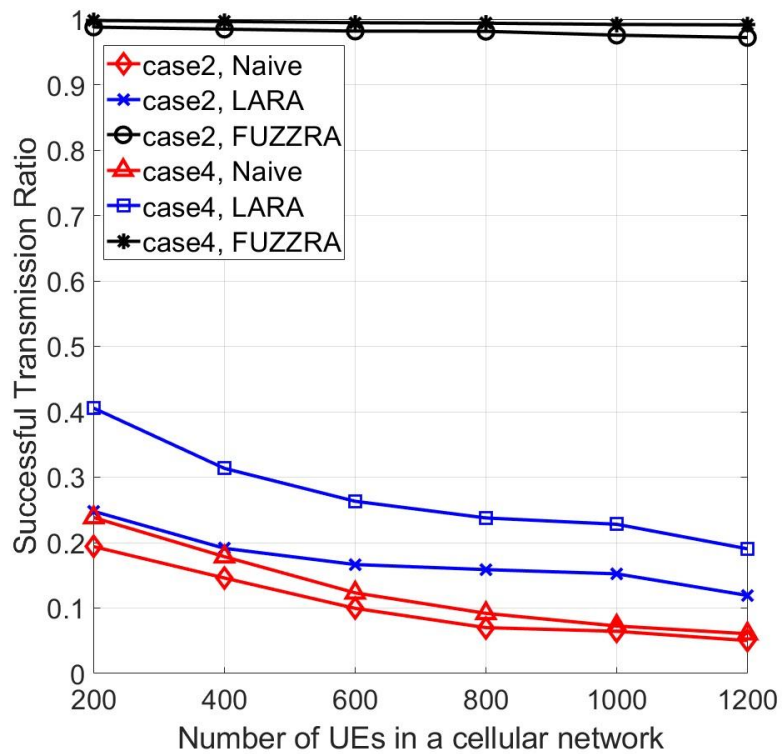
(b)

Fig. 5.9: Successful transmission ratio for V2X communications applying various resource allocation schemes.

different types of services equally and work in a first-come-first-serve mode, which may be always affected by the proportion among the requests with different priority.

Fig. 5.12 further shows the constituent of transmitted packets of different applications. The results are obtained under the circumstance of case 2. The naive and LARA treat all kinds of requests equally, so applications with higher request frequency yet less resource consumption account for the most, which can be validated by the proportions represented in (a) and (b). Therefore, the transmissions of CAT1 make up the most in the naive and the LARA. In contrast, in FUZZRA, messages of CAT2 and CAT3 have the highest priority, so they take up the most part in the total number of transmissions. Among all transmissions, packets of CAT2 are transmitted most frequently. The priority of CAT1 and CAT4 is moderate, so the CAT1 has the third largest proportion. CAT4 occupies the smallest part as its transmission frequency is the lowest, although it has higher priority than the non-safety related categories of CAT5 and CAT6, and the observation meets our expectation.
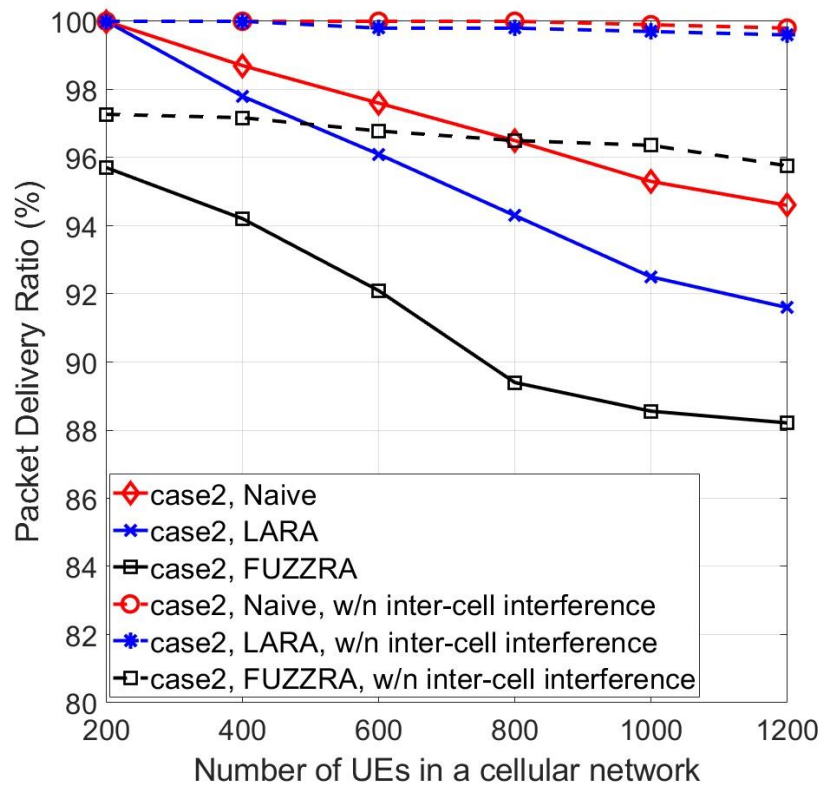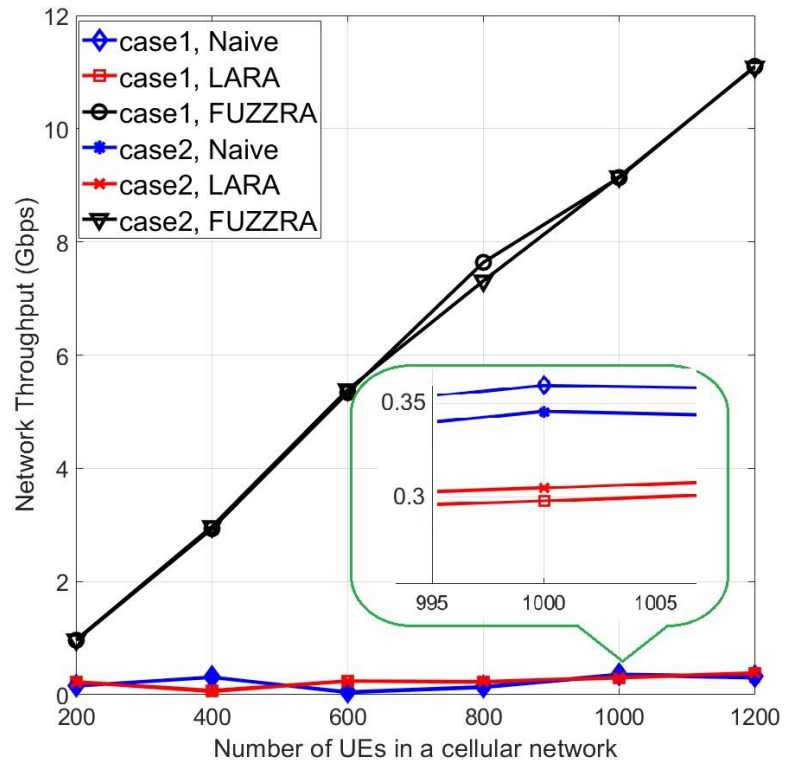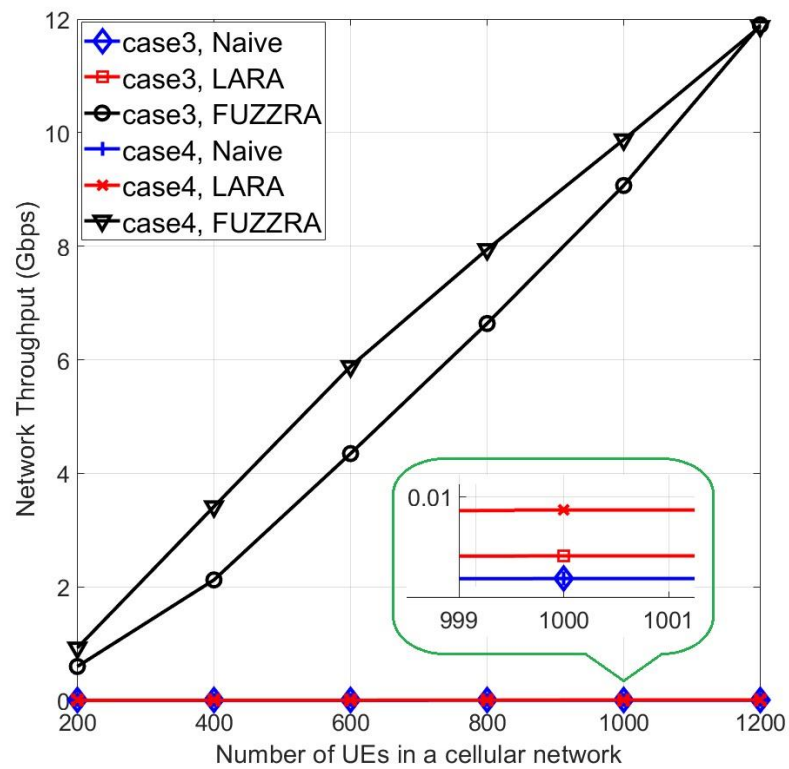

Fig. 5.10: PDR performance comparison among three allocation strategies for packet delivery ratio.

(a)

(b)

Fig. 5.11: Network throughput for C-V2X applying four different resource allocation algorithms.
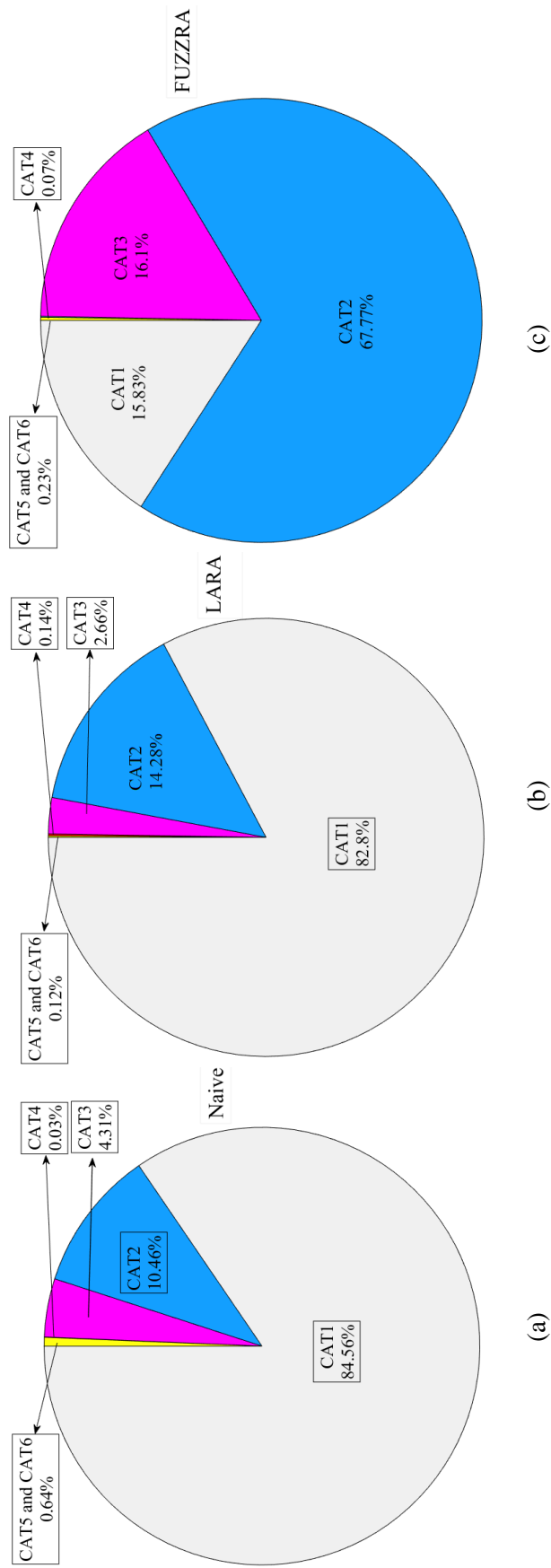
Fig. 5.12: Constituent of different types of packets in V2X communications applying different algorithms of resource allocation for: (a) Naive; (b) LARA; and (c) FUZZRA.

5.4 Summary

In this chapter, we investigate the strategy of resource allocation for 5G V2X communications. We first introduce the two types of resource allocation in mode 3. Since vehicles and other UEs are within the coverage of the base station, we focus on the dynamic resource allocation, in which the base station manages all two-dimensional time-frequency resources. However, the V2X standard proposed by 3GPP does not mandate any dynamic resource allocation for mode 3. Predicated on such fact, three distinct resource allocation algorithms have been proposed: 1) a straightforward method (i.e., the naive); 2) a location-aware one (i.e., the LARA) and 3) a fuzzy-logic based adaptive approach (i.e., FUZZRA). The naive randomly assigns resources to transmitters but it avoids concurrent transmissions in a cell. The LARA tries to reuse the spectrum and improve the effectiveness of information dissemination based on the knowledge of vehicles' instant locations. The FUZZRA takes multiple variables as input factors and comprehensively considers how to allocate appropriate resources to various UEs by advantage of fuzzy logic. It can also dynamically adjust the parameters in the fuzzy system according to the network status in order to ensure the full utilization of resources and QoS. A system model is developed by NS-3 and SUMO to simulate V2X communications in a cellular network, in which both the inter-cell and intra-cell interference exist. Simulation results demonstrate that although the naive and the LARA scheme can prevent the intra-cell interference, thus leading to a higher PDR than the FUZZRA, they cannot satisfy the requirement of certain services, especially enhanced safety-related services. On the other hand, the FUZZRA can help to effectively boost the resource utilization, exchange information between UEs and UEs/infrastructure and make the network achieve a high throughput than the other two schemes.

Chapter 6 Conclusions and Future Work

In this Chapter, the entire thesis is concluded, and potential future studies are pointed out.

6.1 Conclusions

In this Thesis, research on V2X safety-related information dissemination in diverse vehicular communication scenarios has been conducted. The dissemination of safety-related information, which has various functionalities closely associated with different applications in ITS, is deemed as a key technology to ensure road safety, fulfil autonomous driving, and improve traffic efficiency in the near future. Motivated by the existing problems like high packet loss rate and large delivery latency as well as research gaps in resource allocation, we first review the existing data dissemination schemes for safety message broadcasting in DSRC and strategies of multiple access in C-V2X, and our proposed algorithms focus on the MAC protocol in DSRC and resource allocation in 5G C-V2X networks. The proposed hybrid MAC protocol, the optimization method based on the analytical model, and the fuzzy logic based adaptive algorithm for resource allocation significantly improve the reliability and efficiency for safety message dissemination in their respective networks. The features and achievements of different proposed schemes are summarised as follows.

We have studied periodic broadcast of BSM in vehicular network based on the DSRC. Distinguishing from the unicast information and event-trigger safety messages, BSMs are massively generated by all vehicles in the networks and needed to be delivered timely. Due to lossy channels, dynamic topology of networks transmission collisions and stringent requirements, BSMs cannot be disseminated reliably and efficiently in vehicular networks, especially in dense networks, even if more complicated and enhanced schemes are employed. To tackle such problem, a novel hybrid MAC protocol, namely NC-PNC MAC, is proposed in this thesis. The hybrid NC-PNC MAC contains both the distributed and centralized sessions in each broadcast period. Such hybrid characteristics, on the one hand can effectively suppress transmission collisions because the centralized session dominate the whole BSM broadcast; and on the other hand, it keeps the flexibility and compatibility with DSRC from the distributed manner. Moreover, with the assistance of PNC and RLNC, which are integrated in both one-hop V2V and V2I communications, the proposed MAC protocol is able to greatly improve the efficiency and reliability for BSM broadcasting in both roadway and intersection scenarios, regardless of sparse or dense networks. In terms of the delivery latency, BSMs can be delivered within one CCH interval without causing extra delay. Based upon both the theoretical analysis and simulation results, the NC-PNC MAC shows a linear communication complexity, which proves it possesses good scalability and feasibility.

We extend our research to BSM broadcast in V2X communications and enhance the NC-PNC MAC by proposing two distinct approaches. At first, theoretical analysis is performed to analyse collision probability in the OFDMA uplink session, the total number of transmissions implemented in all three sessions, and the average PDR performance of the network. The derived mathematical model explicitly shows the relationship between the parameters of the MAC protocol and the PDR performance. From the model, the tuneable parameters are identified. By adjusting one parameter of the MAC, the PDR performance is boosted without extra cost and endeavour (i.e., the increase of complexity or use of extra resources). For the second approach, we improve the PDR performance by designating a pair of auxiliary relay nodes that make use of the remaining idle time at the end of every dissemination interval and forward network-coded packets to distant nodes. This strategy is based on observations from the simulations and deep consideration of the working mechanism in the NC-PNC MAC. Finally, the two enhanced schemes are compared and the trade-off between the consumed time and PDR are discussed.

Cellular V2X communication in 5G era is another technology that is promising to support more advanced services envisioned in ITS. Since the resource allocation plays a pivotal role in dedicating limited time-spectrum resources to different UEs and coordinating those UEs to exchange data, we studied the strategy of resource allocation in mode 3 and how it affects the network performance. In fact, most of the other researchers pay more attention on transmission scheduling in mode 4 or link-level performance analysis. From the elementary principle in physical-layer working procedures specified in 3GPP standard, a straightforward method of random-based resource allocation and a location-aware resource allocation are proposed and studied at first. Although both methods can preclude transmission collisions and obviate inter-UE interference, they cannot satisfy the requirement of ultra-reliable low-latency communications like enhanced V2X services, in which safety or sensing data are generated enormously and frequently, because of the low reuse of the spectrum. A self-adaptive fuzzy-logic based resource allocation algorithm (FUZZRA) proposed in the thesis is a promising solution. By taking into account multiple factors other than only the interference from the concurrent links existing in the network, resources are assigned more wisely to different UEs. Extensive simulations show that the FUZZRA can significantly boost the network throughput and maintain the intra-cell interference at a low level.

6.2 Future Work

There are really a few of potential research directions that are worthy of further exploration in order to advance the V2X communications based on both the DSRC and 5G cellular networks. Based upon the research work in Chapter 3, 4 and 5, we will discuss those research topics in the following paragraphs.

In Chapters 3 and 4, we worked on enhancing the performance for BSM dissemination in vehicular networks in DSRC. The proposed MAC protocol realises the BSM interchange among all vehicles in a region via the assistance of both the V2I and V2V communications. In the protocol, the RSU functions as a coordinator, selects relay nodes and executes PNC encoding. However, RSUs are usually placed in urban areas and busy motorways. They may not be available in some remote places and small towns. How to apply the NC-PNC MAC in those areas is a challenge. One possible solution is to elect an appropriate vehicle to play a role as a RSU. However, due to the mobility of vehicles, the selection of a coordinator should be done autonomously and dynamically with the consideration of multiple factors, including instant positions, travelling velocity, direction and so on. On the other hand, cross-region dissemination of BSMs should also be considered. As pointed out before, the interchange of BSM packets are conducted in a RoI. That means our proposed MAC protocol only considers how to make sure all vehicles in the same RoI to mutually receive each other's safety messages. However, some vehicles also need to receive BSMs sent by other RoI, i.e., adjacent regions, because every vehicle needs to receive BSMs around them, regardless of which RoI they belong to, according to the requirement of safety applications in ITS. Unfortunately, vehicles near the boundary of a RoI may not receive BSMs from vehicles in the adjacent RoI as the NC-PNC MAC only ensure the BSM exchange within the same RoI. Therefore, cross-region broadcast of certain BSMs turns to be necessary; especially for those sent by vehicles close to the border of the two regions. To solve this problem, vehicles at the border of two regions should not only take part in the local NC-PNC sessions, but also get an opportunity to have cross-border exchange of BSMs without causing interference to the communications in their own region. One potential solution is that the RSUs allow those remote vehicles to broadcast their BSMs autonomously or via the assistance of a relay node during the distributed session (i.e., *CSMA session or MAC setup session*), since they are too far to receive data from their own associated RSUs. Nevertheless, whichever method is adopted, such as via relay or leveraging RLNC like in [46], the scheme should be deliberated and carefully studied. Otherwise, it may interfere with the original protocol.

In Chapter 5, we proposed a fuzzy-logic based resource allocation in 5G C-V2X. The proposed algorithm, FUZZRA, can effectively balance the spectrum reuse and intra-cell interference, thereby achieving a high successful allocation ratio and network throughput. However, as discussed and pinpointed in the Chapter, the inter-cell coordination is not considered while implementing tasks of resource allocation as the FUZZRA at different cells works independently. The lack of cross-cell coordination obviously lowers the packet reception radio of the vehicles at the boundary of two adjoining cells and brings hidden hazards to those vehicles. Therefore, a further research on resource allocation should seriously consider the problem and provide effective solutions. Moreover, although the proposed FUZZRA can adaptively change the allocation strategy

in according to the network conditions, the input factors like interference level are obtained based on inaccurate calculation and channel model. As we know, the reception power and the interference closely relate to channels and the environment. Even with the same transmission power and distance between a sender and a receiver, the probability of packet reception at the receive may change dramatically if there are obstructions in between. Therefore, in order to accurately calculate the interference and other input variables, we can resort to machine learning, which can quickly find the optimal resources for different transmissions, according to their distinct features, including the current positions, dissemination type (broadcast or unicast) and so on. For example, if broadcast and unicast transmissions take place at the same time, then the unicast may cause interference to the recipient nodes of the broadcast. The current solution may either be choosing different time or different subchannels for them. By leveraging the machine learning, power control may be adopted to the unicast without utilizing extra resources. Such method depends on accurate calculation of interference and channel conditions. The machine learning may play an important role in such scenario to further improve the resource allocation.

Author's Publications

The following part lists the author's publications during the period of pursuing the PhD degree in Auckland University of Technology.

Publications related to the thesis:

- **Journal Papers**

1. **M. Zhang,** G. G. M. N. Ali, P. H. J. Chong, B. C. Seet and A. Kumar, "A Novel Hybrid MAC Protocol for Basic Safety Message Broadcasting in Vehicular Networks," *IEEE Transactions on Intelligent Transportation Systems*, vol. 21, no. 10, pp. 4269-4282, Oct. 2020.

2. **M. Zhang**, P. H. J. Chong and B. C. Seet, "Performance Analysis and Boost for a MAC Protocol in Vehicular Networks," *IEEE Transactions on Vehicular Technology*, vol. 68, no. 9, pp. 8721-8728, Sept. 2019.

- **Conference Papers**

1. **M. Zhang,** P. H. J. Chong, B. Seet, S. U. Rehman and A. Kumar, "Integrating PNC and RLNC for BSM dissemination in VANETs," in *Proceedings of IEEE 28th Annual International Symposium on Personal, Indoor, and Mobile Radio Communications (PIMRC)*, pp. 1-5, Montreal, QC, 2017.

2. **M. Zhang**, A. Kumar, P. H. J. Chong, H. C. B. Chan and B. Seet, "Resource Allocation Based Performance Analysis for 5G Vehicular Networks in Urban Areas," in *Proceedings of IEEE Wireless Communications and Networking Conference Workshops (WCNCW)*, pp. 1-6, Seoul, Korea (South), 2020.

Other publications:

- **Journal Paper**

M. Zhang, I. C. Lam, A. Kumar, K. K. Chow, P. H. J. Chong, "Optical environmental sensing in wireless smart meter network", *AIMS Electronics and Electrical Engineering*, *vol.* 2, *no.* 3, *pp.* 103-116, Oct. 2018.

- **Conference Paper**

M. Zhang, K. K. Chow, P. H. J. Chong, "Optical fibre-based environmental sensors utilizing wireless smart grid platform," in *Proceedings of Smart Grid Inspired Future Technologies*, *pp.* 253-258, Aug. 2017.

Bibliography

[1]   W. H. O. Violence, I. Prevention, and W. H. Organization, Global status report on road safety 2018. World Health Organization, 2018.

[2]   L. Figueiredo, I. Jesus, J. T. Machado, J. R. Ferreira, and J. M. De Carvalho, "Towards the development of intelligent transportation systems," in *Proceedings of the IEEE Intelligent Transportation Systems*, pp. 1206-1211, 2001.

[3]   ETSI TC ITS, Intelligent Transport Systems (ITS); Vehicular Communications; Basic Set of Applications; Definitions, *Std. ETSI* TR 102 638 V1.1.2, 2015.

[4]   3GPP, "Enhancement of 3GPP Support for V2X Scenarios," *3GPP* TS 22.186 v16.0.0, Sep. 2018.

[5]   M. Boban, A. Kousaridas, K. Manolakis, J. Eichinger and W. Xu, "Use cases, Requirements, and Design Considerations for 5G V2X", *IEEE Vehicular Technology Magazine*, vol. 13, no. 3, Sept. 2018.

[6]   J. Hu, C. Chen, T. Qiu and Q. Pei, "Regional-Centralized Content Dissemination for eV2X Services in 5G mmWave-Enabled IoV," *IEEE Internet of Things Journal*, vol. 7, no. 8, pp. 7234-7249, Aug. 2020.

[7]   Z. Yang, M. Li, and W. Lou, "CodePlay: Live multimedia streaming in VANETs using symbol-level network coding," *IEEE Transactions on Wireless Communications,* vol. 11, no. 8, pp. 3006-3013, 2012.

[8]   P. Papadimitratos, A. De La Fortelle, K. Evenssen, R. Brignolo, and S. Cosenza, "Vehicular communication systems: Enabling technologies, applications, and future outlook on intelligent transportation," *IEEE Communications Magazine,* vol. 47, no. 11, pp. 84-95, 2009.

[9]   3GPP, "V2X services and requirements," *3GPP* TS 22.185 v15.0.0, Jun. 2018.

[10]   E. B. Hamida, H. Noura, W. Znaidi, "Security of Cooperative Intelligent Transport Systems: Standards, Threats Analysis and Cryptographic Countermeasures," *Electronics*, *vol* 4, *no.* 3, *pp.* 380-423, 2015.

[11]   H. Hartenstein and L. Laberteaux, "A tutorial survey on vehicular ad hoc networks," *IEEE Communications Magazine*, vol. 46, no. 6, pp. 164-171, 2008.

[12]   F. J. Martinez, C.-K. Toh, J.-C. Cano, C. T. Calafate, and P. Manzoni, "Emergency services in future intelligent transportation systems based on vehicular communication networks," *IEEE Intelligent Transportation Systems Magazine,* vol. 2, no. 2, pp. 6-20, 2010.

[13]   J. B. Kenney, "Dedicated short-range communications (DSRC) standards in the united states," *Proceedings of the IEEE*, vol. 99, no. 7, pp. 1162-1182, 2011.

[14]   E. ETSI, "302 637-2 v1. 3.1-Intelligent Transport Systems (ITS); vehicular communications; basic set of applications; part 2: Specification of cooperative awareness basic service," ETSI, Sept. 2014.

[15]   F. C. Commission et al., "FCC allocates spectrum in 5.9 GHz range for intelligent transportation systems uses," Report No. ET, pp. 99-105, 1999.

[16]   Final Report, U.S. Dept. Trans., National Highway Traffic Safety Admin., "Vehicular safety communications project," Rep. DOT HS 810 591, Apr. 2006.

[17]   IEEE Standard 802.11p-2010, *Std*., 2011.

[18]   IEEE Standard 1609.1, Trial-Use Standard for Wireless Access in Vehicular Environments (WAVE) — Resource Manager, 2006.

[19]   IEEE Standard 1609.2, Trial-Use Standard for Wireless Access in Vehicular Environments (WAVE) — Security Services for Applications and Management Messages, 2006.

[20]   IEEE Standard 1609.3, IEEE Trial-Use Standard for Wireless Access in Vehicular Environments (WAVE)-Networking Services, 2007.

[21]   IEEE Standard 1609.4, Trial-Use Standard for Wireless Access in Vehicular Environments (WAVE) — Multi-Channel Operation, 2006.

[22]   Y. L. Morgan, "Notes on DSRC & WAVE standards suite: Its architecture, design, and characteristics," *IEEE Communications Surveys & Tutorials,* vol. 12, no. 4, pp. 504-518, 2010.

[23]   R. A. Uzcategui, A. J. De Sucre, and G. Acosta-Marum, "WAVE: A tutorial," *IEEE Communications Magazine,* vol. 47, no. 5, 2009.

[24]   3GPP, "Study on LTE-based V2X services," TR 36.885, v.14.0.0, July, 2016

[25]   3GPP, "Evolved Universal Terrestrial Radio Access (E-UTRA) and Evolved Universal Terrestrial Radio Access Network (E-UTRAN); Overall Description," TS 36.300, Dec. 2018.

[26]   3GPP, "Physical layer procedures," TR 36.213, Sept, 2016.

[27]   3GPP, "Architecture enhancements for V2X services," TR 23.285, Dec. 2016.

[28]   3GPP, "Enhancement of 3GPP Support for V2X Scenarios," 3GPP TS 22.186 v16.0.0, Sep. 2018.

[29]   3GPP, "Evolved Universal Terrestrial Radio Access (E-UTRA); Physical layer procedures (V15.4.0, Release 15)," 3GPP TS 36.213, Dec. 2018.

[30]   N. Bonjorn, F. Foukalas and P. Pop, "Enhanced 5G V2X services using sidelink device-to-device communications," in *Proceeding of IEEE 17th Annual Mediterranean Ad Hoc Networking Workshop*, pp. 1-7, Jun. 2018.

[31]   5G Americas White Paper: Cellular V2X Communications Towards 5G, available at: https://www.5gamericas.org/cellular-v2x-communications-towards-5g/.

[32]   K. Abboud, H. A. Omar and W. Zhuang, "Interworking of DSRC and Cellular Network Technologies for V2X Communications: A Survey," *IEEE Transactions on Vehicular Technology,* vol. 65, no. 12, pp. 9457-9470, Dec. 2016.

[33] S. Ucar, S. C. Ergen, and O. Ozkasap, "Multihop-cluster-based IEEE 802.11p and LTE hybrid architecture for VANET safety message dissemination," *IEEE Transactions on Vehicular Technology,* vol. 65, no. 4, pp. 2621-2636, 2016.

[34] Y. P. Fallah, C. Huang, R. Sengupta, and H. Krishnan, "Congestion control based on channel occupancy in vehicular broadcast networks," in *Proc. IEEE Veh. Technol. Conf.*, Fall 2010.

[35] F. Bai, D. D. Stancil, and H. Krishnan, "Toward understanding characteristics of dedicated short-range communications from a perspective of vehicular network engineers," in *Proc. ACM Int. conf. on Mobile computing and networking*, Sept. 2010.

[36] Q. Xu, T. Mak, J. Ko, and R. Sengupta, "Medium access control protocol design for vehicle-vehicle safety messages," *IEEE Trans. Veh. Technol.,* vol. 56, no. 2, pp. 499–518, 2007.

[37] F. Farnoud, B. Hassanabadi, and S. Valaee, "Message broadcast using optical orthogonal codes in vehicular communication systems," in *Proceeding of The First International Workshop on Wireless Networking for Intelligent Transportation Systems*, 2007.

[38] R. Ahlswede, N. Cai, S.-Y. R. Li, and R. W. Yeung, "Network information flow," *IEEE Transaction on Information Theory,* vol. 46, no. 4, pp. 1204-1216, 2000.

[39] T. Ho, M. Medard, R. Koetter, D. R. Karger, M. Eros, J. Shi, and B. Leong, "A random linear network coding approach to multicast," *IEEE Transactions on Information Theory,* vol. 52, no. 10, pp. 4413-4430, 2006.

[40] J. Sahoo, E. H.-K. Wu, P. K. Sahu, and M. Gerla, "Congestion-controlled-coordinator-based MAC for safety-critical message transmission in VANETs," *IEEE Trans. Intelligent Transportation System,* vol. 14, no. 3, Sept. 2013.

[41] Y. Kim, M. Lee, and T.-J. Lee, "Coordinated multichannel MAC protocol for vehicular ad hoc networks," *IEEE Trans. Veh. Technol.,* vol. 65, no. 8, Aug. 2016.

[42] W. Guo, L. Huang, L. Chen, H. Xu, and J. Xie, "An adaptive collision-free MAC protocol based on TDMA for inter-vehicular communication," in *Proceedings of International Conference on Wireless Communications and Signal Processing (WCSP)*, Oct. 2012.

[43] Y. Wu, K. W. Shum, W. S. Wong, and L. Shen, "Safety-message broadcast in vehicular ad hoc networks based on protocol sequences," *IEEE Trans. Veh. Technol.,* vol. 63, no. 3, Mar. 2014.

[44] M. F. Tsai and C. H. Chang, "A reducing broadcast message method in vehicular networks," in *Proceedings of Tenth International Conference on Intelligent Information Hiding and Multimedia Signal Processing*, Aug. 2014.

[45] B. Hassanabadi and S. Valaee, "Reliable periodic safety message broadcasting in VANETs using network coding," *IEEE Trans. Wireless Commun.,* vol. 13, no. 3, pp. 1284–1297, 2014.

[46] Y. Gao, P. H. J. Chong, and Y. L. Guan, "BSM dissemination with network coded relaying in VANETs at NLOS intersections," in *Proc. IEEE Int. Conf. on Comm. (ICC)*, May 2017.

[47] K. Liu, J. K.-Y. Ng, J. W. V. C. S. Lee, W. Wu, and S. H. Son, "Network coding-assisted data dissemination via cooperative vehicle-to-vehicle/-infrastructure communications," *IEEE Trans. Intelligent Transportation System,* vol. 17, no. 6, pp. 1509-1520, June 2016.

[48] Q. Yang, J. Zheng, and L. Sheng, "Modelling and performance analysis of periodic broadcast in vehicular ad hoc networks," in *Proc. IEEE Glob. Telecom. Conf.* (*GLOBECOM*), Dec. 2011.

[49] M. Khabazian, S. Aissa, and M. M. Ali, "Performance modeling of safety messages broadcast in vehicular ad hoc networks," *IEEE Trans. Intelligent Transportation System,* vol. 14, no. 1, pp. 380–387, 2013.

[50] R. M. Masegosa and J. Gozalvez, "LTE-V for Sidelink 5G V2X Vehicular Communications: A New 5G Technology for Short-Range Vehicle-to-Everything Communications," *IEEE Vehicular Technology Magazine,* vol. 12, no. 4, pp. 30-39, Dec. 2017.

[51] N. Bonjorn, F. Foukalas, F. Cañellas and P. Pop, "Cooperative Resource Allocation and Scheduling for 5G eV2X Services," *IEEE Access,* vol. 7, pp. 58212-58220, 2019.

[52] M. G. Martín, M. Sepulcre, R. M. Masegosa and J. Gozalvez, "Analytical Models of the Performance of C-V2X Mode 4 Vehicular Communications," *IEEE Transactions on Vehicular Technology,* vol. 68, no. 2, pp. 1155-1166, Feb. 2019.

[53] B. Toghi, M. Saifuddin, H. N. Mahjoub, M. O. Mughal, Y. P. Fallah, J. Rao and S. Das, "Multiple Access in Cellular V2X: Performance Analysis in Highly Congested Vehicular Networks," in *Proceeding of IEEE Vehicular Networking Conference* (VNC), Dec. 2018.

[54] M. Wang, Z. Zhong and Q. Liu, "Resource allocation for SC-FDMA in LTE uplink," in *Proceeding of IEEE International Conference on Service Operations, Logistics and Informatics,* July 2011.

[55] S. Rostami, K. Arshad and P. Rapajic, "Resource Allocation in LTE-Based MIMO Systems with Carrier Aggregation", in *Proceeding of IEEE 84th Vehicular Technology Conference* (*VTC-Fall*), Sept. 2016.

[56] X. Wang, X. Li, H. Shwe, M. Yang and P. H. J. Chong, "Interference-aware resource allocation for device-to-device communications in cellular networks," in *Proceeding of IEEE 10th International Conference on Information, Communications and Signal Processing* (*ICICS*), Dec. 2015.

[57] H. S. Chae, J. Gu, B. Choi and M. Y. Chung, "Radio resource allocation scheme for device-to-device communication in cellular networks using fractional frequency reuse," in *Proceeding of the 17th Asia Pacific Conference on Communications*, pp. 58-62, Sabah, 2011.

[58] L. Melki, S. Najeh and H. Besbes, "Radio resource allocation scheme for intra-inter-cell D2D communications in LTE-A," in *Proceeding of IEEE 26th Annual International*

Symposium on Personal, Indoor, and Mobile Radio Communications (PIMRC), pp. 1515-1519, Hong Kong, 2016.

[59]   T. Kanai, "Autonomous reuse partitioning in cellular systems," in *Proceeding of Vehicular Technology Society 42nd VTS Conference - Frontiers of Technology*, pp. 782-785 vol. 2, Denver, CO, USA, 1992.

[60]   I. C. Wong, Zukang Shen, B. L. Evans and J. G. Andrews, "A low complexity algorithm for proportional resource allocation in OFDMA systems," in *Proceeding of IEEE Workshop on Signal Processing Systems,* SIPS 2004., pp. 1-6, 2004, Austin, TX, 2004.

[61]   A. A. Khan, M. Abolhasan, W. Ni, J. Lipman and A. Jamalipour, "A Hybrid-Fuzzy Logic Guided Genetic Algorithm (H-FLGA) Approach for Resource Optimization in 5G VANETs," *IEEE Transactions on Vehicular Technology,* vol. 68, no. 7, pp. 6964-6974, July 2019.

[62]   S. Zhang, S. C. Liew, P. P. Lam, "Hot topic: Physical-layer network coding," in *Proc. ACM MOBICOM*, *pp*. 358-365, 2006.

[63]   The Network Simulator tool: ns-3 (version 3.27), available at: https://www.nsnam.org

[64]   P. A. Lopez, M. Behrisch, L. B. Walz and J. Erdmann, Y. Pang, "Microscopic Traffic Simulation using SUMO," in *Proceeding of the 21st IEEE International Conference on Intelligent Transportation Systems*, Nov. 2018.

[65]   "Dedicated short range communications (DSRC) message set dictionary," Nov. 2009.

[66]   D. Jiang, V. Taliwal, A. Meier, W. Holfelder, and R. Herrtwich, "Design of 5.9 GHz DSRC-based vehicular safety communication," *IEEE Wireless Communications,* vol. 13, no. 5, 2006.

[67]   IEEE Standard for Wireless Access in Vehicular Environments (WAVE)–Multi-channel Operation, IEEE Standard 1609.4, 2011

[68]   Ahmed, Shereen AM, Sharifah HS Ariffin, and Norsheila Fisal, "Overview of wireless access in vehicular environment (WAVE) protocols and standards," *Indian Journal of Science and Technology,* vol. 6, July 2013.

[69]   3GPP, "Physical layer procedures," TR 36.213 (V15.4.0), Dec. 2018.

[70]   3GPP, "Medium Access Control (MAC) protocol specification," TS 36.321 (V15.4.0), Dec. 2018.

[71]   S.-Y. Li, R. W. Yeung, and N. Cai, "Linear network coding," *IEEE transactions on information theory,* vol. 49, no. 2, pp. 371-381, 2003.

[72]   P. A. Chou, Y. Wu, and K. Jain, "Practical network coding," in *Proceeding of Allerton Conference on Communication, Control, and Computing*, Monticello IL, October 2003.

[73]   G. L. Mullen and D. Panario, Handbook of finite fields. CRC Press, 2013.

[74]   K. E. Atkinson, An introduction to numerical analysis. John Wiley & Sons, 2008.

[75] N. Cai and R. W. Yeung, "Secure network coding on a wiretap network," *IEEE Transactions on Information Theory,* vol. 57, no. 1, pp. 424-435, 2011.

[76] T. Ho, B. Leong, R. Koetter, M. Medard, M. Effros, and D. R. Karger, "Byzantine modification detection in multicast networks with random network coding," *IEEE Transactions on Information Theory,* vol. 54, no. 6, pp. 2798-2803, 2008.

[77] S. Jaggi, M. Langberg, S. Katti, T. Ho, D. Katabi, and M. Medard, "Resilient network coding in the presence of byzantine adversaries," in *Proceeding of IEEE International Conference on Computer Communications*, pp. 616-624, 2007.

[78] N. Cai and R. W. Yeung, "Network coding and error correction," in *Proc. of IEEE Inform. Theory Workshop*, 2002.

[79] R. Koetter and F. R. Kschischang, "Coding for errors and erasures in random network coding," *IEEE Transactions on Information Theory,* vol. 54, no. 8, *pp*. 3579-3591, 2008.

[80] X. Chu and Y. Jiang, "Random linear network coding for peer-to-peer applications," *IEEE Network,* vol. 24, no. 4, pp. 35-39, 2010.

[81] Z. Liu, C. Wu, B. Li and S. Zhao, "UUSee: Large-Scale Operational On-Demand Streaming with Random Network Coding," in *Proceedings of IEEE INFOCOM*, San Diego, CA, 2010.

[82] A. Nandan, S. Das, G. Pau, M. Gerla, and M. Sanadidi, "Cooperative downloading in Vehicular Ad-hoc Networks," in *Proceedings of IEEE Second Annual Conference on Wireless On-demand Network Systems and Services*, pp. 32-41, 2005.

[83] Z. Yang, M. Li, and W. Lou, "CodePlay: Live multimedia streaming in VANETs using symbol-level network coding," *IEEE Transactions on Wireless Communications,* vol. 11, no. 8, pp. 3006-3013, 2012.

[84] M. Li, Z. Yang, and W. Lou, "Codeon: Cooperative popular content distribution for vehicular networks using symbol level network coding," *IEEE Journal on Selected Areas in Communications,* vol. 29, no. 1, pp. 223-235, 2011.

[85] F. Mirani, A. Busson, and C. Adjih, "Improving delay-based data dissemination protocol in VANETs with network coding," *REV Journal on Electronics and Communications,* vol. *2*, no. 3-4, 2013.

[86] D. W¨ubben and Y. Lang, "Generalized sum-product algorithm for joint channel decoding and physical-layer network coding in two-way relay systems," *in Proc. 2010 IEEE Glob. Telecom.* Conf., 2010.

[87] L. Lu and S. C. Liew, "Asynchronous physical-layer network coding," *IEEE Trans. Wireless Commun.,* vol. 11, no. 2, Feb. 2012.

[88] M. Zhang, L. Lu and S. C. Liew, "An Optimal Decoding Strategy for Physical-Layer Network Coding Over Multipath Fading Channels," *IEEE Transactions on Vehicular Technology,* vol. 64, no. 9, pp. 4365-4372, Sept. 2015.

[89] F. Rossetto and M. Zorzi, "On the design of practical asynchronous physical layer network coding," in *Proc. of IEEE Workshop on SPAWC,* 2009.

[90] L. Lu, T. Wang, S. C. Liew, and S. Zhang, "*Implementation of physical-layer network coding," Physical Communication,* vol. 6, no. 1, pp. 74–87, Mar. 2013.

[91] P. K. Sahu, A. Hafid, and S. Cherkaoui, "M-PNC: Multi-hop physical layer network coding for shared paths in vehicular networks," in *Proc. Wireless Communications and Mobile Computing Conf.*, Oct. 2015.

[92] E. D. N. Ndih and S. Cherkaoui, "Toward neighborhood prediction using physical-layer network coding," in *Proc. IEEE Int. Conf. on Comm.* (*ICC*), Jun. 2012.

[93] E. D. N. Ndih and S. Cherkaoui, "MAC for physical-layer network coding in VANETs," *International Journal of Business data communication and networking,* vol. 8, no. 4, Oct. 2012.

[94] H.-J. Zimmermann, "Fuzzy Set Theory and Its Applications", Fourth Edition, Springer Science and Business Media, LLC, 2001.

[95] Zadeh, L.A. "Fuzzy Sets", Inform. Control 8, 338-353, 1965.

[96] W. V. Leekwijck, E. E. Kerre, "Defuzzification: criteria and classification", *Fuzzy Sets and Systems,* vol. 108, pp. 159-178, 1999.

[97] N. Chaabouni, A. Hafid, and P. K. Sahu, "A collision-based beacon rate adaptation scheme (CBA) for VANETs," in *Proceedings of IEEE International Conference on Advanced Networks and Telecommunications Systems (ANTS)*, Dec. 2013.

[98] Y. Park and H. Kim, "Collision control of periodic safety messages with strict messaging frequency requirement," *IEEE Trans. Veh. Technol.,* vol. 62, no. 2, Feb. 2013.

[99] J.-S. Park, U. Lee, S. Y. Oh, M. Gerla, D. S. Lun, W. W. Ro, and J. Park, "Delay analysis of car-to-car reliable data delivery strategies based on data mulling with network coding," *IEICE Trans. on Information and Systems,* vol. E91-D, no. 10, pp. 2524–2527, Jan. 2008.

[100] Y. Gao, G. M. N. Ali, P. H. J. Chong, and Y. L. Guan, "Network coding based BSM broadcasting at road intersection in V2V communication," in *Proc. IEEE Veh. Technol. Conf.*, Fall 2016.

[101] IEEE 802.11-2007: A new release of the standard that includes amendments a, b, d, e, g, h, i, and j, July 2007.

[102] I. W.-H. Ho, S. C. Liew, and L. Lu, "Feasibility study of physical-layer network coding in 802.11p VANETs," in *Proc. IEEE Int. Symp. Info Theory*, Jun. 2014.

[103] L. F. Xie, I. W.-H. Ho, S. C. Liew, L. Lu, and F. C. M. Lau, "Mitigating doppler effects on physical-layer network coding in VANET," in *Proc. IEEE Int. Symp. on Person Indoor and Mobile Radio Comm.* (*PIMRC*), Aug. 2014.

[104] E. D. N. Ndih and S. Cherkaoui, "Reliable broadcasting in VANETs using physical-layer network coding," in *Proc. International Conference on Communications and Information Technology*, Jun. 2012.

[105] C. Wu, S. Ohzahata, Y. Ji, and T. Kato, "Joint fuzzy relays and network coding-based forwarding for multihop broadcasting in VANETs," *IEEE Trans. Intelligent Transportation System,* vol. 16, no. 3, Jun. 2015.

[106] C. Wu, X. Chen, Y. Ji, S. Ohzahata, and T. Kato, "Efficient broadcasting in VANETs using dynamic backbone and network coding," *IEEE Trans. Wireless Commun.,* vol. 14, no. 11, Nov. 2015.

[107] Y. Bi, H. Shan, X. S. Shen, N. Wang, and H. Zhao, "A multi-hop broadcast protocol for emergency message dissemination in urban vehicular ad hoc networks," *IEEE Trans. Intelligent Transportation System*, vol. 17, no. 3, Mar. 2016.

[108] O. S. Eyobu, J. Joo, and D. S. Han, "Cooperative multi-channel dissemination of safety messages in VANETs," in *Proceedings of IEEE Region 10 Conference* (*TENCON*), Nov. 2016.

[109] J. Y. Lee and H. S. Lee, "A performance analysis model for IEEE 802.11e EDCA under saturation condition," *IEEE Transactions on Communications,* vol. 57, no. 1, pp. 56-63, 2009.

[110] M. Gas, K. Kosek-Szott, M. Natkaniec, and A. Pach, "3D Markov chainbased saturation throughput model of IEEE 802.11 EDCA," *Electronics letters,* vol. 47, no. 14, pp. 826-827, 2011.

[111] K. Kosek-Szott, M. Natkaniec, and A. R. Pach, "A simple but accurate throughput model for IEEE 802.11 EDCA in saturation and non-saturation conditions*," Computer Networks,* vol. 55, no. 3, pp. 622-635, 2011.

[112] R. Reinders, M. van Eenennaam, G. Karagiannis, and G. Heijenk, "Contention window analysis for beaconing in VANETs," in *Proceedings of 7th International Wireless Communications and Mobile Computing Conference* (*IWCMC*), pp. 1481-1487, 2011.

[113] G. V. Rossi and K. K. Leung, "Optimised CSMA/CA protocol for safety messages in vehicular ad-hoc networks," in *Proceedings of IEEE Symposium on Computers and Communications* (*ISCC*), pp. 689-696, 2017.

[114] Y. Gao, X. Xu, Y. Zeng, and Y. L. Guan, "Optimal scheduling for multi-hop video streaming with network coding in vehicular networks," in *Proceedings of IEEE 87th Vehicular Technology Conference* (*VTC Spring*), 2018.

[115] G. Nardini, A. Virdis, C. Campolo, A Molinaro, G Stea, "Cellular-V2X Communications for Platooning: Design and Evaluation." *Sensors*, no. 5, 2018.

[116] X. Wu, Y. Hou, X. Tao and X. Tang, "Maximization of Con-current Links in V2V Communications Based on Belief Propagation", in *Proceedings of IEEE Wireless Communications and Networking Conference* (*WCNC*), May 2020.

[117] L. Gao, Y. Hou, X. Tao and M. Zhu, "Energy-Efficient Power Control and Resource Allocation for V2V Communication", in *Proceedings of IEEE Wireless Communications and Networking Conference* (*WCNC*), May 2020.

[118] C. Xu et al., "Efficiency Resource Allocation for Device-to-Device Underlay Communication Systems: A Reverse Iterative Combinatorial Auction Based Approach," in *IEEE Journal on Selected Areas in Communications,* vol. 31, no. 9, pp. 348-358, September 2013.

[119] X. Wu, M. Safari and H. Haas, "Three-state fuzzy logic method on resource allocation for small cell networks," in *Proceedings of IEEE 26th Annual International Symposium on Personal, Indoor, and Mobile Radio Communications* (*PIMRC*), Hong Kong, 2015.

[120] L. Lu, L. Z. You, and S. C. Liew, "Network-coded multiple access," *IEEE Jour. Select. Areas in Comm.,* vol. 13, no. 12, pp. 2853 – 2869, Dec. 2014.

[121] S. Sen, R. R. Choudhury, and S. Nelakuditi, "No time to countdown: migrating backoff to the frequency domain," in *Proc. ACM int. conf. on Mobile computing and networking*, Sept. 2011.

[122] L. Cheng, B. E. Henty, D. D. Stancil, F. Bai, and P. Mudalige, "Mobile vehicle-to-vehicle narrow-band channel measurement and characterization of the 5.9 Ghz dedicated short range communication (dsrc) frequency band," *IEEE Journal on Selected Areas in Communications,* vol. 25, no. 8, pp. 1501-1516, 2007.

[123] J. Yin, G. Holland, T. ElBatt, F. Bai, and H. Krishnan, "DSRC channel fading analysis from empirical measurement," in *Proc of IEEE First International Conference on Communications and Networking in China*, Oct. 2006.

[124] P. Ferrand, J. M. Gorce, and C. Goursaud, "Approximations of the packet error rate under slow fading in direct and relayed links," *Research Report*, 2013.

[125] A. AI-Sobky and R. M. Mousa, "Traffic density determination and its applications using smart phone," *Alexandria Engineering Journal,* vol. 55, no. 1, pp. 513 – 523, 2016.

[126] ETSI TC ITS, Intelligent Transport Systems; Vehicular Communications; Basic Set of Applications; Part 2: Specification of Cooperative Awareness Basic Service, Std. ETSI EN Std 302 637-2 V.1.3.0, 2013.

[127] Martin Döttling; Werner Mohr; Afif Osseiran, "WINNER II Channel Models," in Radio Technologies and Concepts for IMT-Advanced, Wiley, 2010.

[128] Interoperability Issues of Vehicle-to-Vehicle Based Safety Systems Project (V2V-Interoperability), Project Order 0004, Technical Proposal Statement of Work, U.S. Dept. Trans., Nat. Highway Traffic Safety Admin., Cooperative Agreement DTNH22-05-01277, Dec. 2009.

[129] European Commission, CVIS projects, available at: http://www.cvisproject.org/.

[130] European Commission, SAFESPOT Integrated Project, available at: http://www.safespot-eu.org/.

[131] 5GAA, "V2X Functional and Performance Test Report", available at: https://5gaa.org/news/5gaa-report-shows-superior-performance-of-cellular-v2x-vs-dsrc/, Oct, 2018.

[132] C. Campolo, A. Molinaro, G. Araniti and A. O. Berthet, "Better Platooning Control Toward Autonomous Driving : An LTE Device-to-Device Communications Strategy That Meets Ultralow Latency Requirements," *IEEE Vehicular Technology Magazine,* vol. 12, no. 1, pp. 30-38, March 2017.

[133] 5GCAR project, available at: https://5gcar.eu/.

[134] C. M. Kozierok, "The TCP/IP Guide: A Comprehensive, Illustrated Internet Protocols Reference," Oct. 2005.

[135] L. Cheng, B. E. Henty, R. Cooper, D. D. Stancil, and F. Bai, "A Measurement Study of Time-Scaled 802.11a Waveforms over the Mobile-to-Mobile Vehicular Channel at 5.9 GHz*," IEEE Communications Magazine,* vol 46, no. 5, pp. 84-91, May 2008.

[136] X. Zhang, M. Peng, S. Yan and Y. Sun, "Deep-Reinforcement-Learning-Based Mode Selection and Resource Allocation for Cellular V2X Communications," *IEEE Internet of Things Journal*, vol. 7, no. 7, pp. 6380-6391, July 2020.

[137] Cohda Wireless, V2X products, available at: https://cohdawireless.com/wp-content/uploads/2018/08/CW_Product-Brief-sheet-V2X.pdf.

[138] Cohda Wireless, Autonomous Platooning, available at: https://cohdawireless.com/platooning/.

[139] DINIGET-PS, available at: https://diginet-ps.de/en/home/.

[140] NYC Connected Vehicle Project, available at: https://cvp.nyc/.

[141] P. K. Singh, S. K. Nandi, S. Nandi, "A tutorial survey on vehicular communication state of the art, and future research directions", *Vehicular Communications,* vol. 18, 2019.